Bioprospecting and pathovar profiling of plant pathogenic bacteria using novel high throughput technology platforms

PhD Candidate - Paulina Focht

Newcastle University

School of Natural and Environmental Sciences

Faculty of Science, Agriculture and Engineering

Supervisors - Dr. Catherine Tétard-Jones, Professor William Willats & Dr. John Elphinstone

Acknowledgements

I would like to thank my supervisors; Dr. Catherine Tetard-Jones, Professor William Willats from Newcastle University for their insight, advice, support, and patience throughout the duration of my PhD and Dr. John Elphinstone for his supported of my activities at FERA Science ltd in York.

To my long-time friend, and soon to be a Dr., Abigail Smith. I wouldn't have embarked on the journey to start a PhD if it wasn't for you. Your support, help and friendship have helped me through many difficult times. I will always value the times we spent together trying to get the machines to cooperate with us, and the times we'd scratch our heads trying to troubleshoot issues. Thanks to you these last 4 years weren't lonely, and were filled with laughter.

Thank you, Dr. Sarah Sommer, for always offering a friendly ear and wealth of knowledge. Your friendship and professional help have been greatly appreciated.

Dr. Sarah Sommer was a post-doctoral research in the research group and has offered many innovative ideas and words of support throughout the last 3 years of my PhD. Sarah has helped with R analysis that is included in chapter 5, in the form of jitter plots.

Finally, I'd like to thank my family, Andrzej, Katarzyna and Oscar for pushing me and listening to me whenever I struggled. Luke Francis for being my rock, and the Francis family for their support during these last few years.

COVID-19 Statement

In February 2020, the COVID-19 pandemic has struck the world. Newcastle University had restricted access to laboratories and cease in-person teaching. Majority of experiments that were planned for the 3rd year, did not take place due to time restrictions imposed by COVID-19. The university re-opened for planned and socially distanced laboratory activity in August. With being granted an 8-week extension, it was possible to complete data collection and analysis for the 5th chapter, which focused on alginate production. However, the timeframe wasn't sufficient to perform any purification and categorisation work on enzymatic activity mentioned in chapters 3,4 and 5.

List of Acronyms

List of acronyms used throughout the thesis.

AGP	-	Arabinogalactan-Proteins
AMP	-	Antimicrobial Peptide
BCIP	-	5-Bromo-4-Chloro-3-Indolyl Phosphatase
CAZy	-	Carbohydrate Active Enzymes
CBM	-	Carbohydrate-Binding Module
CDC	-	Centre For Disease Control And Prevention
CDTA	-	Cyclohexane Diamine Tetraacetic Acid
CoMPP	-	Comprehensive Microarray Polymer Profiling
CRA	-	Congo Red Agar
CTCF	-	Corrected Total Cell Fluorescence
DAMPs	-	Damage-Associated Molecular Patterns
DAP	-	Defined Alginate Polysaccharide
DFMO	-	DL-Alpha-Difluoromethylornithine
eDNA	-	Environmental DNA
EPS	-	Extracellular Polysaccharides
ETI	-	Effector-Triggered Immunity
FTIR	-	Fourier Transform Infrared Spectrometry
G-block	-	A-L-Guluronate Residues
GC-MS	-	Gas Chromatography-Mass Spectrometry
GFP	-	Green Fluorescent Protein
HG	-	Homogalacturonan
HPAEC-PAD	-	Chromatography With Pulsed Amperometric Detection
HPLC	-	High-Performance Liquid Chromatography
HRGPs	-	Hydroxyproline-Rich Glycoproteins
IMP	-	Integral Protein Membrane
KB	-	Kings Broth
LP	-	Lipopolysaccharide
mAbs	-	Monoclonal Antibodies
mAGP	-	Mycolyl-Arabinogalactan-Peptidoglycan
M-block	-	B-D-Mannuronate Residues
MLST	-	Multilocus Sequence Typing Analysis
MS	-	Mass Spectrometry
NBT	-	Nitro Blue Tetrazolium
NCPPB	-	National Collection Of Plant Pathogenic Bacteria
NLR	-	Nucleotide Binding Leucine-Rich Repeat
PAG	-	Poly(Aldehyde Guluronate
PAMPs	-	Pathogen-Associated Molecular Patterns
PASTA	-	Penicillin-Binding-Protein And Serine-Threonine Kinase-Associated
PAT	-	Pectin-Alginate-Titania
PCW	-	Primary Cell Wall
PGA	-	Polygalacturonic Acid

PIA	-	Polysaccharide Intercellular Adhesin
RG	-	Rhamnogalacturonan
RGI	-	Rhamnogalacturonan I
T3E	-	Type 3 Effectors
T3SS	-	Type 3 Secretion System
TCP	-	Tissue Culture Plate
TFA	-	Trifluoracetic Acid
TM	-	Tube Method

Table of Contents

Abstract

Pseudomonas syringae is one of the most common and abundant plant pathogens, it invades damaged tissues and produces toxins that kill the surrounding cells, allowing for the bacteria for multiply further. *P. syringae* has many pathovars, which are bacterial subspecies strains with similar characteristics but different pathogenicity and host specificity. Plants affected by *P. syringae* can develop blight, cankers, discolouration, and dead dormant buds. All of these symptoms make plants more susceptible to harsh abiotic and biotic stress, such as extreme weather, moisture extremes, insects and additional pathogens. Plant pathogens are a world-wide issue as they affect crop health and therefore yield of economically important crops. This project aims to establish high-throughput methodology for the identification of bacterial cell wall polysaccharides, exopolysaccharides and exoenzymes, which can be utilised as a biomarker for identification of *Pseudomonas syringae* pathovars. Initial experiments indicated that thin layer chromatography (TLC) is not an appropriate method for a large-scale study, due to complex sample preparation and limited success with obtaining viable fractions for poly- and monosaccharide identification. Comprehensive microarray polymer profiling (CoMPP) is a high-throughput method most commonly used for polymer profiling in plants, therefore was a candidate of interest for exploring viability of this methodology when applied to bacterial samples. Due to lack of P. syringae monoclonal antibodies findings were limited when bacterial material was analysed using CoMPP.

CoMPP was used at a platform for developing epitope depletion methodology for bacterial supernatant, where enzymatic activity was identified. This methodology was applied further on plant material and immunofluorescent microscopy, where enzyme containing bacterial supernatants visibly depleted relevant epitopes in plant structures, such as root hair cells. *P. syringae* forms biofilms which is aids in surface adhesion and therefore host infection. Alginate, which is a main component of bacterial biofilms was identified using CoMPP at different monoclonal antibody binding patterns, indicating potential for alginate to be utilised as biomarker for pathovar identification. Together, these approaches have the potential to uncover novel enzymes and be developed further into a tool for pathovar identification.

1.General Introduction

Abstract

Agricultural industry has been battling many issues that affect the crop yield and quality, in order to tackle world hunger. Crop yield is affected by soil fertility, availability of water, climate, diseases, and pests. *Pseudomonas syringae,* a key pathogen, has been studied extensively due to the fact it has many closely related strains (pathovars), that have different host specificities. This plant pathogen causes plant blight, cankers, discolouration, and dead dormant buds, these symptoms have a severe effect on plant health, and therefore crop yield. This group of plant pathogens has also been found to produce biofilm, that aids in infection and proliferation of bacteria. Biofilm build up can occur on machinery and medical instruments, linking bacterial biofilms as a causal agent of up to 80 % of bacterial infections in America. The main methodology for differentiating between *P. syringae* pathovars is genomics, however due to its lengthy process and high cost, an alternative methodology must be considered.

Microarray robot is a versatile instrument that prints molecules onto nitrocellulose membrane through non-contact printing, allowing for further analysis of the molecules in a high-throughput fashion. By utilising comprehensive microarray polymer profiling (CoMPP), thin layer chromatography (TLC), utilising polysaccharides present in the bacterial cell wall as biomarkers was explored. Further studies were carried out in order to establish a methodology for utilising the microarray printer as a novel enzyme discovery platform. By printing a selection of defined polysaccharide standards, and incubating them with crude microbial broths, it was possible to explore enzymatic activity produced by plant pathogens of interest, *P. syringae*. Same methodology was applied to plant samples, and with using fluorescent probes, it was possible to visualise the effect of enzymes on specific polysaccharides within plant tissue. Use of microarray technology as a means of detection and monitoring of alginate containing biofilms was explored.

1.1 Microorganisms

Bacteria are thought to be the first organisms to appear on earth, estimated to be roughly 3.5 billion years ago. They are single celled organisms that usually exist in communities of millions. They serve a variety of functions in ecosystems, many of them survive on organic compounds, and some have evolved to survive in extreme conditions, such as extreme pH and temperatures (Fredrickson et al., 2004). Bacteria can also live in symbiotic and parasitic relationships with their hosts, which can be plants, insects and animals including humans. Most of these bacteria have not been characterised, partly due to the complex environments that they can be found in. It is estimated that only 27 % of bacteria can be grown in the lab, where it can be studied in more detail (Dudek et al., 2017).

Despite microorganisms being able to be cultured in the laboratory, conditions from their original environment and/or host cannot be replicated perfectly in the lab. The microorganism's physiology and regulatory mechanisms will be different than what may be observed in Nature (Palková, 2004). Microorganisms in their natural setting are able to modify their responses according to the nutrient supply, such as decreasing their metabolic rate and survive using scarce and rare nutrient sources, sometimes even their own waste products, such as ammonia (Palková and Váchová, 2003). Such a complex environment is nearly impossible to recreate in laboratory settings, which is further supported by difficulty of growing bacterial biofilms in artificial setting. Multicellular communities of bacteria and yeasts produce biofilms in order to attach to solid surfaces in liquid environment (Ghigo, 2003).

Often microorganisms grown in laboratory setting are considered to be "domesticated". This can be observed when comparing freshly isolated microorganisms and those that have been grown in laboratory conditions long term. The changes are most likely caused by accumulation of mutations that lead to selection of strains that thrive in laboratory settings. This example is best supported by wild yeast, which in nature can grow fluffy colonies, but in lab settings the colonies tend to be flat and shiny (Kuthan et al., 2003).

1.2 Agricultural importance

There is a high demand for optimising and increasing crop yield, due to a growing world population and environmental stressors. It is estimated that plant pests and diseases have the potential to deprive the world's population of up to 82 % of cotton, and up to 50 % of other major crops. Rice losses noted between 2001 and 2003 reached a 37.4 %, where 10.8 % was due to pathogens and rest was due to pests, viruses, and weeds (Oerke, 2005). It is estimated that globally 10-16 % of plant harvest is lost to plant diseases, and this is estimated to be worth US$220 billion (Strange and Scott, 2005).

A lot of research currently undertaken focuses on various aspects affecting crop production in different countries. There are many biotic and abiotic factors that affect growth efficiency of agriculturally and economically important plants. Areas of interest include genetically modifying plants, crop rotation, use of fertilisers, pesticide, and insecticide, and use of bioinoculants. A key research area is bacterial-plant interactions, which span from looking at bacteria in the soil, and how that can affect crop yield, as well as plant pathogens that can be detrimental to the crop once they infect the plant. By better understanding plant-bacterial interactions, it may be possible to find less energy intensive practices, which can be utilised to increase crop yield. This is of importance as bacteria is responsible for a plethora of devastating diseases in plant fields and cause issues with plant derived product storage, as of yet there is no adequate control in place to combat them. Use of chemical treatments to combat bacteria is very costly and can still be inefficient, while contributing to bacterial colonies developing resistance to those chemicals. Bacteria are highly associated with plants as many of them have symbiotic relationships with them, best example of this would be rhizobia (Van Der Heijden et al., 2006), which are considered to play a key role in ecosystems due to their nitrogen fixing ability. The chemicals used to treat plants are depleting associated bacteria, the parasitic and symbiotics ones alike.

Microorganisms such as bacteria and fungi evolved before plants, and the evolutionary relationships and interactions between the microbes and plants have developed over millions of years. Bacteria are thought to have been prevalent in aerial and subterranean plant organs, despite there being no geologic records to prove those interactions existing so early in evolution. In spite of various openings on the plant surface area, such as stomata, hydathodes

and lenticles, and wounds on the plant surface which can be caused by insects, abrasive elements carried by the winds or agricultural practices, it is often difficult for a bacterium that has entered the plant, to multiply and colonise it. Living plants can inhibit the growth of bacteria that has gained access to intercellular spaces within the leaf, or lumen of xylem vessels, they do so by producing antimicrobial chemicals, proteins or enzymes that can fight the pathogen (Hammerschmidt and Schultz, 1996).

The main parasitic bacterial sub-groups are considered to be extracellular and intracellular. In mammals, extracellular pathogens can resist or inhibit phagocytosis, promoting virulence. Whereas intracellular pathogens have adapted to exploit being ingested by phagocytes to colonise the host (Mitchell, Chen and Portnoy, 2016).

Most common phytopathogenic bacteria are extracellular parasites and their virulence is assumed to come from their ability to prevent attachment to the hosts' cell walls. For example, rhizobia are able to penetrate plant cell, and *Agrobacterium tumefaciens* can transfer part of their genome into the plant cell. Although rhizobia are considered to be symbiotic, there are strains of *Rhizobium japonicum* that produce toxins that inhibit plant growth. It is hard to find a clear distinction between symbiosis and parasitism (Sequeira, 1984).

1.3 Plant Pathogens

Correct identification of plant pathogens is crucial, as it determines the control measures needed to be taken to prevent the spread of the disease. Many plant health issues can be due to environmental factors such as nutrients lacking in the soil, over or underwatering and temperatures. The first steps of investigation are looking for signs of biotic causal agents, such as insects or microorganisms (Riley, Williamson and Maloy, 2002). Signs of a fungal infection include leaf rust, stem rust, sclerotinia (white mould) and powdery mildew, with symptoms being birds-eye spot on berries, damping off of seedlings, lead spot and chlorosis (Figure 1.1). Signs of bacterial infection include oozing, water-soaked lesions and streaming in water from a cut stem which can present as a variety of symptoms, such as leaf spots with yellow halo, fruit spot, cankers, crown gall and shepherd's crook stem ends on woody plants (Figure 1.2) (Isleib, 2012).

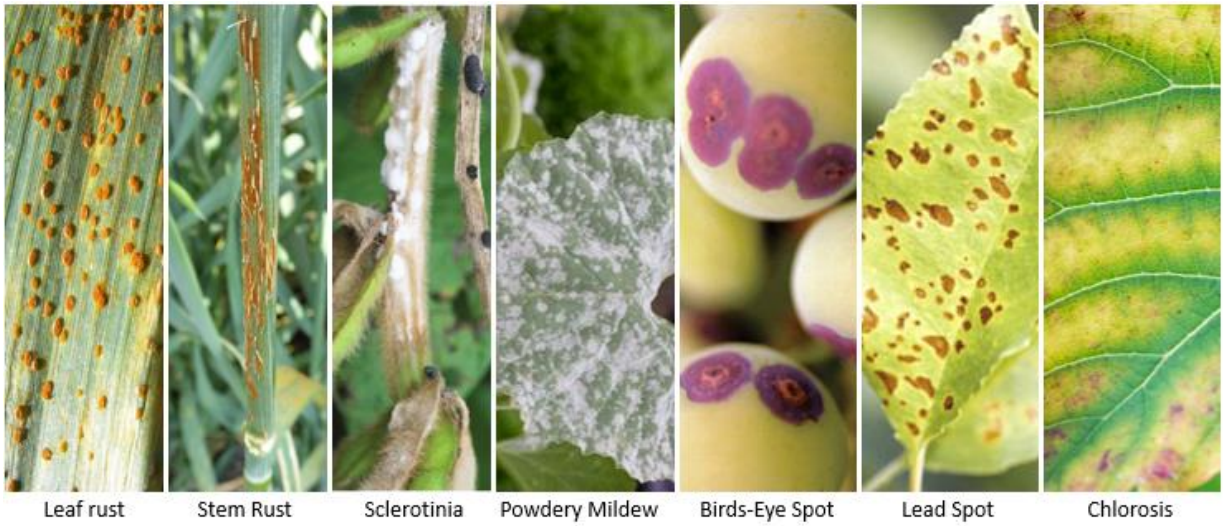

Figure 1.1. Signs of fungal disease in plants.
Photo credit for: leaf rust (Rust, 2022), stem rust (Stem Rust of Wheat, 2022), sclerotinia (Peltier et al., 2012), powdery mildew (Powdery Mildew Treatment & Prevention (A How-To Guide) - Garden Design, 2022), birds-eye spot (Anthracnose, 2022), lead spot (Rainy spring weather may lead to more leaf spot pathogens in the nursery, 2022) and chlorosis (How to Spot, Treat and Prevent Chlorosis, 2022).

Figure 1.2. Signs of bacterial disease in plants.
Photo credit for: bacterial ooze (Thomas et al., 2016), blight spots (Holcus Leaf Spot of Corn, 2022), Bacterial Halo (Nelson, 2007), fruit spots (How to get rid of Passionfruit Spots, 2021), cankers (Bacterial canker, 2022), crown gall (Ellis, 2016) and shepherd's crook (Cleveland, 2019).

In an effort to prevent infection and combat these pathogens, plants produce cysteine-rich antimicrobial peptides (AMPs), that are composed of 45 to 54 amino acids (Veronese et al., 2003). They are capable of inhibiting the growth of many fungi and bacteria at micromolar concentrations. They are non-toxic to both mammalian and plant cells (Castro and Fontes, 2005). Despite this immune response, plants are still at risk of infection from fungi and bacteria.

Bacterial pathogens are also responsible for substantial crop yield losses. Bacteria attack the host in various ways, such as a complex mixture of degrading enzymes, and manipulation of plant defences. There are many well studied bacteria that cause substantial yield losses, such as *Erwinia carotovora* and its subspecies *atrospeticia* and *carotovora*. These bacteria are well known and well-studied producers of plant cell wall degrading enzymes, that are associated with causing soft rot (Toth, Bell, Holeva and Birch, 2002). Another pathogen of key importance is *Pseudomonas syringae* and its many pathovars. *P.syringae* infects plants by injecting effectors into the plant via the type 3 secretion system (T3SS), these effectors then suppress or manipulate the host defences, allowing the bacterial population to grow. With sufficient bacterial growth, the plant will start exhibiting disease symptoms (Alfano and Collmer, 2004).

Initially the scientific community put the *E.carotovora* and *P.syringae* in different categories when it came to their mode of infection, which are thought to be vastly different. Recent studies have shown that the genes that encode for the plant cell wall degrading enzymes in *E.carotovora* have also been identified in *P.syringae* (Toth and Birch, 2005).

1.4 Use of Pesticides

It is estimated that at least 10-20 % of total world food production is lost to plant diseases and range of chemicals have been used, especially since the 1960s for controlling agricultural pathogens and pests. However the overuse of agrichemicals has led to serious ecological issues and there is growing appreciation of the value of beneficial microbes, such as nitrogen fixing bacteria (Ritika and Utpal, 2014).

There are multiple health and environmental issues associated with pesticides. Use of pesticides have been linked with a decline in amphibian populations (Hayes et al., 2006), bird population decline (Goulson, 2014) , toxicity to humans (Public health impact of pesticides used in agriculture, 1990), and a depressive effect on soil microbial communities (Lo, 2010). Residues of these pesticides can accumulate overtime in soil and water, and they can be found in everyday foods and beverages (McGill and Robinson, 1968), though the concentrations of these pesticides do not exceed legislatively determined safe levels (Chourasiya, Khillare and Jyethi, 2014).

Further study of plant pathogen plant cell wall degrading enzymes may offer more solutions on preventing pathogens from infecting and colonising crops. DFMO (DL-alpha-Difluoromethylornithine) is an inhibitor of polyamine biosynthetic enzymes ornithine decarboxylase, which significantly slows down the growth of many phytopathogenic fungi (Rajam, Weinstein and Galston, 1985). The current use of pesticides, and the negative effects they have on many aspects of the environment, highlight the need for novel agricultural practices, and a drastic reduction in use of pesticides. Further investigation into microorganisms' enzymes may provide more alternatives for pest control in agriculture and food industry.

1.5 Polysaccharides

Polysaccharides are the most abundant biological polymer, and the most abundant organic material on earth (Teegarden, 2004). They comprise chains of monosaccharides, which are bound by glycosidic bonds. Monosaccharides such as glucose, fructose and glyceraldehyde follow a general formula of $(CH_2O)_n$, with n being 3 or higher. Oligosaccharides vary between 3 and 10 monosaccharides, whereas polysaccharides usually consist of 10 or more monosaccharide units, following a $C_x(H_2O)_y$ formula, where x is usually a large number between 200 and 2500 (Mathews, Holde and Ahern, 2000). Polysaccharides may be branched and also decorated with a number of substitutions such as acetyl and methyl groups, sulphate (in marine ecosystems) and ferulate (Reem et al., 2016).

Polysaccharides play vital roles in all living organisms, they usually fall into two broad categories; storage and structural. Starch, a plant storage polysaccharide is composed of two glucose-based polymers, amylopectin, and amylose (Brust, Orzechowski and Fettke, 2020). Mammals utilise a different polysaccharide for storage, glycogen, made up of amylopectin and amylose, just like starch. Starch and glycogen both have α-1,4-glycosidic linkages, with branch points introduced by α-1,6-glycosidic linkages. The key difference between the two is structural, glycogen has minimal branching, whereas starch's major constituent, amylopectin, has nonuniform branching (Roach and Zeeman, 2016).

There are several structural polysaccharides, such as cellulose, xylans, arabinoxylans, cellulose, mannans, mixed linkage glucans chitin and pectins. Arabinoxylan has two major constituents, arabinose, and xylan. Arabinoxylan is found in primary and secondary cell walls of plants, and has been found to be a main component of dietary fiber, therefore playing a key role in human health (Mendis and Simsek, 2014). Cellulose is a primary component of primary cell wall of viridiplantae (green plants) (De Clerck, Bogaert and Leliaert, 2012) and is the most abundant organic biopolymer on earth (Klemm, Heublein, Fink and Bohn, 2005). It consists of hundreds of β(1→4) linked D-glucose units, arranged in a straight chain, unlike starch, which coils and branches.

Pectin is abundant in the cell wall of non-graminaceous plants and fruits, where it plays a key role in cell adhesion and separation (Daher and Braybrook, 2015), and modulates cell growth and shape (Yang and Anderson, 2020). Pectin is one of the most structurally complex polysaccharides, as it is made up of homogalacturonan, rhamnogalacturonan-I, rhamnogalacturonan-II, arabinogalacturonan, and xylogalacturonan regions (Ropartz and Ralet, 2020).

Chitin is a biopolymer produced by fungi, arthropods, and some fish and lissamphibians (Tang, Fernandez, Sohn and Amemiya, 2015), making it the second most abundant polysaccharide in nature after cellulose.

Bacteria and other microbes produce a variety of exopolysaccharides that play a role in cell protection, cell adhesion and cell to cell interactions (Nicolaus, Kambourova and Oner, 2010),such as xanthan, dextran, levan and pullulan (Ates, 2015). Lipopolysaccharides are molecules made up of O-antigen, a lipid, and a polysaccharide. They are a major component of outer membrane of gram-negative bacteria (Rietschel et al., 1994).

The complexity and abundance of polysaccharides has made them a promising choice as a biomarker. They are utilised in medicine as biomarkers for cancers (Adamczyk, Tharmalingam and Rudd, 2012), and other diseases. The have also been used as carrier for bioactive agents, for targeted therapeutics and diagnostic applications (Mukwaya, Wang and Dou, 2018).

Polysaccharides are versatile and diverse molecules that need have applications in food industry, pharmaceuticals, biofuels, cosmetics, and many others. They have been a key area of research for decades, with much still left to uncover.

1.6 Bacterial Cell Walls

The bacterial cell wall is a complex structure, comprising of many components. It has been a key area of study for decades due to its complexity and the vital role of bacteria in many areas of interest, such as antibiotic resistance and biofilm formation. Bacterial cell walls are essential to the survival of bacteria, as they provide structure, protection, signalling and adhesion (Van Meer, Voelker and Feigenson, 2008). Unlike bacteria, plant cell walls have an elaborate extracellular matrix that encloses each cell in a plant. The plants' thick cell walls allow for withstanding harsh weather conditions, and was an adaptation to sedentary lifestyle, whereas bacterial and prokaryotic cells thrive due to their ability to remain mobile.

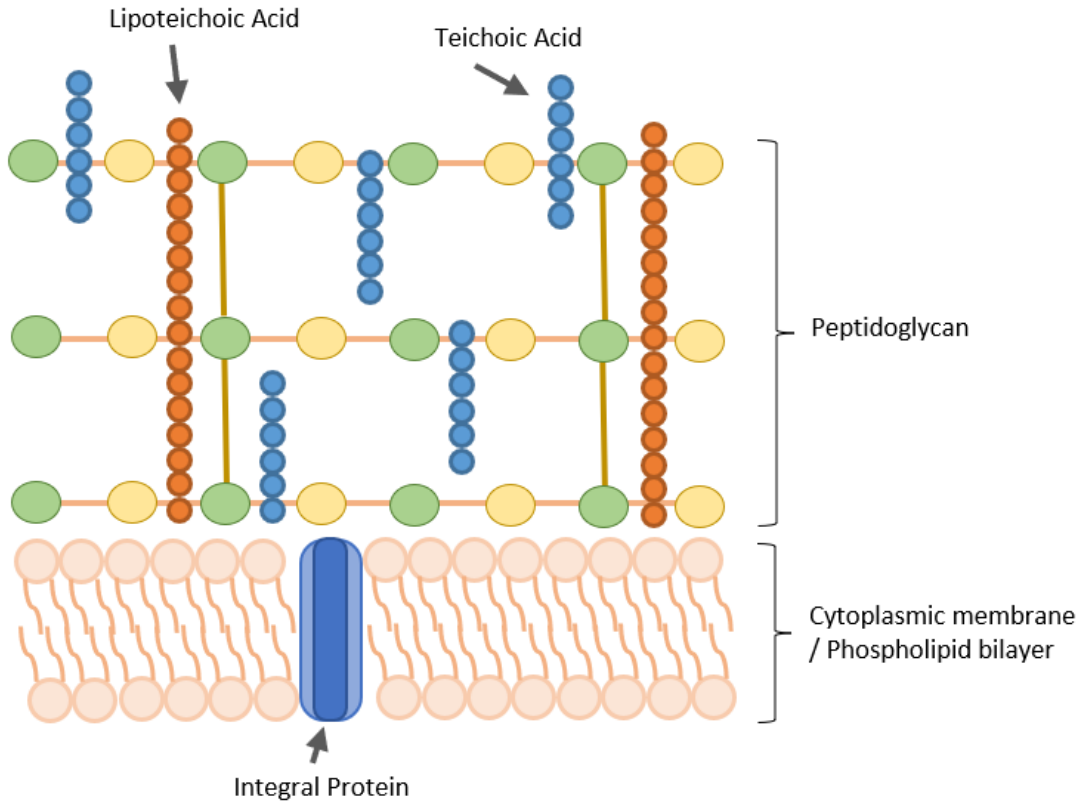

Figure 1.3. Structure of gram-positive bacterial cell wall and its' main components.

The main and most abundant component within the bacterial cell wall, is peptidoglycan. It is a mesh-like structure of polysaccharides, containing poly-[N-acetylglucosamine (GlcNAc)-N-acetylmuramic acid (MurNAc)] backbone) cross-linked via short peptide bridges attached to the MurNAc residues (Vollmer, Blanot and De Pedro, 2008). Peptidoglycan serves a mainly a structural role, as it provides strength to the bacterial cell wall, but it also counteracts the osmotic pressure that is applied by the cytoplasm.

Research has shown that peptidoglycans are significantly thicker in gram-positive bacteria where its thickness can vary anywhere between 30 to 100 nanometers and comprises of many layers, whereas in gram-negative bacteria is estimated to be under 10 nanometers thick, comprising of one or a handful of layers (Silhavy, Kahne and Walker, 2010). When investigating the dry weight of peptidoglycan within the bacterial cell wall, in gram-positive bacteria is can make-up up to 20-25 %, whereas in gram negative bacteria it is only around ~10 % (Esko, Doering and Raetz, 2009).

The bacterial cytoplasmic membrane is composed of roughly equal proportions of lipids and proteins. The main lipid components are phospholipids, which vary in acyl chain length, saturation, and branching and carry head groups that vary in size and charge. Phospholipid variants determine membrane properties such as fluidity and charge that in turn modulate interactions with membrane-associated proteins (Strahl and Errington, 2017).

In gram positive bacteria, the peptidoglycan mesh contains secondary cell wall polymers, these include teichoic acids and lipoteichoic acid. These polymers are covalently bonded to the peptidoglycan (Rajagopal and Walker, 2015).

Lipoteichoic (LTA) acid plays a key role in bacteriolysis. It is a surface-associated adhesion amphiphile from Gram-positive bacteria and regulator of autolytic wall enzymes. LTA is released from the bacterial cells after bacteriolysis induced is by lysozyme, cationic peptides from leucocytes, or beta-lactam antibiotics (Ginsburg, 2002) .

An integral protein membrane (IMP) is a protein that is permanently attached to the biological membrane. These integral membrane proteins have two types, α-helical and β-barrel. The α-helical IMP is more abundant and is often found in cytoplasmic membranes, whereas β-barrel are found in outer membranes of bacteria (Schulz, 2002). The most common type of IMP is a transmembrane protein, which act as pumps that transfer substances which are vital to the organism's survival (Williams and Fraústo da Silva, 2006).

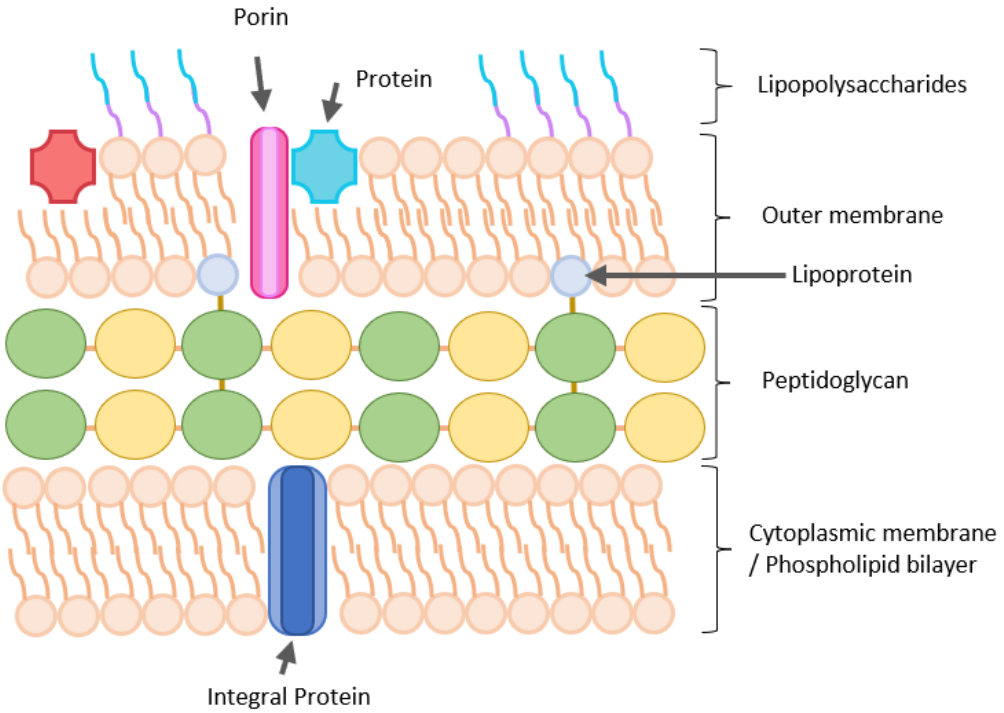

Figure 1.4. Structure of gram-negative bacterial cell wall and its' main components.

Porins, which are specific to gram negative bacteria, are the proteins present on the outer membrane of the cell wall. Porins act as pores and channels, passively transporting hydrophilic molecules across the membrane. Porins can be further divided into 2 main types, general and selective. General porins do not have a substrate specificity, but they do show a preference to anions and cations (Novikova and Solovyeva, 2009). Selective porins are smaller and have substrate specificities, they are determined by the size of the porin and amino acids present (Galdiero et al., 2012).

Lipopolysaccharides, consist of a hydrophilic polysaccharide and a hydrophobic lipid A. Lipid A is responsible for majority of bioactivity related to the endotoxin. These lipopolysaccharides are recognised by the immune cells of the host, via pathogen associated molecule through toll-like receptors (Wang and Quinn, 2010).

Bacterial lipoproteins are hydrophilic proteins, they are anchored to the cell membrane by N-terminally linked fatty acids. Majority of lipoproteins are held in the inner membrane or transferred to the inner leaflet of the outer membrane (Figure 1.4). There have been reports of lipoproteins report on the surface of the cells but are considered to be rare (Wilson and Bernstein, 2016). They have been shown to play key roles in nutrient uptake, signal transduction, adhesion, conjugation, and sporulation (Kovacs-Simon, Titball and Michell, 2011).

1.6.1 Type 3 secretion system and *Pseudomonas syringae* Pathovars

Many bacterial pathogens use the type 3 secretion system (T3SS) to inject protein effectors into the host cell, these proteins cause the symptoms of a disease as they disrupt the hosts' normal cellular activities. When looking at the example of *Pseudomonas syringae* pv. tomato, there are more than 20 effectors that this bacterium injects into the host plant, these effectors need combined activity to successfully infect the host and enable growth of the pathogen. This bacterium is also known to produce a AvrPto protein, which mimics a substrate of a highly conserved plant kinase, the kinase activity enhances the virulence (Anderson et al., 2006). Groups of kinases are responsible for control of essential processes in bacteria, necessary for their survival. In most pathogens, penicillin-binding-protein and serine-threonine kinase-associated (PASTA) domains have been associated with regulating biofilms, antibiotic resistance and virulence, due to their ability to regulate bacteria physiology under stress (Pensinger, Schaenzer and Sauer, 2018).

The plant innate immune system is comprised mostly from extracellular pattern recognition and nucleotide binding leucine-rich repeat (NLR) proteins. These proteins recognise bacterial effectors present in the host cells, such as type 3 secretion system. Pathogen-Associated Molecular Patterns (PAMPs) are surface localised and can recognise bacterial flagellin, which in turn triggers pattern recognition immunity. There are other surface based receptors, Damage-Associated Molecular Patterns (DAMPs), which are triggered as a result of wounding, eliciting a similar response. There is also an effector-triggered immunity (ETI), which is utilised to recognise bacterial effectors intracellularly. Due to these mechanisms working together, even when a bacterium can enter the plant through a lesion or an opening, it struggles with colonising the plant (Henry, Yadeta and Coaker, 2013). The plants also have gene for gene interaction, where the plant resistance protein recognises the pathogens Avr avirulent protein. This interaction causes an immune response within the plant that results in cell wall thickening, upregulation of gene expression and hypersensitive response, which causes localised cell death. ((Martin et al., 2003), (Anderson et al., 2006))

Plant diseases are caused by fungi and bacteria, *Ralstonia (Pseduomonas) solanacearum* can cause diseases in more than 200 host species, where 50 of them belong to the potato family. Other hosts include bananas, tomatoes, eggplant, peppers, geraniums, ginger and mulberries (Strange and Scott, 2005). Variety of *Pseudomonas* species has been the perpetrator of blight

across various plants, as well as other diseases. *Pseudomonas syringae* is responsible for a loss of crop damage worldwide, as it has more than 60 pathovars, each with distinct host ranges. This complex group relies on a range of type 3 effectors (T3E) to successfully infect varieties of host plants (Table 1.) (Block and Alfano, 2011).

Table 1.1. Activity, plant targets and localisation in planta of type 3 effectors (T3E) of *Pseudomonas* complex pathovars (Block and Alfano, 2011).

T3E	Pathovar	Activity	Target(s)	Subcellular Localization
AvrB	*Glycinea* Race 0	Unknown	RIN4/RAR1/MPK4	Plasma membrane
AvrPphB	*Phaseolicola* Race3	Cysteine protease	PBS1/BIK1/PBLs	Plasma membrane
AvrPto	*Tomato* JL1065	Kinase inhibitor	Pto/Fen/PAMP RLKs/BAK1	Plasma membrane
AvrPtoB	*Tomato* DC3000	E3 ubiquitin ligase	Pto/Fen/PAMP RLKs/BAK1	Non-discrete
AvrRpm1	*Maculicola* M6	Unknown	RIN4	Plasma membrane
AvrRpt2	*Tomato* Jl1065	Cysteine protease	RIN4	Non-discrete
HopAI1	*Tomato* DC3000	Phosphothreonine lyase	MPK3/MPK6 and other MPKs	Unknown
HopAO1	*Tomato* Dc3000	Protein tyrosine phosphatase	Unknown	Non-discrete
HopI1	*Maculicola* Es4326	J domain protein	Hsp70	Chloroplast
HopF2	*Tomato* Dc3000	Mono-ADP-ribosyltransferase	RIN4/MKK5	Plasma membrane
HopG1	*Tomato* Dc3000	Unknown	Unknown	Mitochondria
HopM1	Tomato Dc3000	Unknown	MIN7 and others	Endomembrane
HopU1	Tomato Dc3000	Mono-ADP-ribosyltransferase	GRP7 and other RNA-binding proteins	Non-discrete
HopZ1	Syringae A2	Cysteine protease/ Acetyltransferase	Unknown	Plasma membrane
HopZ2	Pisi 895A	Cysteine protease/ Acetyltransferase	Unknown	Plasma membrane
HopZ3	Syringae b728a	Cysteine protease/ Acetyltransferase	Unknown	Non-discrete

P. syringae pv. *syringae* has the biggest host range among all the pathovars in this complex, however it mostly affects woody and herbaceous plants.

P. syringae pathovars have been a controversial topic from a taxonomic point of view as currently there are over 15 bacterial species that fall under the complex and 60 pathovars. The classification of these pathovar groups is based on host range and pathogenicity. There have been many genomic studies, some based on DNA-DNa hybridisation, allowing to classify the pathovars further into 9 genomospecies. This approach has been widely accepted until recently, where further multilocus sequence typing analysis (MLST) analysis has been carried out, and a new classification was proposed. Until recently the classification proposed by Berge et al. 2014 has been widely accepted, until a recent study using comparative genomics has shown delineation of *P. syringae* complex. The results that indicated that a large proportion of these bacteria have been misclassified (Gomila et al., 2017)

These pathovars have been isolated from different sources, plants, snow and irrigation water. Despite being isolated from different environments that have been identified to belong to the same evolutionary lineage (Monteil et al., 2016). This has pointed towards the pathogen evolution being linked to water cycles, related to colonisation of agricultural and non-agricultural surroundings (Morris et al., 2008).

P. syringae complex has proven to be an interesting subject to study, due to its wide host range, numerous pathovars. These pathovars are suspected of having different effectors, toxic compounds, exopolysaccharides, cell wall degrading enzymes and ice nucleation (Xin, Kvitko and He, 2018, Gutiérrez-Barranquero, Cazorla and de Vicente, 2019).

1.6.2 Identifying Pathovars

The *Pseudomonas syringae* complex offers an interesting set of effectors and cell wall degrading enzymes. It is still unknown what underpins the host specificity of each pathovar. Despite many DNA based studies, there is only a few pathovars that have been studied in depth. *Pseudomonas syringae* pv. Tomato (DC3000) and tomato, which is the host plant, have been used to study the plant-bacterial interaction, however that data cannot be applied to the rest of the pathovars. DC3000 has been fully sequenced, however sequences for most of the pathovars are not available. This impacts the starting point of most experiments, as proteins of interests are inferred from homology of DC3000. This may cause a lot of research to be unsuccessful as specific activities or sequences may not present in the genome of a specific pathovar. The experiments required to understand simple processes take months and are very costly. There are singular experiments focusing on specific enzymes across various pathovars. The toxin found in *Pseudomonas syringae* pv. *Tabaci*, tabxoin, is responsible for wildfire disease across tobacco plants. Exploring a pathway, which has enzymes responsible for formation of this toxin requires many techniques and significant resources. A study done by M. E. Manning et al. (2018) had to make use of DNA extraction kit to clone relevant genes. The clones were then overexpressed, in a specific medium. Once colonies showing the expression on IPTG medium were selected, they could be grown up on a larger scale where the protein could be isolated and purified. Protein isolation and purification required a french press, resins, and various buffers. Once the proteins were isolated, further assays were performed to ensure the specific genes were responsible for formation of active enzyme complexes (Manning, Danson and Calderone, 2018). Exploring enzyme activities across 60 pathovars and various metabolic pathway using these methods is not feasible, due to time limitations and resource limitations that most researchers have to comply with.

So far screening for enzymes has been a challenging and long process. Often based on knowledge already present from the bacteria's natural environment or host. Most processes which require enzymes, such as juice production that use pectinases (Magro et al., 1994) and xylanases, have been discovered and established decades ago (Raveendran et al., 2018). A mix of pectolytic enzymes is utilised in fruit juice production. Pectin which can be found in the middle lamella of plant tissue is degraded by protopectinase, pectin methylesterase, pectin lyase and polygalacturonase. Using this mix of enzymes allowed for viscous polymers to be

fully dissolved, which in turn improves product yield and clarity of the juice (Nighojkar, Patidar and Nighojkar, 2019).

There are resources like the CAZy, a database of Carbohydrate-Active enzymes which can be utilised to view carbohydrate active enzymes; however, these are often inferred from homology a closely related organism, or pathovar. A lot of research has been done trying to uncover one or two novel enzymes, or to confirm their presence and/or activity. It is not common for enzymes to be researched in groups beyond specific individual metabolic pathways, however due to new technologies these ideas can be explored.

Due to agricultural pressure, many laboratories are pursuing a fast routine method for pathogen identification, which offers sensitive and accurate detection. Plants are often infected by various and multiple pathogens; therefore, the assay has to offer multiplex screening for multiple pathogens. Currently DNA array technology is the most suiTable, due to its ability to screen a large sample set for multiple DNA sequences of interest (Lievens and Thomma, 2005). However, when screening for *Pseudomonas syringae* pathovars which have such similar DNA sequences, non-specific primer binding may occur, resulting in an unreliable data set (Ruiz-Villalba et al., 2017).

1.7 Microarray robots as high throughput screening tools

Microarray robots were first developed for DNA analysis but have since found a wide range of other uses (Lemuth and Rupp, 2015). Microarray robots can print small quantities of liquid onto a desired medium, a nitrocellulose membrane or glass via non-contact printing. Liquid which can be loaded into the machine and printed is mixed with a buffer to provide a suiTable molecular environment and printing conditions. The range of samples that can be printed is wide, it can vary from proteins to sticky and viscous polysaccharides. Once printed, these small amounts of liquid can be interacted with, using dyes, antibodies, and enzyme treatments to name a few. By printing polysaccharides, which can be extracted from specific plants, or purchased standards, the arrays, that can have as many as 100 different polysaccharides on 1 array, can be treated with enzymes to investigate enzymatic activity against these polysaccharides. The change caused by the enzyme can be detected by using monoclonal antibodies. These antibodies can bring to specific structures, in this case polysaccharides. Changes in molecular probe binding can be detected, and enzymatic activity can be inferred

(Uttamchandani and Moochhala, 2010). This technology can be applied to research cell wall degrading enzymes of *Pseudomonas syringae* complex and its many pathovars.

The same concept can be applied to immunofluorescent microscopy. Plant sections can be treated with enzyme treatments and immunolabelled antibodies can be used to visualise and quantify what effect a specific enzyme or group of enzyme has on specific plant structures. Other studies have been carried out, where plant sections were treated with a known enzyme in order to characterise polysaccharides in stem internodes of plants (Marcus et al., 2008).

1.8 Molecular Probes

Molecular probes are tools used to study the properties, or interact with molecules of interest. There is a variety of probes which are utilised in different areas of science, such as DAPI (4'-6-diamidino-2-phenylindole) which penetrated bacterial cell wall and binds to dsDNA (Paczesny and Mierzejewski, 2021), fluorescent dyes which can be conjugated to other molecules (Brinsko et al., 2011), often specific sequences of DNA and RNA are used to detect and identify an organism within samples (Hill, 2009).

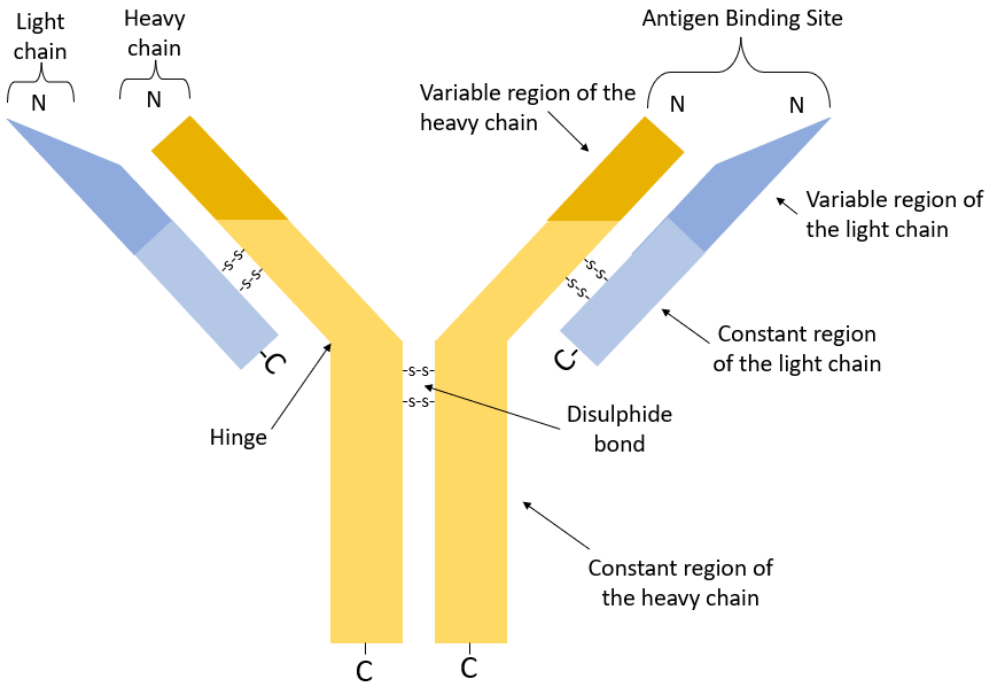

Figure 1.5. Diagram showing the structure of an antibody, made up of two chain types – light and heavy chains. Antibodies contain variable and constant regions, with N and C terminals. The chains are bound together by sulphide bonds.

Monoclonal antibodies (mAbs) are often used as molecular probes due to their properties. The main function of antibodies within the human body is to bind foreign molecules and in most cases, label them for elimination. An antibody is a Y shaped molecule, it consists of four polypeptide chains, two heavy chains and two light chains. These molecules are secreted from B-cells, they are nearly identical to receptors on the B-cell, apart from a small region of the C-terminus of the heavy chain constant region. Antibodies have a hydrophilic sequence, allowing them to be soluble, and since they are secreted in large quantities, they are the often utilised as molecular probes. There are five different isotypes of antibodies, determined by the heavy chain – IgM, IgD, IgG, IgA and IgE (Janeway, Travers, Walport and Schlomchik, 2001). IgG is the most abundant out of all 5 antibody types in human serum and is estimated to make up 10-20 % of plasma protein, and 75 % of serum antibodies (Vidarsson, Dekkers and Rispens, 2014).

An IgG antibody consists of two heavy and two light chains, with light chains being bound to the heavy chains with disulphide bonds. The two pairs of chains are attached and mirror each other, providing the molecule two identical antigen binding sites (N terminus). There are two varieties of the light chain lambda (λ) and kappa (κ), and an antibody will have a pair of one of these, never a mixture. Though there have not been any functional differences found between the two, the ratio of these two chains varies between different species. Heavy and light chain contribute to forming of two identical antigen binding sites by forming the V regions at the N terminals. The trunk of the Y is made up of carboxy-terminal domains of the heavy chains, where the joined arms of the trunk make flexible hinge regions. All antibody isotypes have similar organisation of domains (Janda, Bowen, Greenspan and Casadevall, 2016)

Carbohydrate antigens play a role in many biological processes. Toxins, hormones, viral receptors, and bacterial endotoxins are often carbohydrates. The mouse hybridoma method has been often used for the production of mAbs for therapeutic use and diagnostic (Köhler and Milstein, 1975). The animals are immunised with desired molecule, and due to the natural immune response, B cells are produced with relevant antigens that can be harvested from the spleen. Monoclonal antibodies show superb specificity and sensitivity towards target antigen, making them a great diagnostic tool to utilise (Siddiqui, 2010).

In order to produce desired antibodies, the animals are immunised with a target antigen, e.g., purified polysaccharide. The host's immune system produces B cells which are removed and fused with myeloma cells. These cells result in hybridoma cell lines which secrete the

antibodies (Nelson, Dhimolea and Reichert, 2010). Although the process appears simple, there are many difficulties when trying to produce antibodies against larger polysaccharides, which are far less immunogenic than proteins due to their simple structure of repeating monomers. Polysaccharides often need to be conjugated with proteins in order to elicit an immune response (Zhou et al., 2009), (Rydahl et al., 2017). Though carbohydrate specific mAbs were thought to have a low affinity and specificity, recent studies have shown the existence of high-affinity carbohydrate specific antibodies (Rollenske et al., 2018). Monoclonal antibodies generated by identical B cells which are cloned from a single parent cell, meaning they all recognise the same epitope. Polyclonal antibodies are a mixure of different B cells produces by the body, so they will bind to different epitopes of a single antigen (Lipman et al., 2005).

By utilising microarray technology, which focuses on work with small volumes, it was identified as a technique which allows for a cost reduction, when compared to standard DNA based technology. Molecular probes are highly sensitive and highly specific, and therefore are the ideal tool to use when trying to identify molecules which may be present in very low quantities, such as lipopolysaccharides within a bacterial cell wall. Microarrays can also be utilised as a novel enzyme discovery tool for extracellular enzymes with optimised methodology. Currently the main challenges of discovering novel enzymes are finding their optimal conditions and the substrate. Thus far, enzyme discovery has been using metagenomics, however it is costly and yields an active enzyme after significant work. Novel enzyme discovery platform would allow for screening of multiple crude enzyme extract against a library of 1000s of target molecules with the corresponding molecular probes. Methodology for novel enzyme screening can also be applied to immunofluorescent microscopy in-situ. With plants having complex polysaccharides structures, application of crude enzymatic broths would also allow for observing enzymatic action on target host with the use of fluorescently conjugated molecular probes. Providing additional insight into metabolic pathways involved into pathogenicity of *P. syringae*, and its pathovars. These methodologies aim to explore the potential of polysaccharides and enzymes being utilised as biomarkers for pathovar identification, and their applications beyond.

2. Optimisation of analytical techniques for detection of bacterial derived polysaccharides

Abstract

The aims of these experiments were to compare microarray and thin layer chromotography as method to identify biomarkers that can be used to distinguish between several different *Pseudomonas syringae* pathovars. The bacterial cell wall is complex and contains many molecules that can be utilised as a biomarker. Despite successful identification of 4 compounds (rhamnose, manno-oligosaccharide, fucose, and raffinose) of bacterial cell wall via TLC, it was proven to be too time consuming and not in line with high-throughput nature of this project. Comprehensive Microarray Polymer Profiling (CoMPP) was a better fit for the project, due to the high-throughput nature of the methodology. A major limiting factor for identification of biomarkers was lack of *Pseudomonas syringae* specific monoclonal antibodies.

2.1 Introduction

2.1.1 Bacterial Cell Wall

Bacterial cell wall polysaccharides, play a key role in maintaining the structure of the organism, as well as mediate the interactions between the bacteria and the environment (Sadovskaya and Guérardel, 2019). In the past it has been a key subject of research, due to its necessity for bacterial survival and the absence of it in eukaryotic domain. The cell wall is of utmost importance when researching pathogenesis and diseases (Jutras et al., 2019). The main cell wall components are a mesh of polysaccharide strands (poly-[N-acetylglucosamine (GlcNAc)-N-acetylmuramic acid (MurNAc)] backbone) cross-linked via peptide bridges attached to the MurNAc, that make up the peptidoglycan layer (Vollmer, Blanot and De Pedro, 2008), which is present in all bacteria. Peptidoglycan synthesis is a key target for antimicrobial compounds and enzymes, as invading pathogens often produce antimicrobial compounds to outcompete already present organisms (Malanovic and Lohner, 2016). *Pseudomonas syringae* is a well-studied plant pathogen, and is considered a model organism for host-microorganism interaction, as it lead to the discovery of a mechanism that allow the bacterium to colonise the host (Passera et al., 2019). Significant effort has been put into use of genomics to understanding metabolic processes and virulence factors. With use of metagenomics a lot of DNA sequences have their activity inferred from homology, which may not always be accurate. The bacterial cell wall has taken the backseat, there several of *Pseudomonas syringae* pathovars have the capacity to infect multiple hosts. The pathovars are so similar genetically (Bereswill et al., 1994), and have been split into different genomospecies. Genomospecies is a term used for species that can be differentiated using genotyping. There have not been many attempts at utilising the bacterial cell wall as a means of identification of these pathovars, due to complexity of the required work and lack of relevant molecular probes.

2.1.2 Thin Layer Chromatography

Thin layer chromatography (TLC) has been routinely used by organic chemists to characterise natural products, namely carbohydrates. Carbohydrates are highly polar molecules, which allows for them to interact with the mobile (solvent mixture) and stationary phase (silica plate), to be characterise them further depending on size of the molecule (Zhang, Xiao and Linhardt, 2009). TLC allows for qualitative and quantitative determination of mono and oligosaccharides from biological materials. When combining TLC with various fractionation techniques, it offers great insight into structures of materials being studied (Gal, 1968). This technique has been commonly used for charactering plant material, due to its simple, versatile

and inexpensive nature (Kharbade and Joshi, 1995). This made it a good technique for attempting to characterise bacterial cell wall components, that are mainly of carbohydrate origin. TLC has limited resolution capability, it cannot be automated and is only compatible with non-volatile compounds (Sherma, 2006) It is often coupled with additional analytical methods such as high-performance liquid chromatography (HPLC), mass spectrometry (MS), and Fourier transform infrared spectrometry (FTIR), as it does not provide sufficient information to infer the molecules of exact characterises.

2.1.3 Comprehensive Microarray of Polymer Profiling (CoMPP) Technology

Comprehensive microarray of polymer profiling (CoMPP) technology utilises the high-throughput capacity of microarrays, automation, and takes advantage of high specificity molecular probes, such as monoclonal antibodies (mAbs) and carbohydrate binding modules (CBMs). This technology has been previously commonly used when studying plant materials. The studies involved studying interactions between many molecules, characterising antibodies with unknown epitope specificity, quantifying relative abundance of molecules and identifying molecules present within sample (Chialva et al., 2019). Whilst DNA microarrays have been commonly used for identifying bacterial pathogens (Cao et al., 2011), use of CoMPP has not been explored. This study aims to apply CoMPP as a meant to identify key differences between *Pseudomonas syringae* pathovars, with the use of a library of mAbs probes.

Due to the recent developments in the field of automation and high-throughput methodology, the viability of microarray robot needs to be evaluated to establish if it can be used to screen for biomarkers of *P. syringae*. TLC will be used for primary analysis, to evaluate methodology for extracting glycans from the bacterial cell wall. By utilising Microarray technology coupled with TLC, is it possible to identify molecules that can be used a biomarkers for pathovar identification.

In this chapter TLC and CoMPP are explored as methods for identification of polysaccharides within the bacterial cell wall, with the hopes of utilising these polysaccharides as biomarkers for pathovar identification. This was done by applying already established techniques such as CoMPP, polysaccharide fractionation and TLC to bacterial cells.

2.2 Material and Methods

2.2.1 Media and Trace Salts Solution Preparation

Kings B media was made according to the Cold Springs Harbor protocols (King's B medium, 2009).

Trace metals solution was prepared with the following: KCl (80 mM), KNO3 (79.12 mM), $FeCl_3$ (1.2 mM), $MnCl_2$ (3.1 mM), $ZnSO_4$ (1.5 mM), H_3BO_3 (2.2 mM) and KI (4 mM) added to 1 L of diH_2O. The solution was titrated to pH 5 ± 0.2 using KOH (1 M) and HCl (1 M) and autoclaved.

Chemically defined media was prepared following methods described by Kim et al., 2009, without the addition of an antifoaming agent. Commonly used antifoaming agents are alcohols, insoluble oils and silicone derivatives (Kar, Chourasiya, Maheshwari and Tekade, 2019), they have not been added as they can affect enzymatic activity (Routledge, 2012). This media has been chosen with exploring novel enzyme activity in mind, and when working on smaller volumes, there was no need for antifoam to be present.

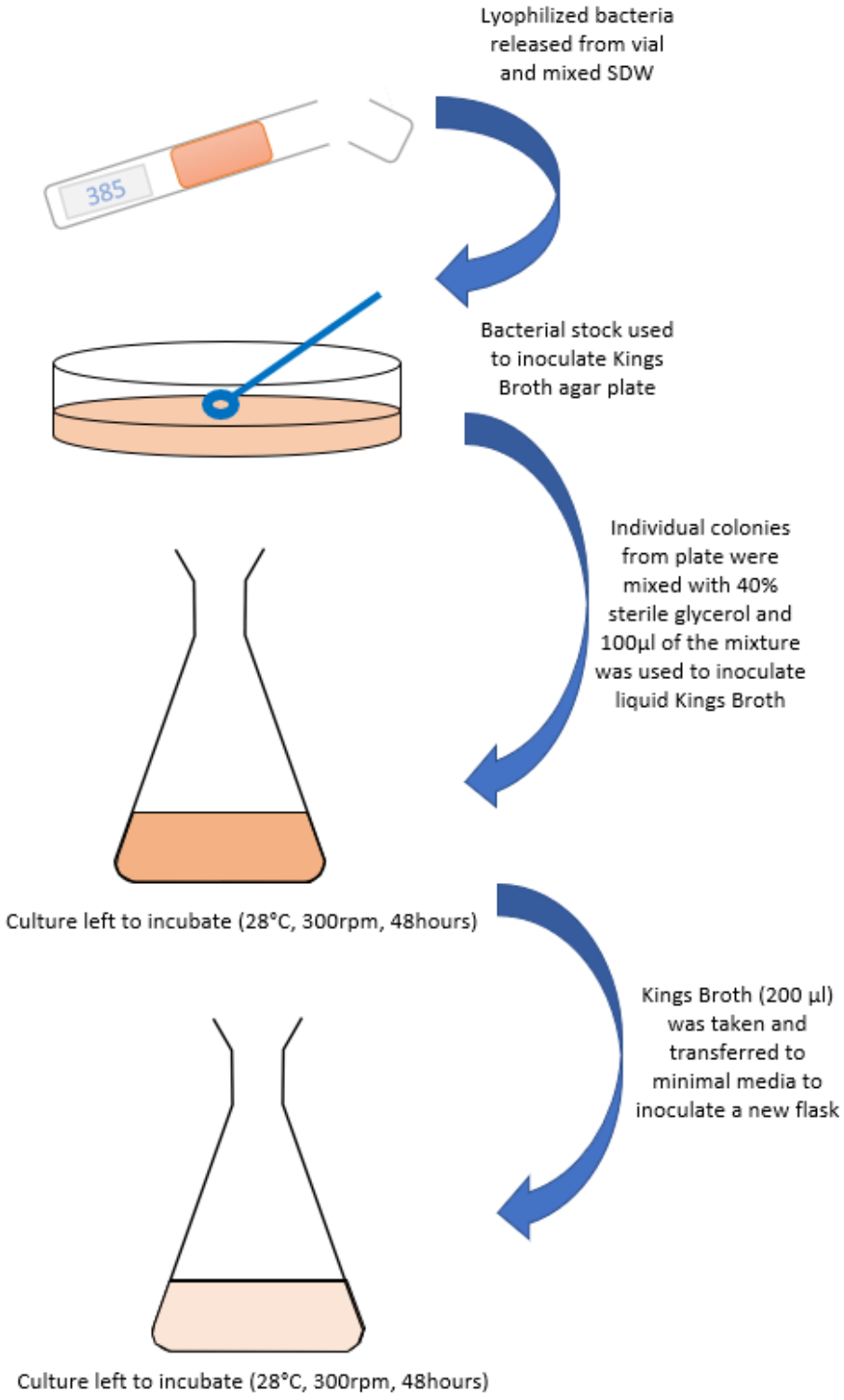

Figure 2.1. Methodoly used for initial bacterial strain creation and inoculation of various minimal media flasks.

A selection of bacterial strains (See Table 2.2. NCPPB catalogue reference number: 218, 600, 635, 639, 1437, 1873 and 2193) were purchased from the National Collection of Plant Pathogenic Bacteria (NCPPB) at Fera Science ltd, the stains arrived in glass vials containing a lyophilised culture on filter paper. The vials were opened and SDW (sterilised distilled water)

was added to resuspend cultures present on filter paper. The water was used to streak the bacteria onto king B agar plates and left to incubate (28 °C, 48 h)(Figure 2.1). Research has shown the optimal temperature for *Pseudomonas syringae* is 28 °C (Arvizu-Gómez, Hernández-Morales, Aguilar and Álvarez-Morales, 2013), with agitation of 300rpm (Kim, Schneider, Cartinhour and Shuler, 2010), though due to circumference of the flask and culture volume it was adjusted to 250rpm to ensure the flask adheres firmly onto the silicone platform of the orbital shaker.

Pseudomonas syringae pv. *Tomato* (NCPPB. 4369, DC3000) was grown in 4 different conditions, alternating glycerol concentration (0.2 % and 2 %), with and without a trace metals solution (1 mL, [x100]). Aliquots were taken and optical density (OD) readings were taken at 600 and 650 nm after 24 h of growth (Table 2.).

Table 2.1. List of bacterial pathogens used for bacterial cell wall analysis using microarray technique. Taken from NCPPB catalogue (NCPPB, 2021).

NCPPB catalogue number	**Catalogue Name**	**Name as Received**	**Host plant**
281	*Pseudomonas syringae* pv. *syringae* van Hall 1902	*Pseudomonas syringae*	*Syringa vulgaris*
600	*Pseudomonas syringae* pv. *coronafaciens* (Elliott 1920) Young, Dye & Wilkie 1978	*Pseudomonas. coronafaciens*	*Avena sativa*
635	*Pseudomonas viridiflava* (Burkholder 1930) Dowson 1939	*Pseudomonas viridiflava*	*Phaseolus sp.*
639	*Pseudomonas savastanoi* pv. *savastanoi* (ex Smith 1908) Gardan et al. 1992	*Pseudomonas savastanoi Smith 1908*	*Olea europaea*
1437	*Pseudomonas cannabina* pv. *cannabina* (ex Šutič & Dowson 1959) Gardan et al. 1999 emend. Bull et al. 2010	*Pseudomonas syringae* pv. *cannabina*	*Cannabis sativa*
1873	*Pseudomonas caricapapayae* Robbs 1956	*Pseudomonas caricapapayae* Robbs 1956	*Carica papaya*
2193	*Pseudomonas tolaasii* Paine 1919	*Pseudomonas tolaasii*	*Agaricus bisporus*
4369	*Pseudomonas syringae* pv. *tomato*	*Pseudomonas syringae* pv. *tomato*	*Lycopersicon esculentum* & *Arabidopsis thalliana*

Optimising growth conditions

Lyophilised Pseudomonas species obtained from the NCPPB collection at FERA, required growth on solid King B media initially. Even when growing the bacteria on chemically defined media, an aliquot had to be taken from a liquid rich media broth to give the bacteria a chance to acclimatise to new environment. When inoculating chemically defined media directly from glycerol stocks, majority of the time the bacteria failed to grow.

It has been proven that an addition of iron to media, can improve the growth rate of *Pseudomonas syringae* and aid with expression of virulence factors. Virulence factors heavily impact on secretion of extracellular enzymes, as they are involved in pathogenicity and host-plant interactions (Kim, Schneider, Cartinhour and Shuler, 2010, Kim et al., 2009).
The effects of varied carbon source dose and addition of a trace metals solution (containing iron alongside other metals and salts) on growth rate have been noted (Table 2.1.)

Per experiment needs, when investigating extracellular enzymes, a simple minimal chemically defined media was necessary. When investigating polysaccharides via microarray and TLC it is possible to exclude a singular polysaccharide when analysing the data, however excluding multiple factors can introduce bias or affect the quality of the results. Hence a simple M9 media containing minimal salts had to be used, alongside a trace metal solution.

It has been proven in other organisms how the presence of heavy metals such as Zinc, can stimulate and improve the biofilm production of *Pseudomonas syringae* species (Teitzel and Parsek, 2003). Bacterial biofilms predominantly consist of polysaccharides, such as polysaccharide intercellular adhesin (PIA), Psl, alginate, colonic acid and levan. (Limoli, Jones and Wozniak, 2015, Colvin et al., 2011).

2.2.2 Polysaccharide extraction and fractionation techniques for TLC and CoMPP

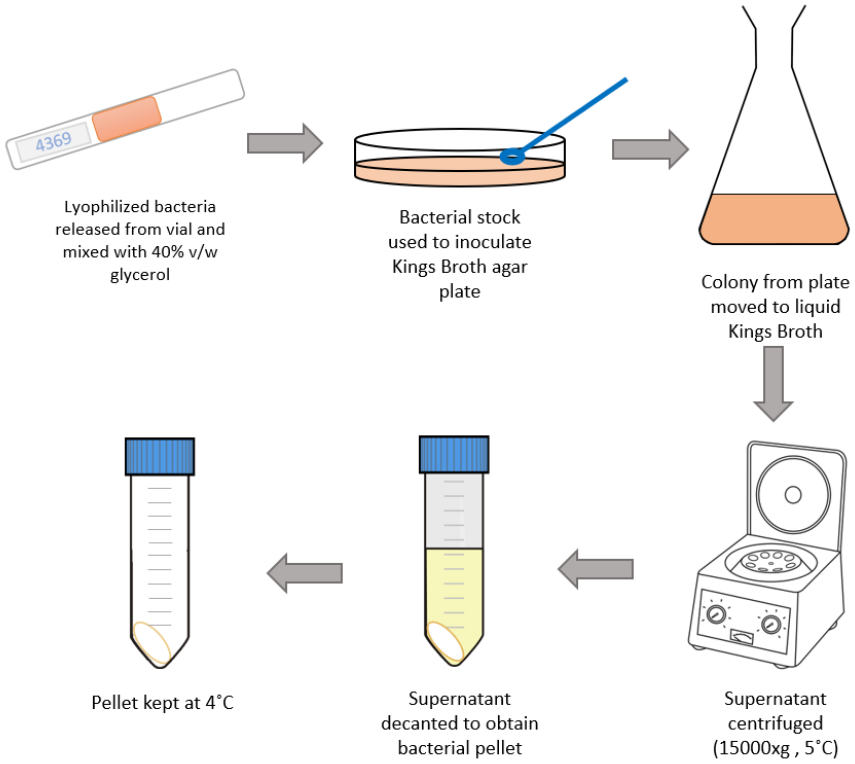

Figure 2.2. Flowchart showing the process of obtaining; bacterial pellets that were used for fractionation and polysaccharide analysis, and supernatant for ethanol precipitated extracellular polysaccharides (EPS).

Ethanol Precipitation of extracellular Polysaccharides

Bacterial supernatant was centrifuged (15000 xg, 15 min) in 50 mL falcon tubes (Figure 2.2). The bacterial pellet was kept for alcohol insoluble residue (AIR) preparation. The supernatant was kept for extracellular polysaccharide (EPS) precipitation. The supernatant was mixed with ethanol (98 %) in a 1:3 ratio, to obtain a final percentage of ethanol to be ≥ 73.5 %. The mixture was kept in a freezer -20 °C for 48 hrs. Once the precipitation was completed, small specs of white solid could be seen. This liquid was then centrifuged (12,000 g, 30 mins). The pellet was kept for further analysis and liquid was decanted kept for further analysis.

Alcohol Insoluble Residue (AIR) Preparation

Each bacterial pellet (1 g) was transferred to a tube with 70 % ethanol (1 mL). The samples were centrifuged (12,000 g, 10 mins) and supernatant discarded. These steps were repeated with methanol:chloroform (1:1 ratio, 1 mL), and acetone. The remaining pellets were left to dry overnight in a fume hood. AIR samples were used in TLC and microarray analysis.

Glycan Extraction

Bacterial AIR sample (10 mg) for each bacterium listed in Table 2.2, was suspended in 300 µL Cyclohexane Diamine Tetraacetic Acid (CDTA) (50 mM, pH 7.5). A steel bead was added to each sample (5 mm), and they were lysed using a tissue lyser (27 shakes per second for 2 mins then 10 shakes per second, for 2 h). The samples were then centrifuged (12,000 g, 10 mins), and the supernatant was decanted and stored at 4 °C. The remaining pellet was mixed with 300 µL NaOH (4 M + 0.1 % $NaBH_4$) and lysed in the same conditions. The sample was centrifuged (12,000 g, 10 mins) and supernatant stored at 4 °C, the pellet was kept for TLC analysis. CDTA and NaOH fractions were used in TLC and microarray analysis.

Fractionation of bacterial cell wall

Bacterial AIR sample (10 mg) was mixed with 500 µl of ammonium oxalate solution (50 mM, pH 7)(Wood et al., 2017). The sample was left to extract overnight (16 h), agitated at room temperature with a steel bead (5 mm) on a rotary wheel (10 rt/min). After extraction the sample was centrifuged (12,000 g, 10 mins), and the liquid was decanted. Extracted polysaccharides in the liquid were lyophilised, then resuspended in milliQ sterile water (100 µl) in order to concentrate the extracted polysaccharides. The fraction was kept in freezer (-20 °C) until further analysis and dialysis. The pellet was washed with water, by adding diH_2O (100 µl) and resuspending the sample, pellet was centrifuged (12,000 g, 10 mins) and liquid decanted (diH_2O wash). Water wash was repeated once again to ensure all extracted polysaccharides were removed from the pellet.

Trifluoracetic Acid (TFA) Hydrolysis

Ammonium oxalate fraction described above (50 µl) was mixed with TFA (100 µl, 6 M) and incubated in a heat block (110 °C, 1 hr). Once the sample has cooled down to room temperature (approx. 1 hr), the sample was lyophilised and kept for further analysis in the freezer (-20 °C), and dialysis.

This was also repeated with the pellet left after glycan extraction for NCPPB. 4369. Due to NCPPB. 4369 being considered the model organism for plant pathogen virulence, T3SS and being studied in most detail, most of the fractionation related TLC work was done on this specific pathovar.

Dialysis

The ammonium oxalate and TFA fractions of bacterial cell walls were loaded in dialysis membrane tubing (3500 Daltons cut off) and left agitated in a cold room in 5 L of diH_2O. The samples had the water changed every 24 h and were left for a total of 3 days. This was done

to remove as much of excess salts present in the samples. When poly and oligosaccharides added onto a TLC plate, the salts interfere with visualisation of carbohydrates, they form pink artifacts that follow all along the well where the sample ascents. Samples were decanted into tubes and lyophilised, then resuspended in 25 µl of sterile diH2O in order to concentrate the sample. The sample was kept in freezer (-20 °C), until TLC could be performed.

2.2.3 Analytical methods used for analysing bacterial derived polysaccharides – Thin Layer Chromatography and Microarrays.

Thin Layer Chromatography

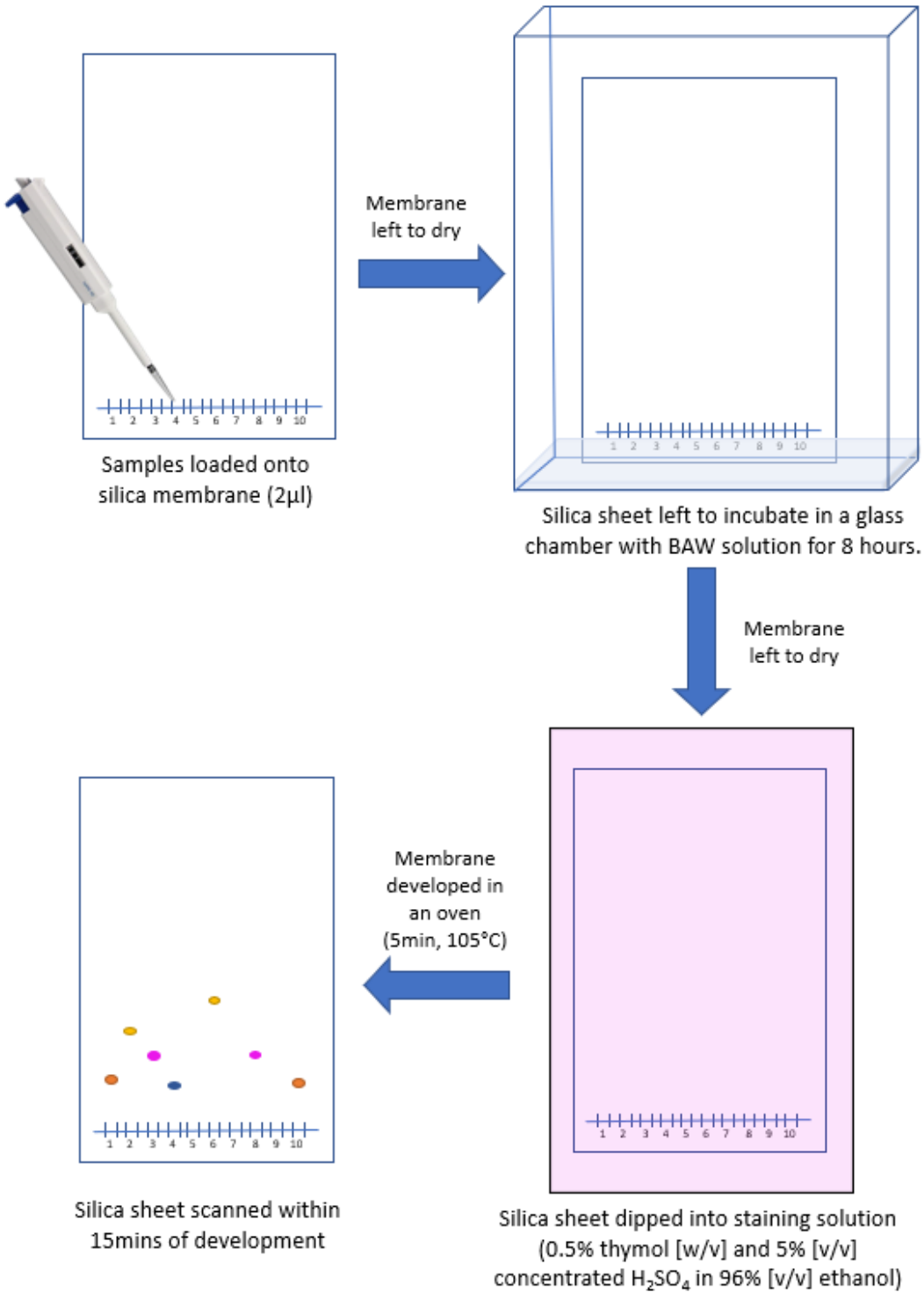

Figure 2.3. Schematic of TLC methodology used, showing the loading of sample, development stage, staining and detection stage.

A silica layer aluminium backed sheet (Macherey-Nagel) was labelled with a pencil and a ruler. A 2 cm gap was left at the bottom of the sheet and 1 cm gaps were left on the sides of the sheet. Wells were marker 2cm from the bottom of the sheet, the wells were 8 mm, and 2 mm gaps were left between the wells. The samples were loaded into marked wells by gently pipetting 2 µl of a sample across the length of the 8 mm well. The bacterial fractions were loaded onto the sheets alongside a defined monosaccharide marker control (2 µl). The marker was prepared by adding Xylan (extracted from beechwood, Megazyme) 0.01 g to 1 mL of diH_2O to achieve a [1 % v/w].

A TLC tank was filled with enough BAW mixture (butanol/ glacial acetic acid/ water, 2:1:1) to fill up the tank 1 cm from the bottom. The tank was covered with a glass cover and left for an h to let the vapours fill the tank. The membrane was left dipped into BAW to ascent for 8 h, dried overnight and put in for a second ascent.

The plates were stained with 0.5 % thymol [w/v] and 5 % [v/v] concentrated H_2SO_4 in 96 % (v/v) ethanol and left to dry in a vertical position. Due to different properties of oligo and monosaccharides, when stained and developed, they present different colours (Table 2.3).

Table 2.3. Table containing list of polysaccharides detecTable by BAW mixture, and colour range that these glycans develop once they are stained with thymol-based solution.

Glycan(s)	**Typical Colour(s) after Staining**
2-O-Methylxylose, Xylose	Blue/Violet
Ribose, Arabinose	Blue
Lamminari-oligosaccharides, Cello-oligosaccharides, Malto-oligosaccharides	Red
Manno-oligosaccharides	Pinkish Red /Coral
Fructose, Sucrose, Raffinose, Stachyose	Pinkish Red /Coral
Rhamnose	Orange
Xyloglucan oligosaccharides	Purple
Galactose	Green/Grey
Fucose	Orange/Green
Sedoheptulose	Green/Blue
Arabino-oligosaccharides	Blue/Violet
Xylan oligosaccharides	Blue/Violet

Plates were put in an oven to allow for detection (5 min, 105 °C). A short heating time prevent the plate from overheating and turning a dark purple colour. Once taken out of the oven, and scanned within 15 mins of coming out of the oven to prevent colours from fading.

Once scanned the image was imported into an image editing software (imageJ), where contract and saturations were adjusted to make any bands/spots present on the plate more visible. Colours of the spots were used as an indication of what was present in each band/spot. Retention factor (Rf) values are calculated using the following equation:

$$Rf = \frac{distance\ of\ substance\ zone\ from\ the\ sample\ origin\ [mm]}{solvent\ front\ migration\ distance [mm]}$$

A higher Rf value means the compound in the substance is less polar, hence travels faster as it is more attracted to the mobile phase (solvent).

A lower Rf value means the compound is the sample is more polar, it travels slower due to it being more attracted to the stationary phase (the silica plate) (Pazos, Otten and Vollmer, 2018).

2.2.4 Microarray Analysis of Bacterial Polysaccharides

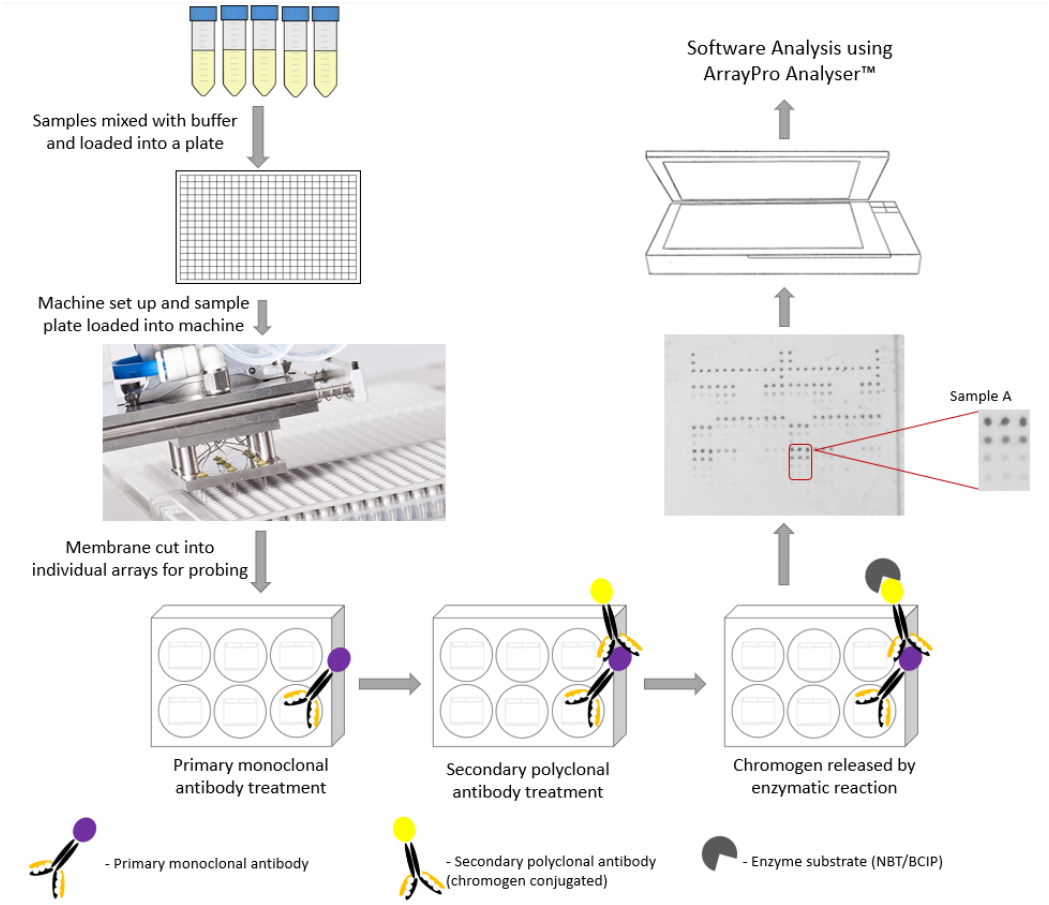

Figure 2.4. A flow chart showing general process of microarray technology applied for specific polysaccharide detection using antibodies as detection probes. The samples, get mixed with glycerol-based buffer. The plate layout is designed, and a file is created, for following where each sample is loaded in the 384-well plate. Once printed, the arrays can be probed with primary monoclonal antibody (mAbs), washed, an alkaline phosphatase polyclonal antibody was applied, washed again then treated with chromogenic NBT/BCIP solution. Presence of a complimentary epitope is detected by relevant mAbs that leads to a presence of an insoluble purple dye, which can be seen in sample A.

Printing

Due to the complexity of the plate layout, a template was used to assign each sample a position that could be easily referred to when analysing the arrays. The samples were placed in a 384 well plate (Greiner Bio-one) where they were diluted with buffer (55.2 % glycerol, 44 % water, 0.8 % Triton X-100, 0.0004 % Proclin). Each sample was loaded in triplicate, in 4 different dilutions, 2-fold, 10-fold, 40-fold, 1000-fold. at dilutions 1000 (0.5 v/v, 0.1 v/v, 0.025 v/v, 0.007 v/v). The samples were printed using a MicroArray Sprint Robot (Newcastle University, UK) onto a nitrocellulose membrane (0.2 µm, Amersham™ Protran). Each sample was printed onto the spot 6 times (6 x 10pL, 60pL total per spot). Nitrocellulose membrane was cut into individual arrays. Each array was labelled and kept in an airtight container, in dry and cool conditions until needed.

Probing

The array was incubated in a blocking solution for 1 h (5 % w/v milk protein in TBST; 20 mM Tris-HCl, 140 mM NaCl, pH 7.5 and 0.1 % Tween-20, v/v) volume used was dependent on the size of well used. The array was incubated for 1.5 h in the blocking solution with a chosen primary antibody (1:10 dilution, or appropriate dilution according to antibody manufacturer suggestion). List of monoclonal antibodies used for this experiment can be seen in Table 2.2, with dilutions used for each monoclonal antibody.

The array was washed thoroughly in TBST, 3 times over the course of 30 mins. The array was incubated for 1.5 h in the blocking solution and secondary antibody conjugated with alkaline phosphatase (1:1000 dilution). The array was washed thoroughly in water, 3 times over the course of 30 mins. An enzyme marker substrate was made according to Bio-Rad NBT-BCIP protocol, the membranes were left to develop in the solution (30 mins). NBT/BCIP is a widely used chromogenic substrate for enzyme linked alkaline phosphatase.

When BCIP (5-Bromo-4-chloro-3-indolyl phosphatase) is hydrolysed by alkaline phosphatases present in the secondary antibody, it produces a blue intermediate. The intermediate is then oxidised by NBT (nitro blue tetrazolium) to produce a dimer, which is the visible and insoluble purple dye.

The reaction was stopped by placing the array in water, then left pressed between filter paper to dry before analysis.

Table 2.3. List of primary monoclonal antibodies used for microarray-based screening of bacterial cell wall extracts (PlantProbes : Paul Knox Cell Wall Lab, 2021).

Polysaccharide	Code	Epitope
Pectin	JIM5	HG partially/de-esterified
Pectin	JIM7	HG partially/de-esterified
Pectin	LM18	HG partially/de-esterified
Pectin	LM19	HG partially/de-esterified
Pectin	LM20	HG partially/de-esterified
Pectin	LM8	Xylogalacturonan
Pectin	LM7	HG/Alginate
RG-I related	LM5	(1→4)-β-D-galactan
RG-I related	LM9	Feruloylated (1→4)-β-D-galactan
RG-I related	LM6	(1→5)-α-L-arabinan
RG-I related	LM13	Linearised (1→5)-α-L-arabinan
RG-I related	LM16	Processed arabinan
RG-I related	LM12	Feruloylate on any polymer
Mannan	LM21	(1→4)-β-D-(galacto)(gluco)mannan
Mannan	LM22	(1→4)-β-D-(gluco)mannan
Glucan	JIM6	No defined Anti-callose like binding
Xyloglucan	LM15	Xyloglucan (XXXG motif)
Xyloglucan	LM24	Xyloglucan
Xyloglucan	LM25	Xyloglucan / unsubstituted β-D-glucan
Xylan	LM10	(1→4)-β-D-xylan
Xylan	LM11	(1→4)-β-D-xylan/arabinoxylan
Xylan	LM23	Terminal (1→4)-β-D-xylan
Xylan	LM27	Anti-grass xylan preparations
Xylan	LM28	Glucuronoxylan
Extensin	LM1	Extensin
Extensin	JIM11	Extensin
Extensin	JIM12	Extensin
Extensin	JIM19	Extensin
Extensin	JIM20	Extensin

AGP	JIM4	AGP
AGP	JIM8	AGP
AGP	JIM13	AGP
AGP	JIM14	AGP
AGP	JIM15	AGP
AGP	JIM16	AGP
AGP	LM2	AGP, β-linked GlcA
AGP	LM14	AGP

The microarrays were stuck flat onto a piece of card, and then were scanned using a 2400 dpi flatbed scanner (Cannon, Newcastle University, UK). The images were converted to greyscale and .TIFF format, then analysed using Array-Pro Analyser (MediaCybernetics, USA). The data was presented using heatmaps, with colours correlating to mean spot intensity produced by NBT/BCIP.

Microarray Data Analysis

Microarray experiments provide thousands of data points, due to a dilution series of 4 and a technical replicate of each sample. Each of these point then provides data for each of the mAbs used, yielding over 7000 data points. An appropriate means of analysis was necessary when handling such large data sets. A heatmap seems the only reasonable visualisation of such a big and complex data set. It allows the reader to easily visualise binding of the monoclonal antibodies to specific epitopes present in each sample.

Array-Pro Analyser applies a grid onto the .TIFF image of a microarray. Each spot of the grid aligns with the spot where the sample was printed. The software then measures degree of greyness, (similar to an optical density reading) and assigns it a value. The data from this software was saved as a .txt file.

Each microarray was analysed in this manner, yielding 38 .txt files, 37 providing data for each antibody, and 38th being a microarray treated with secondary antibody, serving as a control of the probing methodology.

The .txt files were imported into a Microsoft Excel Macro, where each spot in the microarray is labelled with what sample has been printed there. This data is taken from template used for designing the plate layout. Each .txt file corresponds to data obtained from a singular array that has been probed with only one monoclonal antibody, e.g., LM7. The macro, imports all

.txt files and merges them into one file, with rows corresponding to samples, and columns corresponding to antibodies. The background is also subtracted from all values. At this stage there is data for each of the triplicates, and dilutions for each sample (Figure 2.3.).

The dilutions and triplicate values are averaged for each sample, to provide 1 value for each sample and antibody pairing. The data is then normalised, this is done by taking the highest value present in the data set and dividing all data points by the value. All data points are then multiplied by 100, to produce a percentage. A colour scheme is applied via conditional formatting, to visualise where binding has occurred and produce the final heatmap.

2.3 Results and Discussion

2.3.1 TLC

Bacterial strain NCPPB. 4386 was grown on minimal media with addition trace metal solution, as it improved the rate of bacterial growth (Table 2.2), after incubation for 48hrs (28^{o}C, 300rpm).

Table 2.2. Media glycerol percentage and trace salts presence affecting growth of NCPPB. 4369. Aliquots (1 mL) of media were taken 24hrs after inoculation. Optical density readings were taken in triplicate, an average of readings was noted, and standard error values for each reading are included in the Table. A higher content of glycerol yielded a higher optical density, meaning a better bacterial growth. An addition of trace metals solution has improved bacterial growth in the two flasks containing the same account of glycerol, 0.2 % and 2 % [v/w].

	OD 650(nm)	**OD 600(nm)**
Glycerol 0.2 % [v/w]	0.044 ± 3.33 x 10^{-4}	0.056 ± 2.3 x 10^{-4}
Glycerol 2 % [v/w]	0.114 ± 3.33 x 10^{-4}	0.132 ± 1.12 x 10^{-4}
Glycerol 0.2 % [v/w] with trace metals solution	0.076 ± 5.57 x 10^{-4}	0.090 ± 1.01 x 10^{-4}
Glycerol 2 % [v/w] with trace metals solution	0.321 ± 8.82 x 10^{-4}	0.133 ± 0.000335

Bacterial pellet was obtained by centrifugation of the bacterial broth (Figure 2.2). Bacterial pellet was used to obtain fractions of polysaccharides; ammonium oxalate fraction, primary and secondary H_2O wash of the ammonium oxalate pellet, and TFA hydrolysed fraction that included the TFA hydrolysed bacterial cell wall in liquid, the TFA pellet and THE primary and secondary H_2O wash of the TFA pellet. Bacterial supernatant was used to obtain EPS, by precipitating the supernatant with EtOH and pelleting the precipitate, the precipitate was

solubilised in water. These fractions were directly loaded onto a silica membrane (without dialysis), alongside a rhamnose sugar standard (1 % [v/w]). The plate was developed using BAW and stained using a thymol-based solution. The plate was heated up to allow for detection of glycans (Figure 2.5). Due to a high salt presence that was increased due to repeated lyophilising of fractions, pink smears can be seen in wells where samples had a high salt content (lanes 1, 3, 5, 6, 8, 9, 10 in Figure 2.5). There are faint bands present in wells 6 and 7, which correspond to TFA pellet resuspended in diH_2O, and dialysed TFA pellet resuspended in diH_2O respectively. Due to very low intensity of the bands, a clear colour identification can't be made. The dialysed sample in well 7 does not show pink artefact in the line of ascent of the sample, confirming that high salt presence can cause these artifacts and obscure visibility of bands. The rhamnose sugar standard was detected, proving the methodology was successful in detecting glycans. Rhamnose was selected as a control due to rhamnose being previously isolated from lipopolysaccharides in *Pseudomonas* species (Yokota et al., 1990, Ovod et al., 2004)

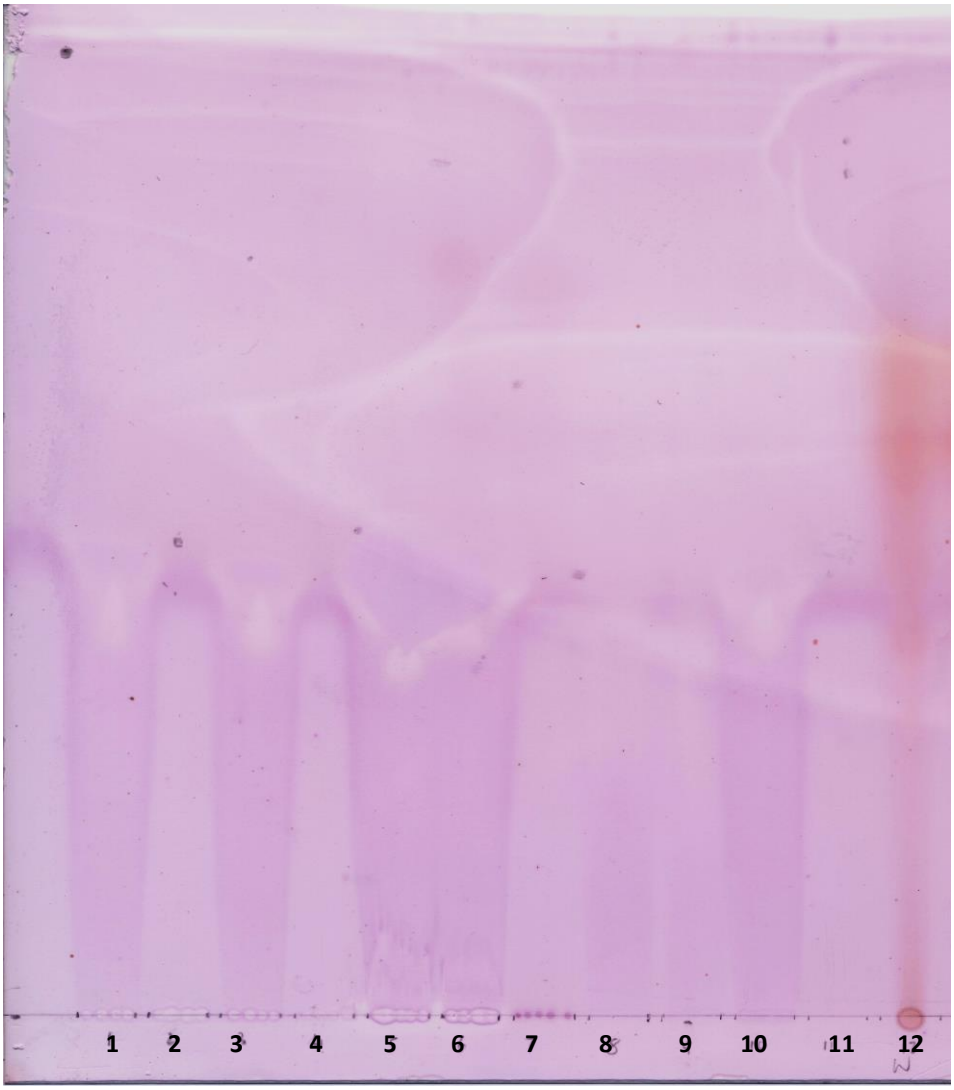

Figure 2.5. TLC with 10 fractions of NCPPB. 4369, and a sugar standard. The plate had two ascents (2 x8hrs) in BAW. Each lane had a different fraction or sugar standard loaded onto it, with lane 9 and 11 being left blank. Lanes present in the TLC plate were loaded with the following:

1. Ammonium Oxalate extract + 2 x H_2O washes.
2. Primary H2O wash of Am Ox extract
3. Secondary H_2O wash of Ammonium Oxalate extract.
4. EtOH extract Bacterial Cell Wall polysaccharides reconstituted in 10 µl diH_2O.
5. TFA Hydrolysed Bacterial cell wall.
6. Pellet after TFA hydrolysis resuspended in diH_2O.
7. Pellet after TFA hydrolysis resuspended in diH_2O and dialysed (3500 Daltons cut off).
8. Ammonium Oxalate extract loaded 5x onto the membrane.
9. Blank.
10. Ammonium Oxalate extract loaded 10x onto the membrane.
11. Blank.
12. Sugar standard – Rhamnose (1 %v/w) and Mannose (1 % v/w).

In Figure 2.6. there are 2 bands visible in well 3, which contains a xylan defined polysaccharide standard (1 % [v/w]). The presence of the second lower band is most likely due to an impurity being present within the standard. From the colour and position of the band, the impurity is

most likely arabinose, as it can be seen in gas liquid chromatography in the data sheet for the product provided by manufacturer (Megazyme). BAW is a very good mobile phase for mono-, di-, tri, tetra- up to deca-saccharides. Due to a clear lack of bands in wells 1 and 2, it appears that only more complex and larger carbohydrates, such as polysaccharides were extracted. There is a faint purple/violet shadow around well 1, where it might indicate presence of xylan / arabino related polysaccharides, however it might also be caused by cell debris interacting with the stain used for these plates. CDTA and NaOH fractions are traditionally used for CoMPP analysis, and are not compatible with BAW solution and thymol based stain for TLC.

Figure 2.6. TLC with CDTA and NaOH extracts of NCPPB. 4369, and a xylan polysaccharide standard serving as a positive control. Two ascents (2 x 8hr) in BAW. Lanes present in the TLC plate were loaded with the following:

1. 2 µl of CDTA extract of NCPPB. 4369 bacterial pellet.
2. 2 µl of NaOH extract of NCPPB. 4369 bacterial pellet and
3. 2 µl of Xylan Standard (1 % v/w)

Additional efforts were made to concentrate samples via lyophilization and multiple loading of sample onto the silica membrane. Samples present in wells 1, 2, 3, 4 were lyophilised and resuspended in minimal amount of liquid needed to resuspend the pellet. The liquid was then loaded until the silica membrane was saturated. EPS in well 1 was loaded x 2, dialysed ammonium oxalate extract in well 2 was loaded x 8, dialysed TFA hydrolysed bacterial cell wall was loaded x4 and TFA hydrolysed pellet was loaded x 3 (Figure 2.7).

A faint band present in well 1, is most likely to be a heat spot produced as a result of overhating the plate in that one space. It is unlikely to be a carbohydrate from the sample as it leans towards the left of where the sample was loaded and all other bands ascended in a straight line.

Fucose monosaccharide is often noted as a component of bacterial polysaccharides (Yi et al., 2009) , and it's been often noted to be a virulence factor, and a determinating factor for bacterium-induced immune reactivity (Ma, Simala-Grant and Taylor, 2006).

Though there is no known bacteria to contain raffinose as the part of its' cell wall, there are plant pathogenic bacterium that utilise and assimilate oligosaccharides such as sucrose and raffinose (Hugouvieux-Cotte-Pattat and Charaoui-Boukerzaza, 2009). It is possible that raffinose was detected, as it was an intermediate in a metabolic process.

Pseudomonas species have been noted to produce lipopolysaccharides (LP), which are considered to play a big role as virulence factors. There is evidence of Pseudomonas aeruginose producing L-Glycero-D-manno-heptose, 3-deoxy-D-manno-oct-2-ulosonic acid, D-galactosamine, D-glucose, and L-rhamnose (Kocincova and Lam, 2011).

Obtaining bands on TLC provided insidght on how time consuming characterising polysaccharides in over 100 pathovars will be. With limited access to a facilities such as the freezedrier and TLC development tanks. An alternative method of exploring bacterial cell wall had to be considered.

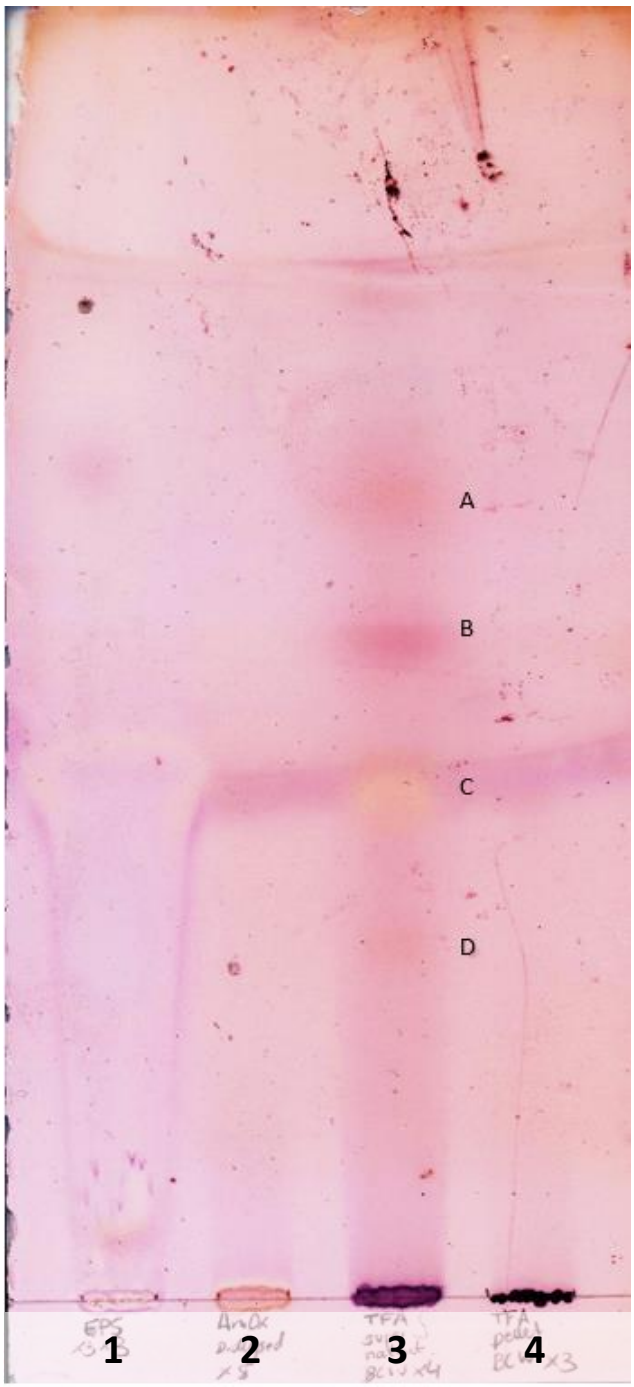

Figure 2.7 . TLC with 4 fractions obtained from NCPPB. 4369. The image was adjusted to increase contrast of the present bands and allow for retention factor (Rf) measurements. Lanes present in the TLC were loaded with the following:

1. Extracellular polysaccharides (EPS) secreted into supernatant, loaded x3 (precipitated with EtOH).
2. Ammonium Oxalate extract dialysed and loaded x8.
3. TFA hydrolysed BCW, loaded x4.
4. Pellet left after TFA hydrolysis, resuspended in 10 µl diH_2O, loaded x3.

The 4 bands present in well 3 are the following: A – Rf 0.667, B – Rf 0.571, C – Rf 0.429 and D – Rf 0.286.

This image was adjusted as follows: brightness – 15 %, contrast + 40 % and sharpness + 12 %.

Comprehensive Microarray Polymer Profiling (CoMPP) was explored. Due to high through-put nature of CoMPP and being able to process and investigate a high number of samples, it was a promising technique. It allows to obtain information on semi-quantitative information on abundance of polysaccharides within samples. An alternative fractionation method was used for CoMPP, a glycan extraction protocol utilising NaOH and CDTA. This extraction method has been commonly used alongside CoMPP to provide excellent results (Baldwin et al., 2017).

2.3.2 CoMPP

CDTA is used for extraction of pectic polymers, and NaOH extract hemicelluloses. With bacterial cell wall not been known to contain hemicelluloses the results provide an interesting outlook. All of the bacterial species used in this study, have reported LM5 (anti-(1→4)-β-D-galactan) binding (Figure 2.8.). This could be explained by LM5 binding to an eitope on arabinogalactan. The mycolyl-arabinogalactan-peptidoglycan (mAGP) has been studied and previously identified to be present in *Mycobacterium tuberculosis* (Alderwick, Harrison, Lloyd and Birch, 2015). Peptidogylcan present in mycobacteria forms the basal layers of the mAGP complex, which consists of alternating N-acetylglucosamine (GlcNAc) and modified muramic acid (Mur) residues, linked in a β(1 → 4) configuration. In plants AGP consists of arabinose, galactan and a protein, with other sugars being previously identified, such as L-rhamnopyranose (L-Rhap), D-mannopyranose (Manp), D-xylopyranose (Xylp), L-fucose (Fuc), D-glucopyranose (Glcp), D-glucuronic acid (GlcA), and D-galacturonic acid (GalA) (Inaba et al., 2015). AGP has a galactan backbone ((1-3)-linked β-D-galactopyranose (Galp)), with branches of (1,6)-linked β-D-Galp (Du et al., 1996).

Antibodies raised specifically against lipoarabinomannan isolated from *Mycobacterium tuberculosis* have proven presence of lipoarabinomannan in *Pseudomonas auruginosa* ((Voisin et al., 2007), this may be proof of mycobacteria and *Pseudomonas spp.,* sharing common lipoarabinomannan epitopes. Though no research has been done on presence of arabinogalactan or mycolyl-arabinogalactan-peptidoglycan (mAGP) complex being present in *Pseudomonas syringae*, the response from LM5 and LM6 (anti-arabinan) could point towards presence of lipoarabinomannan. The function of mAGP has been studied in *Mycobacterium tuberculosis*, where it is key in maintaining structure of the upper myco-membrane. It is mAGP that is thought to play a key role in non-replicative growth during dormancy (Alderwick, Harrison, Lloyd and Birch, 2015).

Binding of LM27 and LM28 can be explained by association to arabinogalactan-proteins (AGP). There is research that tracks AGP and shows binding to LM27 and LM28 (Cornuault et al., 2015). It is unlikely that there is xylan present in bacterial cell wall fragments, it is highly attributed to cross-linking of cellulose microfibrils and lignin in plant cell walls (Balakshin et al., 2011). More work on characterising bacterial cell wall would be required to definitely confirm presence of mAGP.

Extraction	NCPPB	Anti-Galactan LM5	Anti-Arabinan LM6	Anti-HG / Alginate LM7	Anti- processed arabinan LM16	Anti-Heteromannan LM22	Anti-Xylosyl LM23	Anti-xylan (Grass) * LM27	Anti-Glucuronosyl residue LM28	Anti-HG JIM5	Anti-Extensin JIM20
NaOH	281	14	0	0	0	0	12	0	5	0	0
NaOH	600	41	0	0	6	3	5	0	0	0	3
NaOH	635	10	0	0	0	0	0	0	0	0	0
NaOH	639	4	0	0	0	0	0	0	0	0	0
NaOH	1437	15	0	0	0	0	0	0	0	0	0
NaOH	1873	10	0	0	0	0	0	0	0	0	0
NaOH	2193	4	0	0	0	0	5	0	0	0	0
CDTA	281	81	0	7	14	11	19	3	0	7	8
CDTA	600	79	0	6	9	7	10	0	0	0	6
CDTA	635	67	0	12	9	6	11	0	0	7	0
CDTA	639	74	4	8	15	9	13	3	0	8	10
CDTA	1437	100	3	11	18	12	14	0	0	5	6
CDTA	1873	31	0	5	6	4	7	0	0	4	3
CDTA	2193	91	5	4	12	7	11	0	0	3	10

0 10 20 30 40 50 60 70 80 90 100

Figure 2.8. The heat-map generated from microarrays of the pectin fraction and hemicellulose (CDTA & NaOH extracts) from 7 different bacterial species from the NCPPB (281, 600, 635, 639, 1437, 1873, 2193). The fractions were probed against the library of the antibodies (Table 2.3). The highest value observed was obtained by probing CDTA extract of NCPPB with LM5 (anti-(1→4)-β-D-galactan). The legend shows the lowest values starting at 0 % to be grey, with values transitioning to a blue colour as the value increases to 100 %. The bacterial cell wall extract has shown a higher signal intensity in the CDTA fraction, which is used to extract pectin in plant material. This is shown by LM5 anti-galactan having the highest signal intensity across all bacteria and the lower half of the heatmap showing more binding to other antibodies too. A full heatmap showing data for all monoclonal antibodies used can be seen in supplementary Figure 2.9.

Pseudomonas syringae is known to produce biofilms, the main component on bacterial biofilm by this species is alginate (Laue et al., 2006). Biofilm protect the bacteria from environmental factors and aids with adhesion to solid surfaces, this is a key mechanism used for spread and colonisation of new sites and plants (Boyd and Chakrabarty, 1995).

Though there is binding to extensin (JIM20, Figure 2.8.), extensins are a term used for hydroxyproline-rich glycoproteins (HRGPs) of the plant cell wall (Lamport, 1966). The JIM20

antibody must have bound to galactan present in AGP, showing a similar epitope that is present in mAGP within bacterial cell walls. JIM20 has only expressed a low level of binding to samples where a high level of binding was present to LM5, which only supports this hypothesis.

2.4 Conclusion

Thought many attempts have been made at utilising TLC for profiling of bacterial cell wall components, the results have been quite limited. Ultimately TLC is not optimal for analysing a large sample set, due to time and cost limitations. CoMPP fit much better with the high through-put nature of this project. AIR sample preparation and printing on this scale can take up to 2 days, with probing and analysis taking another day or day and a half. CoMPP offered 476 individual data points, whereas TLC requires complex sample preparation which takes approximately 5 days, with additional 2 days needed for 2 separate ascents in BAW solution. Due to microaaray printing being automated, the machine can be left to print overnight with no human intervention, whereas TLC needs careful planning and frequent checking as the mobile phase cannot be allowed to reach the top of the silica plate.

While offering a lot of insight and being able to differences in relative quantities of different epitopes present in each sample (i.e. CDTA extract of 1873 binding to LM5, vs other CDTA extracts), these findings are insufficient in order to develop the methodology further as a potential pathovar identification tool. In order to utilise this technique for identification of bacterial pathovars, a selection of antibodies with specificity directed specifically towards *Pseudomonas syringae* would have to be made. There is a very limited amount of *Pseudomonas syringae* mAbs available on the market. Taking the budget of the project into account and high cost of these antibodies, it was not feasible to explore them as potential probes. Assuming successful and clear profiles of these pathogens being produced by CoMPP, for any future identification, the samples would have to be printed and probed alongside each other, as identification would only be possible by comparison of samples between the sample set. Despite clear limitations of both of these techniques, there is potential for utilising CoMPP as a means of identification of enzymatic activity amongst the bacterial pathogens. Pathovars have different host specificities and produce enzymes that allow them to degrade the bacterial cell wall. These enzymes might differ depending on the pathovar, making them the next possible biomarker that can be identified by using microarray technology.

2.5 Supplementary Material

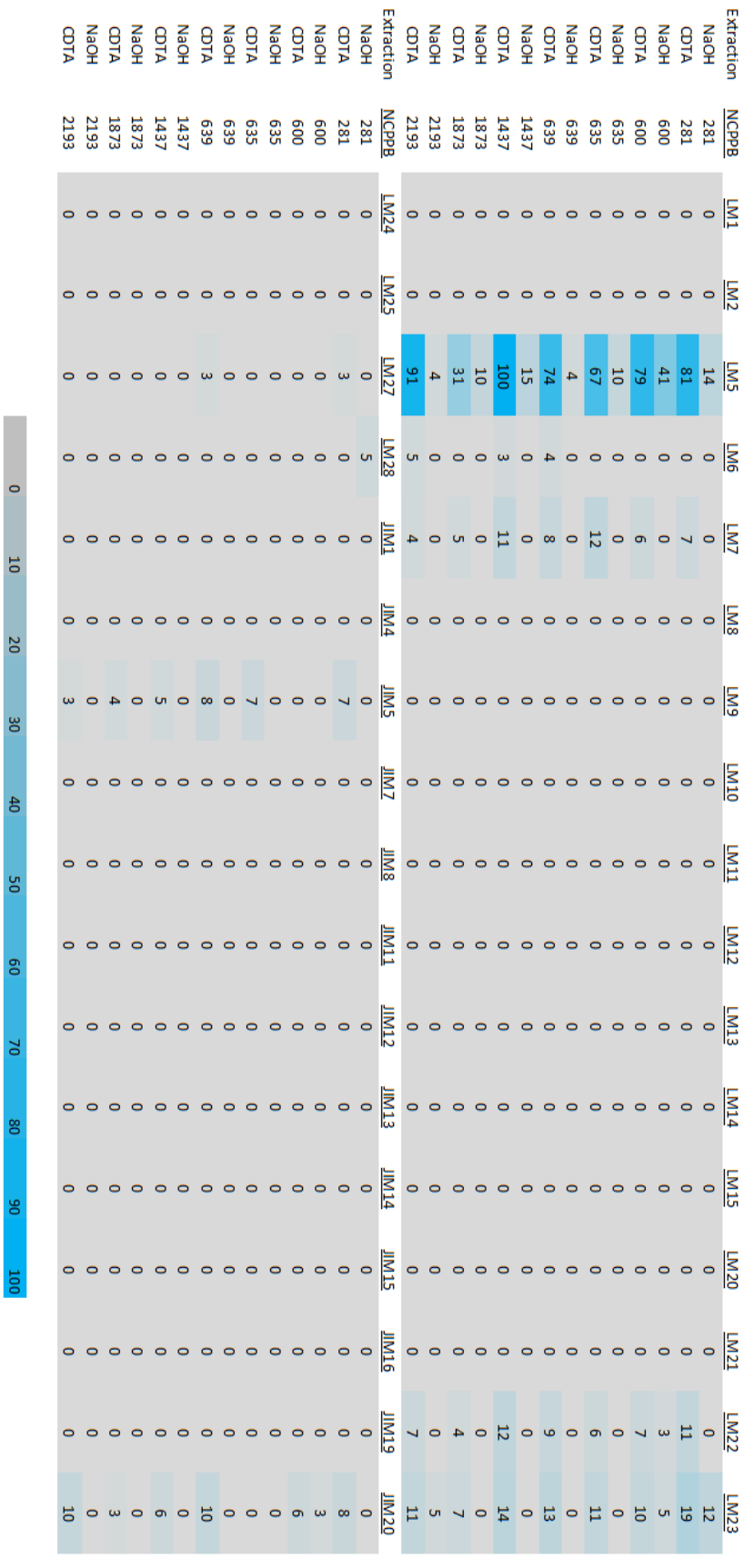

Supplementary Figure 2.9. The heat-map generated from microarrays of the pectin fraction and hemicellulose (CDTA & NaOH extracts) from 7 different bacterial species from the NCPPB (281, 600, 635, 639, 1437, 1873, 2193). The fractions were probed against the library of the antibodies (Table 2.3). The highest value observed was obtaind by probing CDTA extract of NCPPB with LM5 (anti-(1→4)-β-D-galactan). The legend shows the lowest values starting at 0 % to be grey, with values transitioning to a blue colour as the value increases to 100 %. This heatmap shows the binding across all antibodies, where majority of them did not bind to the samples.

3. Development of microarray-based enzyme discovery platform via epitope depletion.

Abstract

Microarray robots have many applications in automation and high-throughput processing of samples. They have been previously applied to characterising plant cell walls, genomics, proteomics, and enzyme screening. This chapter focuses on method development of applying high-throughput microarray approach for enzyme characterisation and discovery, and potential use of enzymes as biomarkers. Biomarkers are biological molecules that can be used to identify a stage, an organism, or a process. With *Pseudomonas syringae* pathovars being phytobacteria that live on plant surfaces, they produce many hydrolytic enzymes that aid in plant entry and infection (Isla et al., 2002).

3.1 Introduction

3.1.1 Biomarkers

Pseudomonas syringae pathovars have been previously identified using of genomics approaches. As described previously, sequencing and use of primers in order to find identification regions across all *Pseudomonas syringae* pathovars is costly and timely (Jung, Han, Jo and Koh, 2003) and alternative biomarkers have to be considered. By definition, biomarkers are molecules that are used to identify a stage, an organism, or a process (Huss, 2015). Polysaccharides have been used as biomarkers for a number of applications, for example food adulteration, as they can be effectively tracked with molecular probes, investigated with thin-layer chromatography (TLC), or high-performance anion exchange chromatography with pulsed amperometric detection (HPAEC-PAD) (Siddiqui, Musharraf, Choudhary and Rahman, 2017). Bacterial cell walls are made up of several polysaccharides, and attempts have been made at utilising cell wall polysaccharides as biomarkers with limited success. Bacteria produce a variety of molecules when infecting plants, one of them being enzymes and enzymes may be an alternative biomarker type of interest.

3.1.2 Use of Microarray Robot for Enzyme Discovery

Enzymes are a crucial part of many biological processes. They are proteins that act as biological catalysis that accelerate chemical reactions and break down substrates converting them into products. Conversion of starch to sugars by plant extract and saliva were known as early as 17th century, but mechanisms behind them were not known (Williams and Williams, 2015) until 18th century where Louis Pasteur, often regarded as the founder of microbiology, discovered that enzymes were the driving force behind fermentation (Manchester, 1995). In 21st century, enzymes are used in a range of industries, from waste management, food industry, pharmaceuticals, detergents, and fashion industry. Many enzymes are crucial to industrial processes, such as rennet in cheese making, or decomposing complex polymers in waste management (Singh, Kumar, Mittal and Mehta, 2016). Enzymes require specific environments and conditions in order to break down substrates, so often finding these novel enzymes from microorganisms is a challenge. High-throughput methodology is of interest to these industries in order to easily find potential enzymatic mechanisms and organisms of interest. Microarray technology is relatively new and has been used in a range of biological applications, enzyme profiling being one of them (Uttamchandani and Moochhala, 2010).

3.1.3 Bridging the gap between metagenomics and application

Thus far, novel enzymes and metabolic pathways have been studied and discovered through DNA sequencing and extensive proteomics. However, there are many steps between DNA extraction, sequencing, genome annotation and actually determining enzyme activity. There is also considerable uncertainty and many of entries in databases such as UniProt or Carbohydrate Active Enzymes (CAZy) are based on sequence homology rather than empirically determined activities (Gerlt, 2016). There are initiatives being taken in order to combat those issues, however the biggest hurdles involve protein expression, activity, and conditions necessary in order to obtain an active enzyme. Many industry and biotechnology laboratories rely on culture-based assays (Vester, Glaring and Stougaard, 2014). The key limitation of culture-based approach is that only relatively small number of microbial organisms can be easily cultured in lab, which is not representative of the microbial ecosystem. It is estimated that less than 2 % of bacteria can be cultured in laboratories (Wade, 2002). Fortunately, *Pseudomonas syringae* is one of the best studied plant pathogens and is considered a model organism for understanding host-microorganism interactions, it has been cultured successfully for decades (Xin, Kvitko and He, 2018).

It requires finding right conditions, such as hosts, inducing hormones, feed, or other chemicals, as well as abiotic factors, or advanced synthetic biology. This would still require a lot of trial and error with operons and much more DNA sequencing and protein expression tests. Once protein is expressed, it still may not be active until set conditions are met. Protein activity is inferred from homology other known proteins and similar activity is assumed, which may not always be the case.

So far, screening for enzymes has been a challenging and long process. Often based on knowledge already present from the bacterial natural environment or host. When limited to only host properties, a lot of key activities that may be utilised in industry may be missed. Most processes which require enzymes, such as juice production that use pectinases and xylanases, have been discovered and established nearly 20 years ago (Raveendran et al., 2018), since then not much progress has been made in this field. There are resources like the CAZy, which can be utilised to view carbohydrate active enzymes which are often homology inferred from a closely related organism. A lot of further research has to been done to confirm enzyme's presence within the organism, and suspected activity.

By utilising microarray technology, which prints variety of samples onto nitrocellulose membrane via non-contract printing. The capabilities of screening bacterial supernatants or crude enzyme extracts against thousands of samples can be achieved in a matter of days. By using monoclonal antibodies (mAbs), the changes in structures of polysaccharides adhered to nitrocellulose can be observed by observing a difference in intensity binding of specific antibodies. Plant extracts, pectic and hemicellulose fractions can also be printed onto such arrays, instead of polysaccharides standards.

This chapter aims to establish a technique for identifying changes in epitopes caused by enzymes present within bacterial broths. This is done by utilising CoMPP as a tool for identifying differences in antibody binding to defined polysaccharides standard after they were treated with bacterial broths. A novel data analysis technique is developed to accuarelty present findings.

3.2 Methodology

3.2.1 Preparation of Ammonium Sulphate and Crude Enzyme Extract

Preparation of crude bacterial enzyme supernatants

Glass vials with lyophilised culture of NCPPB 385. (Fera Science ltd) on filter paper were opened and mixed with SDW (sterile distilled water). The bacteria were prepared according to methods outlines in 2.2.1.

The colonies taken from the plates were used to inoculate flasks of media (100 mL). For rich media, Kings broth was used. For experiments requiring alternating carbon sources, minimal media was used (made according to methodology in 2.2.1) with addition of sterile defined polysaccharide stock. Each polysaccharide was prepared by making a 10 % stock solution with SDW (10 g of polysaccharides standard in 100 mL of SDW), and then autoclaved. Once the polysaccharide stock was cool, 5 mL was added to flasks containing 95 mL of SDW to ensure correct concentration of 0.5 %.

Flasks containing minimal media and no carbon source, were inoculated, then boiled. The broth was used as a control for experiments listed in Figures 3.4, 3.5 and 3.7.

The flasks were left to incubate (28 ^{o}C, 130 rpm for 2 days). The liquid from each flask was collected and centrifuged (12,000 g, 10 mins) to obtain supernatant. Each of the four supernatants were filtered through a 0.2 µm syringe the mixed with sodium azide solution (0.5 mL, 10 % w/v), to achieve a final concentration of 0.0 5 %.

Preparation of ammonium sulphate precipitate

Kings broth and minimal media with addition of xylan (0.5%) were prepared according to 2.2.1. The media were inoculated with NCPPB. 1957 and allowed to incubate (28 ^{o}C, 130 rpm for 2 days).

Supernatants from rich media based on glycerol (Kings broth) and minimal media with addition of xylan were and centrifuged (12,000 g, 10 min) to obtain supernatant. Each of the four supernatants were filtered through a 0.2 µm syringe the mixed with sodium azide solution (0.5 mL, 10 % w/v), to achieve a final concentration of 0.05 %.

Each supernatant was slowly mixed with ammonium sulphate (66.82 g, 95 % saturation) over the course of 2 h at 4 °C and agitated with a magnetic stirrer. Once homogenous, the solution was centrifuged (3500 rpm, 4 °C, 30 min). Once the pellets formed, the supernatant was discarded, and pellets were kept at 4°C.

Individual pellets were mixed with enough water to resuspend (2 mL) and dialysed (4° C, 3500 Daltons cut-off membrane) in milliQ water (10 L), that was changed every 12 h. The dialysis was carried out over a 48 h time period. The enzyme extract was lyophilized and resuspended in 200 µl SDW. Resuspended enzyme extract was split across 2 tubes (100 µl). One tube mixed with succinate (0.5 M, pH 5.00) to final contraction of 100mM (25 µl) and HEPPS (0.5 M, pH 7.20) to obtain a final concentration of 100 mM (25 µl).

3.2.2 Preparation of polysaccharide standards

Selection of polysaccharides were selected based on their presence in a variety of host plants. The polysaccharides Arabinoxylan (wheat), β-glucan (barley), Galactan (lupin), 61-α-D-Galactosyl-mannobiose plus Mannotriose / GMM3 (prepared from galactomannan extracted from carob), Pectin (Citrus), Polygalacturonic Acid / PGA (Citrus), Rhamnogalacturonan (Soy Bean), Xylobiose, Xyloglucan (XG tamarind). All of the polysaccharide standards listed above were purchased from Megazyme. Xanthan gum (isolated from Xanthomonas campestris) and raffinose was purchased from Merck/Sigma Aldrich. PAT (pectin-alginate-titania), PAG (poly(aldehyde guluronate)), DAP (defined alginate polysaccharide), lime pectins; P16 (16 % methylesterified pectin), F43 (43 % methylesterified pectin, obtained by using a fungal plant pectin methylesterase) , E81 (81 % methylesterified pectin) were kindly donated from the University of Copenhagen.

Stocks of each polysaccharide were made by mixing 10 mg of each polysaccharide with SDW (1 mL).

3.2.3 Incubation of enzyme extract with defined polysaccharide extracts

Each defined polysaccharide standard (10 mg/mL) was diluted to 5 mg/mL. In a qPCR 96-well plate, each of 9 standards used (1 µl) was mixed with enzyme extract (4 µl) from relevant enzyme extract mixed with buffer, for final polysaccharide concentration of 1 mg/mL. This results in enzyme activity tested against 9 substrates in 4 different conditions. The 4 conditions the bacteria being raised on glycerol or xylan, then the enzymes from the supernatant being mixed with succinate or HEPPS. Additional sets of substrates were mixed with the succinate and HEPPS buffers, to act as control and provide baseline readings. Buffers were also mixed with enzyme extract as an additional control for polysaccharide presence in the media. The 96-well plate was incubated in a heated shaking block (29 °C, 200 rpm, 24 hrs).

3.2.4 Preparation and printing of microarrays

The incubated samples from the 96 well-plate were directly loaded as the first dilution due to the already low concentration of polysaccharide present in the mixture (1 mg/mL), which is expected to be lower after enzymatic digestion. Following dilutions were made following methods outlined in 2.2.4.

3.2.5 Monoclonal Antibody Probing of Arrays

The arrays were removed from the plates and washed in 5 % Milk TBST solution (30 mins). The microarrays were placed in clean multi-well plates, submerged in 5 % Milk TBST solution (300 µl). Selection of primary monoclonal antibodies (see Table 3.1 for epitope specificity) were added individually to each of the microarrays, and the probing protocol outlined in 2.2.4 was followed.

3.2.6 Analysis

Microarrays were handled and analysed following the method outlined in 2.2.4.

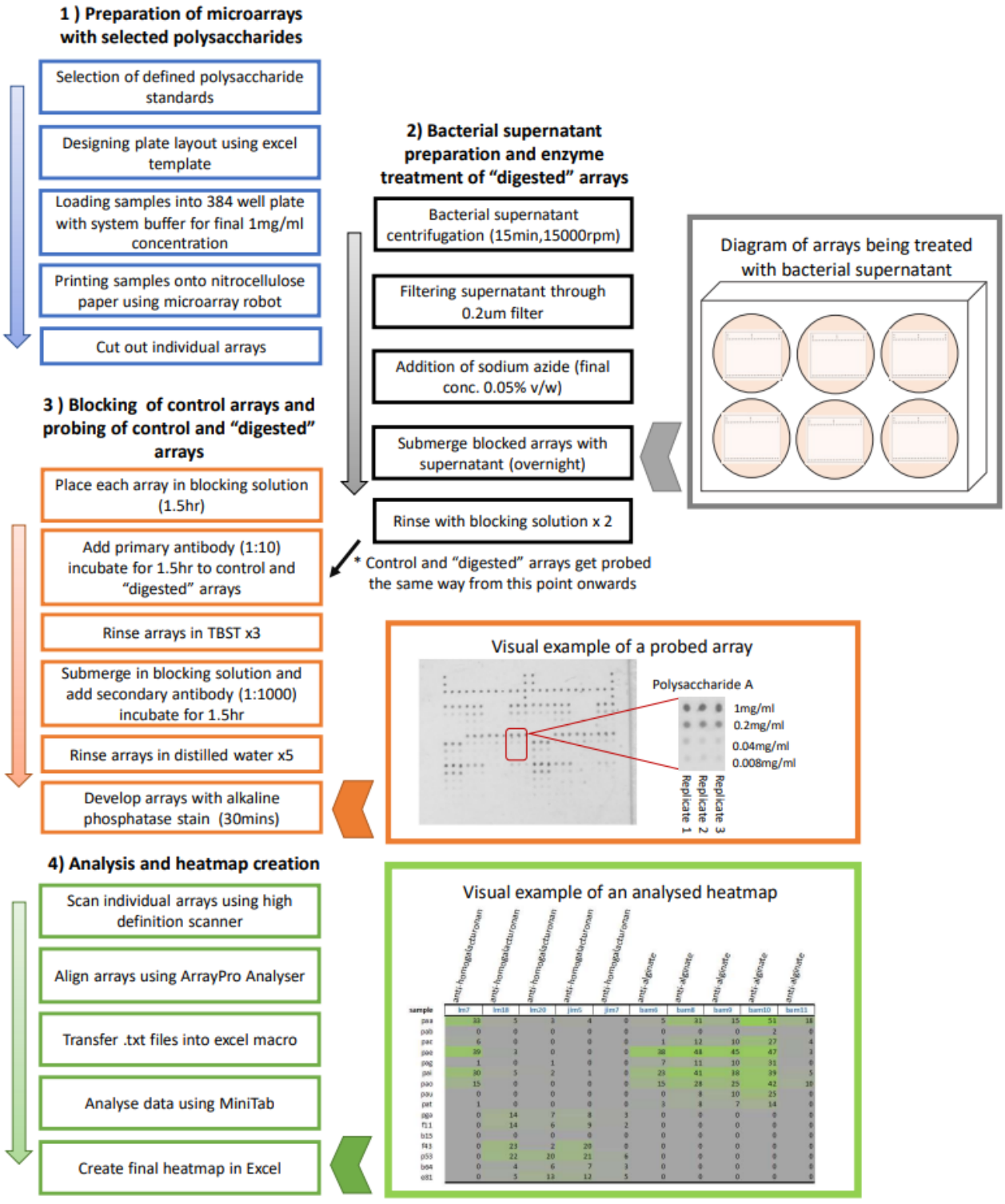

Figure 3.1. Flowchart providing overview of methodology used to investigate enzymatic activity secreted by *P.syringae* pathovars as seen in Figure 3.5. Blue section (1) of the flowchart shows steps taken during preparatrion and priting of the microarrays. Black/grey section (2) of the flowchart shows steps taken during enzymatic treatment with the bacterial supernatant of the individual arrays, with a diagram showing how they are treated. The control and "digested" array are then probed, as seen in the orange section (3), with an example of a probed individual array. The arrays are then analysed as outlined in the green section (4), with the outcome being a heatmap also shown in the flowchart.

Table 3.1. List of primary monoclonal antibodies used for microarray-based screening of bacterial enzymatic activity by tracking epitope changes on defined plant polysaccharides and plant CDTA and NaOH fractions (PlantProbes : Paul Knox Cell Wall Lab, 2021).

Polysaccharide	Code	Epitope
Pectin	JIM5	HG partially/de-esterified
Pectin	JIM7	HG partially/de-esterified
Pectin	LM18	HG partially/de-esterified
Pectin	LM19	HG partially/de-esterified
Pectin	LM20	HG partially/de-esterified
Pectin	LM7	HG/Alginate
RG-I related	LM5	(1→4)-β-D-galactan
RG-I related	LM6	(1→5)-α-L-arabinan
RG-I related	LM13	Linearised (1→5)-α-L-arabinan
RG-I related	LM16	Processed arabinan
Mannan	LM21	(1→4)-β-D-(galacto)(gluco)mannan
Xyloglucan	LM15	Xyloglucan (XXXG motif)
Xyloglucan	LM25	Xyloglucan / unsubstituted β-D-glucan
Xylan	LM10	(1→4)-β-D-xylan
Xylan	LM11	(1→4)-β-D-xylan/arabinoxylan
Xylan	LM28	Glucuronoxylan
Extensin	LM1	Extensin
AGP	LM2	AGP, β-linked GlcA
Alginate	BAM6	Mannuronate-guluronate
Alginate	BAM7	Mannuronate-guluronate
Alginate	BAM8	Mannuronate-guluronate
Alginate	BAM9	Mannuronate-guluronate

3.3 Results & Discussion

Bacterial enzymatic supernatant was produced by precipitation with ammonium sulphate and dialysed to remove excess salts. Enzymes that were now dialysed, were lyophilised in order to concentrate the sample, and reconstituted with 0.1 M sodium succinate. Sodium succinate was used due to succinic acid having many biological roles as metabolic intermediates, involved in ATP synthesis, playing a key role in cellular metabolism (Giorgi-Coll et al., 2017).

A)

Substrate	Control VS Digested	Anti-extensin LM1	Anti-arabinogalactan-protein LM2	Anti-(1-4)-b-D-galactan LM5	Anti-(1-5)-a-L-arabinan LM6	Anti-homogalacturonan LM7	Anti-xylan LM10	Anti-xylan / arabinoxylan LM11	Anti-(1-5)-a-L-arabinan (linear) LM13	Anti-xyloglucan LM15	Anti-processed arabinan /RG-I LM16	Anti-homogalacturonan LM18	Anti-homogalacturonan LM19	Anti-homogalacturonan LM20	Anti-mannan LM21	Anti-xyloglucan LM25	Anti-glucuronoxylan LM28	HG partially/de-esterified JIM5	HG partially/de-esterified JIM7
ArabinoXylan	Control	0	0	0	3	0	0	40	0	0	0	0	0	0	0	0	0	0	0
ArabinoXylan	Digested	0	0	0	6	0	0	48	0	0	0	0	0	0	0	0	2	0	0
β-Glucan	Control	0	0	0	0	0	0	1	0	0	0	0	0	0	20	0	0	0	0
β-Glucan	Digested	0	0	0	0	0	0	0	0	0	0	0	0	0	17	0	0	0	0
Galactan	Control	4	0	29	65	72	0	0	1	0	0	42	0	0	0	0	16	2	0
Galactan	Digested	4	0	32	66	82	0	0	0	0	0	50	0	1	0	0	12	0	0
GMM3	Control	0	0	0	0	0	0	1	0	0	0	0	0	0	0	3	0	0	0
GMM3	Digested	0	0	0	0	0	0	0	0	0	0	0	0	0	0	3	0	0	0
Pectin	Control	7	6	7	0	0	0	0	0	0	9	25	29	32	0	6	0	34	19
Pectin	Digested	11	5	9	0	0	0	1	0	0	9	22	27	31	0	7	0	31	21
Polygalacturonic Acid	Control	18	0	20	13	0	0	0	0	0	26	8	22	0	0	10	1	0	0
Polygalacturonic Acid	Digested	14	0	19	14	0	0	0	0	0	24	13	25	0	0	12	0	0	0
Rhamnogalacturonan	Control	5	0	3	0	0	0	0	0	0	0	0	0	0	0	0	0	0	0
Rhamnogalacturonan	Digested	6	0	5	0	0	0	1	0	0	0	0	0	0	0	0	0	0	0
XyloBiose	Control	0	0	0	0	0	0	0	0	0	0	0	0	0	0	0	0	0	0
XyloBiose	Digested	0	0	0	0	0	1	0	0	0	0	0	0	0	0	0	0	0	0
Xyloglucan	Control	0	0	4	10	0	0	0	0	52	0	0	0	0	0	84	0	0	0
Xyloglucan	Digested	0	0	7	16	0	0	0	0	63	0	0	3	0	0	100	1	0	0

0 100

B)

Substrate	LM1	LM2	LM5	LM6	LM7	LM10	LM11	LM13	LM15	LM16	LM18	LM19	LM20	LM21	LM25	LM28	JIM5	JIM7
ArabinoXylan	0	0	0	0	1.73	0	0	1.20	0	0	0	0	0	0	0	0	0	0
β-Glucan	0	0	0	0	0	0	0	0	0	0	0	0	0	0	0.84	0	0	0
Galactan	0	1.00	0	1.11	1.00	1.13	0	0	0	0	0	1.20	0	0	0	0	0.74	0
GMM3	0	0	0	0	0	0	0	0	0	0	0	0	0	0	0	1	0	0
Pectin	0	1.56	0.84	1.38	0	0	0	0	0	0	1	0.88	0.91	0.95	0	1.18	0	0.92
Polygalacturonic Acid	0	0.74	0	0.94	1.07	0	0	0	0	0	0.92	1.56	1.15	0	0	1.19	0	0
XyloBiose	0	0	0	0	0	0	0	0	0	0	0	0	0	0	0	0	0	0
Xyloglucan	0	0	0	1.61	1.59	0	0	0	0	1.20	0	0	0	0	0	1.20	0	0

C)

Substrate	LM1	LM2	LM5	LM6	LM7	LM10	LM11	LM13	LM15	LM16	LM18	LM19	LM20	LM21	LM25	LM28	JIM5	JIM7
ArabinoXylan	0	0	0	3	0	0	8	0	0	0	0	0	0	0	0	2	0	0
β-Glucan	0	0	0	0	0	0	-1	0	0	0	0	0	0	-3	0	0	0	0
Galactan	0	0	3	0	9	0	0	-1	0	0	8	0	1	0	0	-4	-2	0
GMM3	0	0	0	0	0	0	-1	0	0	0	0	0	0	0	0	0	0	0
Pectin	4	-1	3	0	0	0	1	0	0	0	-3	-3	-2	0	1	0	-3	2
Polygalacturonic Acid	-5	0	-1	1	0	0	0	0	0	-2	5	3	0	0	2	-1	0	0
Rhamnogalacturonan	2	0	2	0	0	0	1	0	0	0	0	0	0	0	0	0	0	0
XyloBiose	0	0	0	0	0	1	0	0	0	0	0	0	0	0	0	0	0	0
Xyloglucan	0	0	3	6	0	0	0	0	11	0	0	3	0	0	16	1	0	0

-100 -90 -80 -70 -60 -50 -40 -30 -20 -10 0 10 20 30 40 50 60 70 80 90 100

Figure 3.2. A) Using bacteria supernatant (NCPPB 385), grown on rich media to test for epitope depletion. Bacteria supernatant was precipitated using ammonium phosphate (95 % saturation), reconstituted, and dialysed for 24 h 4 ˚C in a 3500 mW membrane. Enzymes were freeze dried and reconstituted in 0.1 M sodium succinate. Enzyme extract was mixed with defined standard polysaccharides to test for any carbohydrate active enzymes.

B) Data shown in Figure 3.2 B), represented as a fold change heatmap. Experimental conditions, aka bacteria digested supernatant was divided by the control conditions. (E / C = fold change). Raw data was used for 3.2 B), unlike 3.2 A) where the data is normalised.

C) Same data presented in a different way. Values in Figure 3.2 C) shown as a percentage, they were subtracted from each other. The control values were subtracted from the experimental (digested) values to show percentage of epitope depleted (E – C = % of epitope change). This results in a representative visualisation of the data.

The heatmap produced by using the standard analysis method offers insight as to what the values are for each polysaccharide standard before and after the enzyme treatment from bacterial supernatant. Figure 3.2A only has 2 colour range, grey to green, this makes seeing

any key differences quite difficult. A new method of presenting the data had to be explored. When considering other data sets of similar nature, a fold change heatmap was done in Figure 3.2B. Fold change heat maps were successfully used to present epitope depletion data (Vidal-Melgosa et al., 2015), however the nature of this experiment was different from previously carried out studies. A fold change heatmap is also not optimal for this data as there were many epitopes and probes that did not show a significant change or showed an increase in intensity binding post-treatment (LM25 binding to xyloglucan after the treatment, Figure 3.2 C).

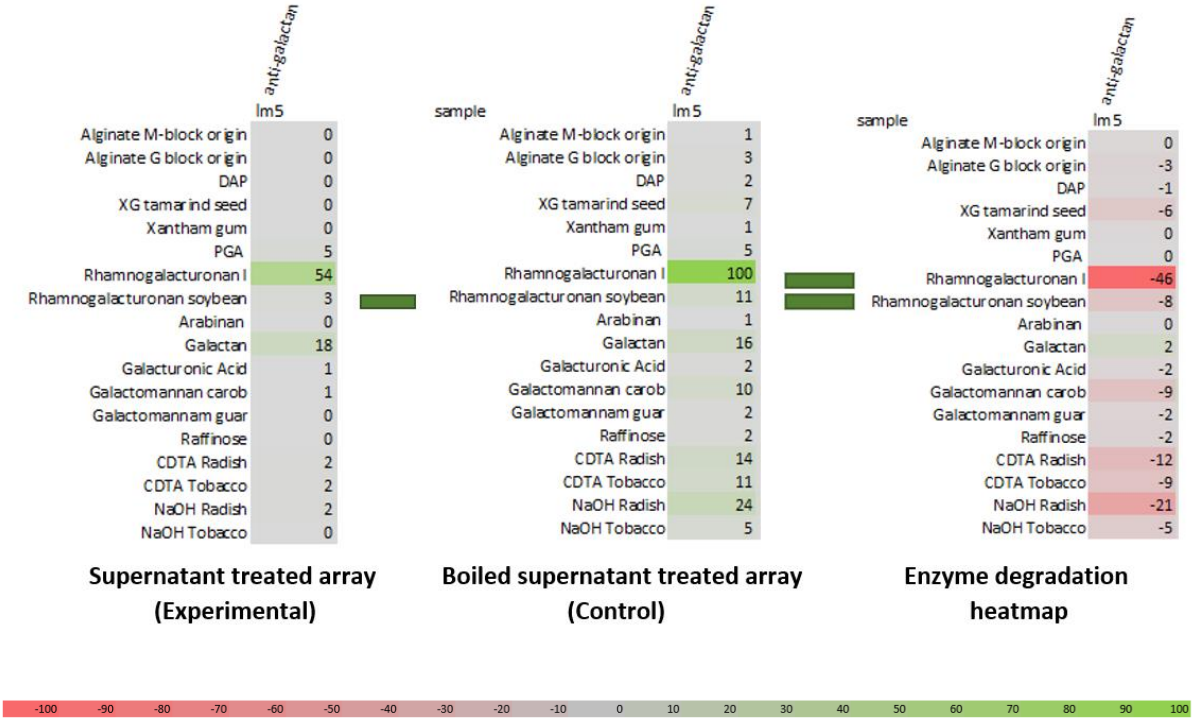

Figure 3.3. Examples of raw data for experimental and control heatmaps. The heatmaps are then subtracted from one another, and conditional formatting with different setting is applied. Lowest values are associated with red, 0 is associated with grey and highest values are associated with green.

A further heatmap was created, showing a percentage change. This was made by subtracting control values from experimental/" digested epitope" values. This method seems to be the most accurate and reliable representation of the data, as it takes into account increases and decreases in antibody binding to the epitopes after the treatment. Both have to be considered, as some of the antibodies, such as JIM5 (anti-homogalacturonan) and JIM7 (anti-homogalacturonan) have a higher binding affinity to partially de-esterified homogalacturonan (HG). Plants naturally produce pectin methyl-esterase as a part of plant cycle (Wolf, Mouille and Pelloux, 2009), however pectinesterases and pectinmethylesterases can also be produced by microorganisms. Some bacteria and fungi are used for industrial processes, such as juice making for their ability to produce pectinesterases (Singh, Kundu, Das and Banerjee, 2019) .

Despite a relatively small increase in binding intensity, NCPPB 385 may be of industrial importance with its ability to produce enzymatic activity that is in line with pectinesterases.

There are many potential limitations with this study. The simplicity of the carbon source in the media is a likely cause of limited enzymatic secretion of the bacteria. *Pseudomonas aeruginosa* when grown on milk casein, produced proteases in order utilise the proteins as a carbon and nitrogen source (Cezairliyan and Ausubel, 2017). The minimal media solution was used, to alternate carbon sources and illicit different responds from the bacterium. A more complex carbon source or a polysaccharide present in the host plant may stimulate a greater extracellular enzymatic response. With more complex plant polysaccharides used the bacterial output of enzyme activity should also increase (Allison and Vitousek, 2005).

Excessive processing of enzymes, such as repeated freeze thaw that occurred when attempting to concentrate the enzyme is detrimental for enzyme denaturation (Cao, Chen, Cui and Foster, 2003). With the enzyme being exposed to extreme conditions, such as high/low temperatures, high/low pH, biological denaturing agents such as proteases and radiation.

Inducer	Buffer	Substrate	Anti-Galactan LM5	Anti-Arabinan LM6M	Anti-Xylan LM10	Anti-Xylan/Arabinoxyla LM11	Anti-Arabinan/RG I LM16	Anti-Homogalacturonar LM18	Anti-Mannan LM21	anti-Xyloglucan LM25	Anti-Glucuronoxylan LM28	Anti-Alginate BAM6	Anti-Alginate BAM7	Anti-Alginate BAM8
Glycerol	HEPPS	Xylan	18	16	-16	-8	9	0	25	2	-8	0	0	0
Glycerol	Succinate	Xylan	0	0	1	4	-2	0	0	0	3	9	0	14
Xylan	HEPPS	Xylan	0	0	2	23	5	0	0	0	19	0	0	0
Xylan	Succinate	Xylan	45	41	-22	-22	26	0	0	6	-25	0	0	0
Glycerol	HEPPS	Galactan	-44	-25	17	45	-19	0	20	-4	44	0	0	0
Glycerol	Succinate	Galactan	14	-5	0	0	-10	0	0	0	4	2	0	0
Xylan	HEPPS	Galactan	-1	14	17	47	10	0	0	2	42	0	0	0
Xylan	Succinate	Galactan	-74	-55	18	40	-45	0	40	-5	39	0	0	0
Glycerol	HEPPS	Galactomannan	0	0	16	41	1	0	-36	0	41	0	0	0
Glycerol	Succinate	Galactomannan	5	6	0	0	1	-1	17	0	0	0	0	0
Xylan	HEPPS	Galactomannan	2	4	18	40	1	0	2	0	39	0	0	0
Xylan	Succinate	Galactomannan	0	-1	17	42	0	-1	-29	0	44	0	0	0
Glycerol	HEPPS	β-Glucan	0	0	17	46	3	0	0	0	47	0	0	0
Glycerol	Succinate	β-Glucan	0	0	0	1	0	0	-4	0	1	0	0	0
Xylan	HEPPS	β-Glucan	0	0	17	42	0	0	7	0	44	0	0	0
Xylan	Succinate	β-Glucan	0	0	11	31	2	0	-8	0	27	9	0	16
Glycerol	HEPPS	Pachyman	0	3	18	48	3	0	0	0	47	0	0	0
Glycerol	Succinate	Pachyman	0	0	0	3	2	0	0	0	0	23	0	50
Xylan	HEPPS	Pachyman	0	0	16	41	1	0	0	0	39	0	0	0
Xylan	Succinate	Pachyman	0	5	0	0	0	0	0	0	0	14	0	20
Glycerol	HEPPS	Lichenan	0	0	0	4	-2	0	0	0	0	23	0	50
Glycerol	Succinate	Lichenan	0	7	0	0	-4	0	0	0	0	6	0	4
Xylan	HEPPS	Lichenan	0	0	19	50	2	0	0	0	51	0	0	0
Xylan	Succinate	Lichenan	0	5	0	26	-4	0	0	0	3	11	0	15
Glycerol	HEPPS	Arabinan	0	2	0	0	0	0	0	0	0	6	0	4
Glycerol	Succinate	Arabinan	-5	-2	0	36	0	0	0	0	4	17	0	22
Xylan	HEPPS	Arabinan	3	1	13	37	3	1	1	1	34	0	1	0
Xylan	Succinate	Arabinan	-5	0	0	41	0	0	0	0	1	16	0	16
Glycerol	HEPPS	Arabinoxylan (26% db)	3	3	3	7	2	2	1	1	3	9	1	9
Glycerol	Succinate	arabinoxylan (26% db)	0	-5	0	-41	1	4	0	0	-5	12	2	13
Xylan	HEPPS	Arabinoxylan (26% db)	0	3	28	68	3	0	0	0	64	0	0	0
Xylan	Succinate	Arabinoxylan (26% db)	5	1	0	-41	0	7	0	0	-5	32	4	63
Glycerol	HEPPS	RG I	0	0	0	0	0	4	0	0	0	15	1	15
Glycerol	Succinate	RG I	7	8	0	0	0	6	0	0	0	44	5	85
Xylan	HEPPS	RG I	1	0	20	51	3	5	0	0	48	0	2	0
Xylan	Succinate	RG I	29	32	0	0	20	32	0	24	0	28	22	28
Glycerol	HEPPS	RG Mix	7	8	0	0	0	6	0	-2	0	44	5	85
Glycerol	Succinate	RG Mix	41	46	0	0	30	47	0	34	0	14	31	2
Xylan	HEPPS	RG Mix	5	7	20	46	4	5	0	1	44	0	1	0
Xylan	Succinate	RG Mix	13	15	23	47	14	16	0	10	43	2	11	1
Glycerol	HEPPS	PGA	5	-3	0	0	-6	4	0	-5	0	15	3	2
Glycerol	Succinate	PGA	-45	-55	36	72	-25	-35	0	-38	66	0	-31	0
Xylan	HEPPS	PGA	-7	-9	19	52	-8	-8	0	-10	53	0	-10	0
Xylan	Succinate	PGA	-17	-29	24	56	-10	-35	0	-34	51	0	-31	0

Figure 3.4. NCPPB 1957 was grown on either glycerol or xylan (inducer). The supernatant samples containing exogenous enzymes were mixed with buffers, succinate (pH 5) or HEPPS (pH 7.5). The supernatant/buffer mixtures were incubated with substrates overnight. These were then printed and probed. Substrates were also printed onto nitrocellulose membrane, those were treated as controls, from which treatments (i.e., weather bacterium was raised on xylan or glycerol, mixed with succinate or HEPPs and substrate used e.g. Xylan) were subtracted.

The cells in Figure 3.4 highlighted in red, indicated decrease in antibody binding intensity signal. This is most likely caused by microbial enzymatic degradation. Key findings show degradation of galactan and PGA (Polygalacturonic acid), these are both pectic polysaccharides. It can be inferred that *Pseudomonas savastanoi* (NCPPB. 1957) has the ability to produce enzymes extracellularly that are capable of digesting these substrates. Pectate lyase and exopolygalacturonate lyase have been inferred from homology (CAZy - PL7, 2021), however the research confirming this enzymatic activity is very limited for various *P.syringae* pathovars.

There are many cells in Figure 3.4, where the cells have been highlighted green. A brighter, more vibrant green colour indicated an increase in antibody binding intensity. The majority of antibody binding increase can be seen in xylan related probes, such as LM11 (anti-xylan/arabinoxylan) and LM28 (anti-glucuronoxylan). This is most likely caused by excess presence of xylan present within the media. Despite a control being printed containing supernatant from the bacterial broth to account for base xylan amount, the data still shows excess xylan that the probes are binding to across many samples.

There are also various samples where hemi-cellulosic polysaccharide, xylan, is being detected by LM5 (anti-galactan) probe under acidic conditions even when the bacterium was grown on xylan. This may be due to impurities within the defined polysaccharides, or the binding of the molecular probes was affected by the pH within the samples printed onto the nitrocellulose. Within this data, there are many examples of unexpected increase in binding intensity, most of the increases of binding intensity can be observed in LM11, LM28, BAM6, BAM7, and BAM8. The BAM antibodies bind to alginate related epitopes (Torode et al., 2016) (see Table 3.1.), with no alginate being introduced to the media or having been used as a substrate for the enzymes, the alginate must be introduced into the reaction by the bacteria. Though this was not the primary objective of the experiment, the assay was able to highlight the bacteria's ability produce alginate synthase. This enzyme has been noted to have been produced from *Pseudomonas syringae pv. syringae*, however its activity has not been confirmed from other pathovars (Fakhr, Peñaloza-Vázquez, Chakrabarty and Bender, 1999).

A lot of unusual binding may be a result of epitope unmasking which has been previously noted when working with complex plant polysaccharides (Leroux et al., 2015). Xyloglucan is highly associated with pectin in plant cell walls (Marcus et al., 2008), upon enzymatic

treatment or exposure to acidic or alkaline environment it is possible that epitopes that were previously undetectable, are now exposed. Another key component of plant cell wall is rhamnogalacturonan, the rhamnogalacturonan backbone is primarily made up of alternating α-D-galacturonic acid and α-L-rhamnosyl residues with extensive branching of galactans, arabinogalactans and arabinans (Harris, 2009). LM5 binds to galactan analogues and linear galactan (Andersen et al., 2016), it is possible that xylan had rhamnogalacturonan impurities that LM5 reacted with.

This method would be an effective screening assay for enzyme activity, however the carbon source in the media is interfering with the molecular probes. It would be possible to use this method for alternative investigations that do not focus on carbohydrates degradation, or by using a microorganism that can survive without a carbon source such as chemolithotrophs (Ye et al., 2017). Alternatively, this can be extrapolated to study the microorganism's ability to produce any extracellular enzymes that can be detected with probes that are not related to carbohydrates or anything in the media composition. By careful design and use of specific carbon sources, it is possible to exclude e.g., all anti-xylan probes, however when studying plant pathogenesis, it is too limiting to exclude such a key carbohydrate. Xylan is one of the most abundant biopolymers on earth, as it is a type of hemicellulose that makes up major cell wall components in most plants, such as dicots and grasses (Mellerowicz and Gorshkova, 2011).

Further method development is necessary in order to fulfil the initial requirement of the experiment. Excluding carbon source from media is not a viable option as *Pseudomonas* pathovars require carbon to fuel all intracellular metabolic processes, such as DNA synthesis etc. With the microarray robot printing the polysaccharides via non-contract printing, an idea was explored the arrays with polysaccharides can be used directly with crude enzyme extract via submersion.

A subsequent experiment was designed, following methods listed in 2.2.3. NCPPB 1957 was grown using multiple carbon sources as inducers, and the bacterial broth supernatant was prepared by centrifugation, filtration through a 0.2 μM filter and addition of sodium azide. These steps were taken to prevent any further bacterial growth, only the enzymes that were produced by stimulation via polysaccharide of choice in media, should be present in this crude enzyme extract.

This crude bacterial enzyme extract was then directly applied onto nitrocellulose arrays with defined polysaccharides printed onto the surface. The arrays can be easily printed in large quantities using an automated microarray robot, in excess of 1000's of arrays. The arrays are cut out individually with scissors and are kept in sets. Each set is used for a different set of conditions, i.e., control, bacteria NCPPB 2716 grown up on PGA (polygalacturonic acid), bacteria NCPPB 2716 grown up on xylan, bacteria NCPPB 281 grown up on PGA and bacteria NCPPB 281 grown up on xylan. These 5 sets of arrays are initially blocked in 2 % Milk TBST solution, to block all nonspecific binding site, i.e., nitrocellulose with no sample printed onto it. Once blocked, the arrays are rinsed in TSB to remove all excess milk, then they are ready to be covered with the crude microbial enzyme extract. Once submerged, the arrays are left on a vertical shaker, agitated gently (10 rpm), for 24 h. Once removed from crude enzyme extract, the arrays are rinsed in TBST to prevent components in the media from sticking to the nitrocellulose. The arrays are then put into 2 % Milk TBST solution and primary antibodies of choice are added. As seen in Figure 3.5, antibodies used were BAM7, BAM8, BAM9, LM10, LM11, LM15, LM16, LM18, LM19 and LM20. With alginate synthase activity observed in Figure 3.4, BAM antibodies which are alginate specific were used to explore alginate related activity further. Similarly, as there was a lot of pectin related activity observed in Figure 3.4, pectic antibodies such as LM16, LM18, LM19 and LM20. With xylan being used as a carbon source, and therefore a hypothetical inducer, xylan related probes were also used, namely LM10, LM11 and LM15.

A) Bacterial strain NCPPB 281

PGA as carbon source

Sample	BAM7	BAM8	BAM9	LM5	LM10	LM11	LM15	LM16	LM18	LM19	LM20
PAT	-0.1	0.0	-61.1	-0.1	-1.3	-1.8	-46.2	-53.3	-94.9	-1.3	-25.0
PAG	0.0	-0.1	-35.5	-0.3	-0.8	-1.8	-27.7	-71.2	-70.7	0.0	-25.5
Galactan	0.0	0.0	-25.0	0.0	0.0	-0.7	-18.8	-58.6	-50.5	-10.6	-10.6
Polygalacturonic Acid	-0.2	-2.7	-47.0	-0.4	-1.5	-7.7	-27.5	-38.6	-72.1	-32.3	-25.6
Xylan	-0.1	-8.9	0.0	0.0	-2.4	-0.2	-4.4	0.0	0.0	0.0	0.0
Lime Pectin - P16	-0.1	-9.3	-28.1	-0.1	-2.0	0.0	-12.6	0.0	-5.3	0.0	-0.1
Lime Pectin - F43	0.0	-4.0	-0.6	0.0	0.0	-0.2	0.0	-0.4	-0.8	-0.4	-0.7
Lime Pectin - E81	0.0	-1.3	-0.1	0.0	-0.9	0.0	0.0	-0.2	-0.7	-0.6	0.0

Xylan as carbon source

Sample	BAM7	BAM8	BAM9	LM5	LM10	LM11	LM15	LM16	LM18	LM19	LM20
PAT	-0.5	0.0	-23.9	-0.8	-2.0	-0.5	-48.9	0.0	-1.2	-10.4	-4.7
PAG	-0.2	-0.1	-19.1	-0.3	-2.1	-2.0	-29.8	-9.3	0.0	0.0	-6.7
Galactan	0.0	-0.4	-11.6	-0.1	-0.6	0.0	-19.9	-0.4	0.0	-10.7	0.0
Polygalacturonic Acid	-0.2	-2.4	-6.0	-0.2	-1.3	-1.6	-30.0	0.0	0.0	-31.8	-11.0
Xylan	-0.1	-8.8	-0.1	-46.9	-60.2	-0.1	-4.5	-0.1	0.0	0.0	-0.5
Lime Pectin - P16	-0.1	-9.0	-13.4	-1.2	-2.9	0.0	-13.8	0.0	0.0	0.0	0.0
Lime Pectin - F43	0.0	-1.8	-0.5	0.0	-0.3	-0.2	0.0	0.0	0.0	-0.3	0.0
Lime Pectin - E81	0.0	0.0	-0.4	0.0	-0.8	0.0	0.0	-0.3	-0.1	-0.3	0.0

B) Bacterial strain NCPPB 2716

PGA as carbon source

Sample	BAM7	BAM8	BAM9	LM5	LM10	LM11	LM15	LM16	LM18	LM19	LM20
PAT	-0.6	0.0	-61.3	0.0	-1.4	-1.5	-48.1	-56.4	-99.0	0.0	-26.0
PAG	-0.3	0.0	-36.4	0.0	-1.6	-2.0	-29.8	-74.1	-72.7	0.0	-41.9
Galactan	0.0	0.0	-25.1	0.0	-0.1	-0.7	-19.5	-59.1	-51.1	0.0	-17.9
Polygalacturonic Acid	-0.2	-2.3	-46.5	0.0	-0.2	-6.3	-28.9	-41.9	-74.0	-41.7	-29.2
Xylan	-0.1	-8.9	-0.2	0.0	0.0	0.0	-4.5	0.0	-0.2	-0.1	-0.5
Lime Pectin - P16	-0.2	-9.1	-27.7	0.0	0.0	0.0	-12.9	-0.1	-5.5	-0.1	-0.1
Lime Pectin - F43	0.0	-4.5	-0.7	0.0	0.0	-0.1	0.0	-0.1	-0.9	-1.1	-0.9
Lime Pectin - E81	0.0	-2.3	-0.2	0.0	0.0	0.0	0.0	-0.3	-0.5	-0.6	0.0

Xylan as carbon source

Sample	BAM7	BAM8	BAM9	LM5	LM10	LM11	LM15	LM16	LM18	LM19	LM20
PAT	0.0	0.0	-32.5	-0.7	-2.3	0.0	-47.5	0.0	-10.9	-6.7	0.0
PAG	-0.1	0.0	-27.5	-0.2	-1.6	0.0	-28.6	0.0	0.0	0.0	-7.0
Galactan	-0.1	0.0	-10.6	0.0	-0.2	0.0	-19.5	0.0	0.0	-9.7	0.0
Polygalacturonic Acid	-0.1	0.0	-11.8	-0.3	-1.7	-1.5	-29.5	-4.7	0.0	-32.1	0.0
Xylan	-0.1	0.0	-0.4	-37.3	-60.3	-0.1	-4.4	0.0	0.0	-0.1	-0.5
Lime Pectin - P16	-0.1	0.0	-20.1	-0.7	-2.6	0.0	-12.8	0.0	0.0	-0.1	0.0
Lime Pectin - F43	0.0	0.0	-0.8	0.0	-0.2	-0.2	0.0	0.0	0.0	-1.0	0.0
Lime Pectin - E81	0.0	0.0	-0.3	0.0	-0.6	0.0	0.0	-0.4	0.0	-0.6	0.0

-100	-90	-80	-70	-60	-50	-40	-30	-20	-10	0

Figure 3.5. Heatmaps comparing enzymatic activity excreted by two pathogenic *Pseudomonas* pathovars, NCPPB 281 and NCPPB 2716.
Both of these pathovars were grown on two different carbon sources, PGA and Xylan. Arrays were prepared with defined polysaccharides printed on nitrocellulose following the standard methodology listed in chapter 1. Selection of pectin related defined polysaccharides were selected – galactan, PGA, Lime Pectin – P16, F43 and E81, defined alginate polysaccharides PAT, PAG and xylan (beech wood). The data was analysed as proposed by method development proposed and showed in Figure 3.2. Antibodies were selected to express binding to selected defined polysaccharide samples, BAM7, BAM8, BAM9, LM5, LM10, LM11, LM15, LM16, LM18, LM19 and LM20. See Table 3.1 for antibody epitope specificities.

The sample was filtered through a 0.2 μm filter, this process is a common a technique in microbiology used to sterilise media. Though it has been proven to not be viable for all microorganisms (Hahn, 2004), *Pseudomonas syringae* cells have the average length of 1.25

μm (Monier and Lindow, 2003). This process should be sufficient for removing of all *Pseudomonas syringae* cells and preventing them from interacting with defined polysaccharides printed onto the nitrocellulose membrane. The samples are mixed with running buffer, that contains Triton x-100 and Tween-20, both of which have antimicrobial properties (Ma et al., 2020). Once the arrays are incubated with crude enzyme extract the concentration of these antimicrobials might become too diluted to be effective. An addition of sodium azide was made, due to its antimicrobial properties, a concentration of 0.05 % was used due to it being successfully used as a sterilisation method in literature alongside other measures (Wolf, Dao, Scott and Lavy, 1989). This concentration should inhibit any further bacterial growth of *Pseudomonas* pathovars or contamination from environment.

In Figure 3.5, activity related to BAM9 is relatively similar between two different inducers (carbon source in media), meaning alginate lyase activity is likely to be cause as a response to a changing carbon source and should be produced by bacteria in all minimal media, possibly even rich media.

Just as in Figure 3.2. LM5 is showing binding towards xylan, disproving that the pH of buffers has affected the antibody's binding specificity. It is most likely that there are highly associated galactan impurities within the xylan polysaccharide standard. Due to the monoclonal antibodys' high specificity and sensitivity, it is providing a strong signal to minimal amounts of galactan present within the xylan polysaccharide standard (Verhertbruggen et al., 2009).

Activity related to LM15 (anti-xyloglucan) is also very similar between the 2 carbon sources, meaning the bacteria produced xyloglucanases as a response to minimal media, or is always secreted by the bacterium. Meaning NCPPB 281 might be of industrial interest with its ability to secrete xyloglucanases. The same can be said for 2716, as it showed similar activity to 281. The only major difference worth noting is the lessened activity of BAM8 when NCPPB. 2716 was induced by xylan as a carbon source, with BAM9 related activity remaining relatively constant. Both, BAM 8 and BAM9 bind to mannuronate-guluronate epitopes on alginate. This is pointing to specific alginate lyase activity that might differ depending on which pathovar secreted the enzymes.

With xylan related activity only being present amongst two of the bacterial species when grown/ induced by xylan as a carbon source, it emphasises the importance of altering the growth conditions and media in order to get a varied and rich enzymatic activity. Both of the

bacterial strains have shown similar digestion patterns. When grown on PGA, NCPPB 281 was able to produce activity that degraded an epitope on galactan that is recognised by LM19 (anti-homogalacturonan) by approximately 10 %, however this activity was not observed in NCPPB 2716.

When analysing the data of enzymatic responses caused by xylan, there is degradation of epitopes recognised by BAM8, however the values are all under 10 %. The sensitivity of this methodology has not been explored, therefore values below 10 % should not be given much significance. It would be best to focus on more significant results, such as NCPPB 2716 showing activity against PAT as detected by LM18 (-10.9 %) and NCPPB 281 showing activity against polygalacturonic acid as detected by LM20 (-11 %).

The differences in enzyme secretion might be a key to using this methodology as a way of differentiating between the *Pseudomonas syringae* pathovars. The alteration of methodology for screening for enzyme activity has yielded good results, however, to be able to use this methodology for pathovar differentiation, much more method development is necessary. In order to make this a viable screening method for pathovars, initial studies would need to look at approximately 20 pathovars to find consistent differences and similarities between pathovars. Each of the sets of pathovars would require a minimum of 2 sets of arrays (2 x 12), requiring an overall 480 arrays to investigate 20 pathovars, each grown on 2 different carbon sources, plus an extra set to act as a control and a baseline, bringing the total up to 492. In order to carry out probing of such a large number of arrays, different lot number of antibodies would be used, and intra-batch variability might introduce differences, that might be interpreted as pathovar specific (Bordeaux et al., 2010). Additional experiments can be carried out to ensure the same performance of antibodies between different batch numbers, however study was not feasible at this moment in time, due to its large scale, time and budget were the limiting factors.

With heatmaps overwhelming the reader with a complex data set forcing the reader to look between multiple heatmaps to get a good grasp on the different activities and what factors may have an effect on the results, it was deemed as an inefficient way to highlight key findings. Bar charts were explored as a way of simplifying data presentation.

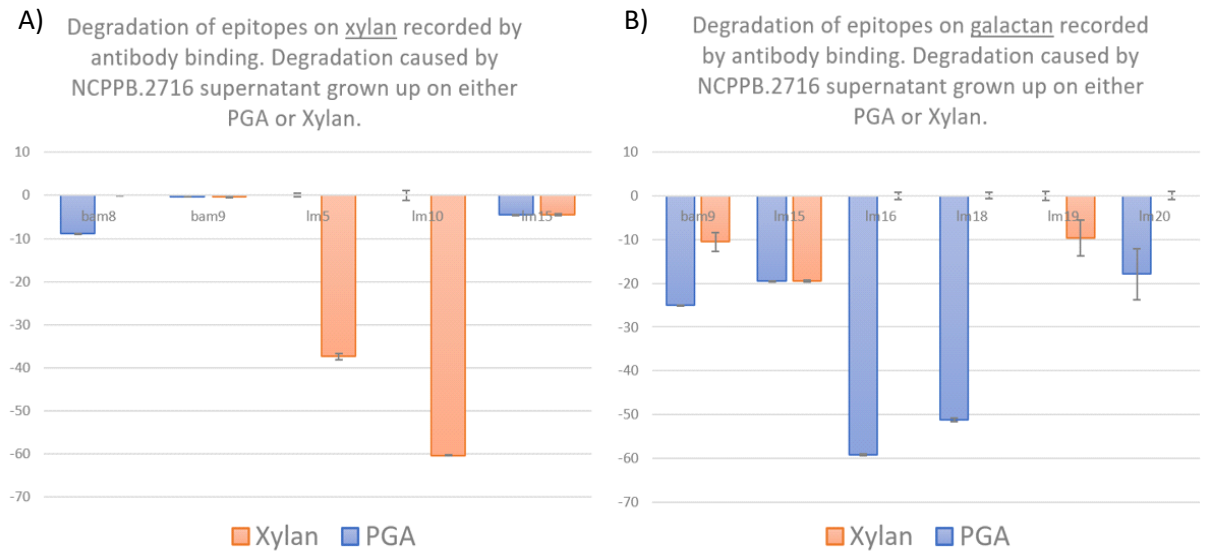

Figure 3.6. Bar charts representing differences brought out in NCPPB 2716 by the selected inducer used in the media, PGA (polygalacturonic acid) or xylan. Bar chart A) , shows degradation of epitopes on xylan recorded by antibody listed in Figure 3.6 A). Degradation caused by NCPPB. 2716 supernatant grown on either PGA (blue) or xylan (orange). The bar chart B) shows degradation of epitopes on galactan recorded by antibody listed in Figure 3.6 B). Degradation caused by NCPPB. 2716 supernatant grown on either PGA (blue) or xylan (orange). The bar chart in orange represents changes caused by NCPPB 2716 that was induced by xylan, and blue columns show changes that were caused by NCPPB 2716 grown on PGA.

Results observed in Figure 3.5 and 3.6, highlight what was expected when starting the experiment. Carbon source use in media would results in enzyme activity specific to it, is it more obvious when data is presented in Figure 3.6, as xylan is only degraded when the bacteria is grown on xylan. The changes in the epitopes were detected by LM5 (anti-galactan) and LM10 (anti-xylan).

Due to the nature of this large data set, a bar chart would have to be produced for every defined polysaccharide for each heat map. This would be able to show intricacies of the data, however it would produce 32 bar charts (8 defined polysaccharides x 4 heatmaps). Only a few of the defined polysaccharides can be selected to highlight key finding (see Figure 3.6.), however when continually displaying partial data, a larger picture can be overlooked, and reliability of the data may become skewed.

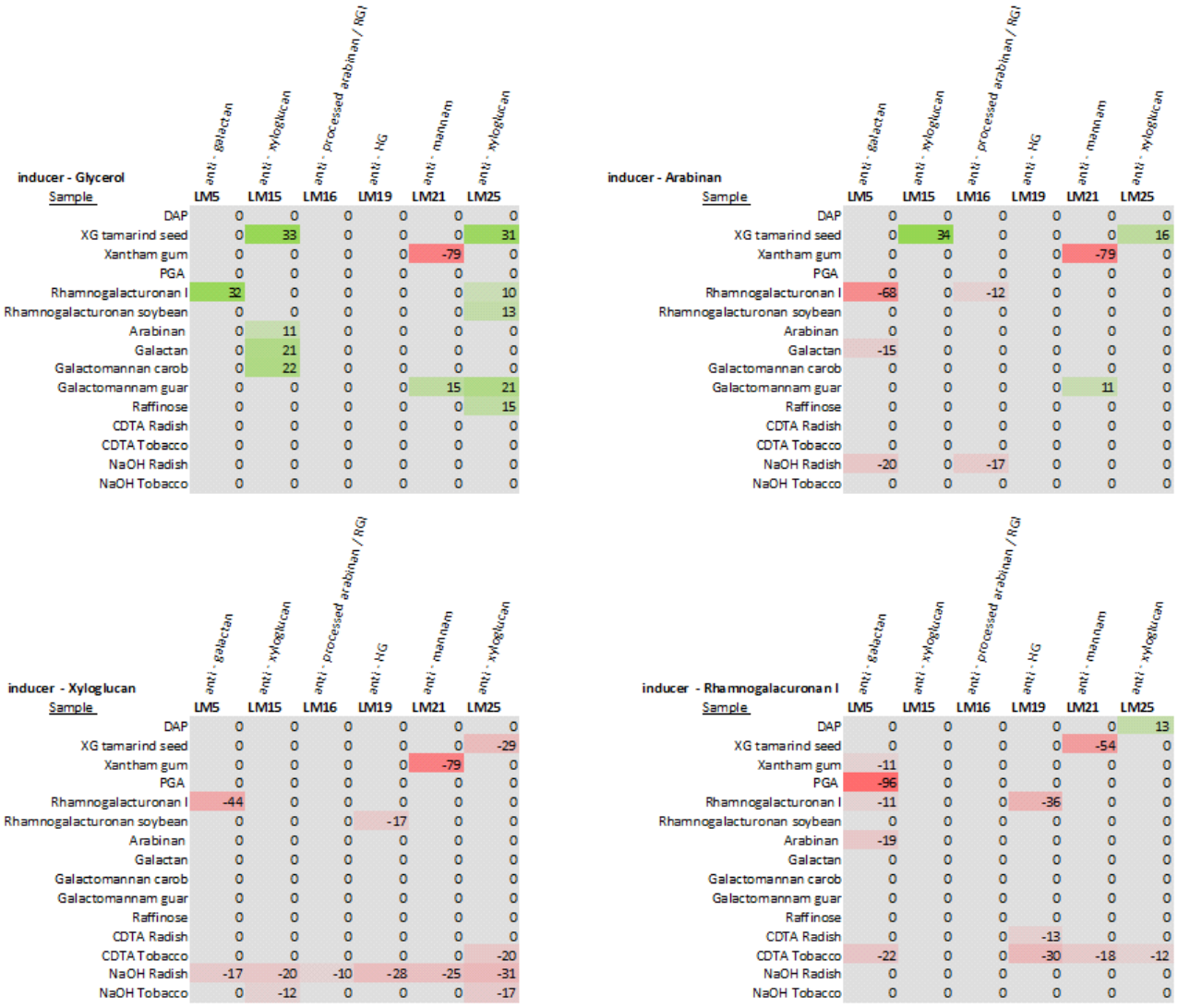

inducer - Glycerol	anti - galactan	anti - xyloglucan	anti - processed arabinan / RGI	anti - HG	anti - mannan	anti - xyloglucan
Sample	LM5	LM15	LM16	LM19	LM21	LM25
DAP	0	0	0	0	0	0
XG tamarind seed	0	33	0	0	0	31
Xantham gum	0	0	0	0	-79	0
PGA	0	0	0	0	0	0
Rhamnogalacturonan I	32	0	0	0	0	10
Rhamnogalacturonan soybean	0	0	0	0	0	13
Arabinan	0	11	0	0	0	0
Galactan	0	21	0	0	0	0
Galactomannan carob	0	22	0	0	0	0
Galactomannam guar	0	0	0	0	15	21
Raffinose	0	0	0	0	0	15
CDTA Radish	0	0	0	0	0	0
CDTA Tobacco	0	0	0	0	0	0
NaOH Radish	0	0	0	0	0	0
NaOH Tobacco	0	0	0	0	0	0

inducer - Arabinan	anti - galactan	anti - xyloglucan	anti - processed arabinan / RGI	anti - HG	anti - mannan	anti - xyloglucan
Sample	LM5	LM15	LM16	LM19	LM21	LM25
DAP	0	0	0	0	0	0
XG tamarind seed	0	34	0	0	0	16
Xantham gum	0	0	0	0	-79	0
PGA	0	0	0	0	0	0
Rhamnogalacturonan I	-68	0	-12	0	0	0
Rhamnogalacturonan soybean	0	0	0	0	0	0
Arabinan	0	0	0	0	0	0
Galactan	-15	0	0	0	0	0
Galactomannan carob	0	0	0	0	0	0
Galactomannam guar	0	0	0	0	11	0
Raffinose	0	0	0	0	0	0
CDTA Radish	0	0	0	0	0	0
CDTA Tobacco	0	0	0	0	0	0
NaOH Radish	-20	0	-17	0	0	0
NaOH Tobacco	0	0	0	0	0	0

inducer - Xyloglucan	anti - galactan	anti - xyloglucan	anti - processed arabinan / RGI	anti - HG	anti - mannan	anti - xyloglucan
Sample	LM5	LM15	LM16	LM19	LM21	LM25
DAP	0	0	0	0	0	0
XG tamarind seed	0	0	0	0	0	-29
Xantham gum	0	0	0	0	-79	0
PGA	0	0	0	0	0	0
Rhamnogalacturonan I	-44	0	0	0	0	0
Rhamnogalacturonan soybean	0	0	0	-17	0	0
Arabinan	0	0	0	0	0	0
Galactan	0	0	0	0	0	0
Galactomannan carob	0	0	0	0	0	0
Galactomannam guar	0	0	0	0	0	0
Raffinose	0	0	0	0	0	0
CDTA Radish	0	0	0	0	0	0
CDTA Tobacco	0	0	0	0	0	-20
NaOH Radish	-17	-20	-10	-28	-25	-31
NaOH Tobacco	0	-12	0	0	0	-17

inducer - Rhamnogalacuronan I	anti - galactan	anti - xyloglucan	anti - processed arabinan / RGI	anti - HG	anti - mannan	anti - xyloglucan
Sample	LM5	LM15	LM16	LM19	LM21	LM25
DAP	0	0	0	0	0	13
XG tamarind seed	0	0	0	0	-54	0
Xantham gum	-11	0	0	0	0	0
PGA	-96	0	0	0	0	0
Rhamnogalacturonan I	-11	0	0	-36	0	0
Rhamnogalacturonan soybean	0	0	0	0	0	0
Arabinan	-19	0	0	0	0	0
Galactan	0	0	0	0	0	0
Galactomannan carob	0	0	0	0	0	0
Galactomannam guar	0	0	0	0	0	0
Raffinose	0	0	0	0	0	0
CDTA Radish	0	0	0	-13	0	0
CDTA Tobacco	-22	0	0	-30	-18	-12
NaOH Radish	0	0	0	0	0	0
NaOH Tobacco	0	0	0	0	0	0

Figure 3.7. NCPPB 1957 was grown on 4 different carbon sources: glycerol, arabinan, xyloglucan and rhamnogalacturonan I. Control supernatant without any carbon sources was left to incubate for the same amount of time, then boiled but heating the tube until liquid reached 100°C. These carbon sources are referred to as inducers, at they are the factor that elicits different responses from the bacteria. A range of defined polysaccharides and plant extracts were printed onto nitrocellulose membrane. When normalising this data set, any values between -10 % and 10 % were excluded. This was done to highlight major activity that was observed on the sample epitopes by the antibodies used.

Whilst glycerol mostly induced pectin related activity, an increase in antibody binding has been noted. Glycerol, arabinan and xyloglucan have induced enzymatic response to xanthan gum, showing the same level of degradation between the 3 inducers. Glycerol has induced enzymatic activity toward xanthan gum, as detected by LM21 (anti-mannan). Xanthan gum is made up of β-1,4-glycosidic bond-linked main chain and a trisaccharide side chain successively

containing mannose, glucuronic acid, and mannose (Hu et al., 2019). High quantity of mannose within xanthan gum may be the reason for cross reactivity of the antibody that was designed for plant cell walls. Xanthan gum is a polysaccharide produced by fermentation of *Xanthomonas campestris,* an endophytic fungus*.* This polysaccharide is of key importance within food industry, as it is used as a thickening agent and a stabiliser (BeMiller, 2019).

There are many instances where an increase in the intensity binding of the antibodies does not have a clear explanation. Due to nature of the assay, it is not known what enzymes are present in the crude enzyme extract, so many of the increased binding intensities may be caused by unknown transferases, esterases, synthases, and so on. Interestingly enough, the majority of the increases in the binding intensities are observed produced by NCPPB 1957 induced by glycerol. When comparing that heatmap to the other three, it is clear that a more complex carbon source induces a more direct enzymatic response.

Including plant extracts has provided additional insight, NCPPB 1957 raised in xyloglucan has produced enzymes that have degraded epitopes on the radish plant NaOH fraction (hemi-cellulosic fraction) of the radish plant, however the activity was much less significant on when compared to tobacco plant NaOH fraction. When comparing that finding to NCPPB induced by rhamnogalacturonan I, the opposite was observed. Pectin related activity was expected, and enzymatic response to CDTA fraction (pectic) of tobacco plant (decrease of antibody binding observed across 4 probes) was more substantial than that of CDTA radish plant fraction (decrease of antibody binding observed in 1 probe).

Enzymatic activity is heavily reliant on the inducer used within the media, the majority of the epitope depletion observed follows a trend of, pectic inducer = pectic enzymatic activity. There is an instance where cross induction is noted, and that is reduction in antibody binding to rhamnogalacturonan I by LM5, when induced by xyloglucan. There was unusual binding associated with LM5 and xylan derived defined polysaccharides (Figure 3.4), so it is also possible for LM5 to be binding to associated xylan within the rhamnogalacturonan I.

An alternative to bar charts has been considered for this data set, a radar chart. Radar chart is a graphical method for presenting multivariate data in form of two- dimensional chart (Chambers, Cleveland, Kleiner and Tukey, 2018). It can represent multiple variables in a way where differences in the data are much more obvious to see. With the need to compare

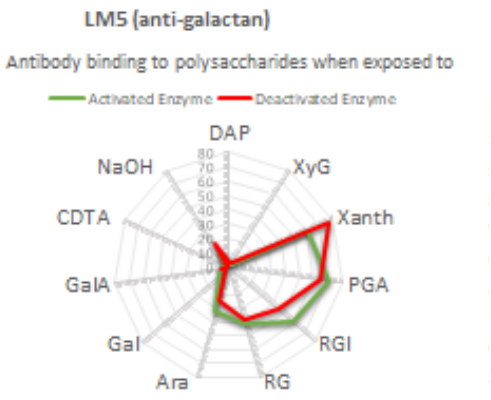

Abbreviation	Full Name
DAP	Defined Alginate Polysaccharide
XyG	Xyloglucan
Xanth	Xanthan Gum
PGA	Polygalacturonic Acid
RG I	Rhamnogalacturonan I
RG	Rhamnogalacturonan
Ara	Arabinan
Gal	Galactan
GalA	Galacturonic Acid
CDTA	CDTA extract from a radish plant
NaOH	NaOH extract from a radish plant
AGP	Arabinogalactan protein
HG	Homogalacturonan

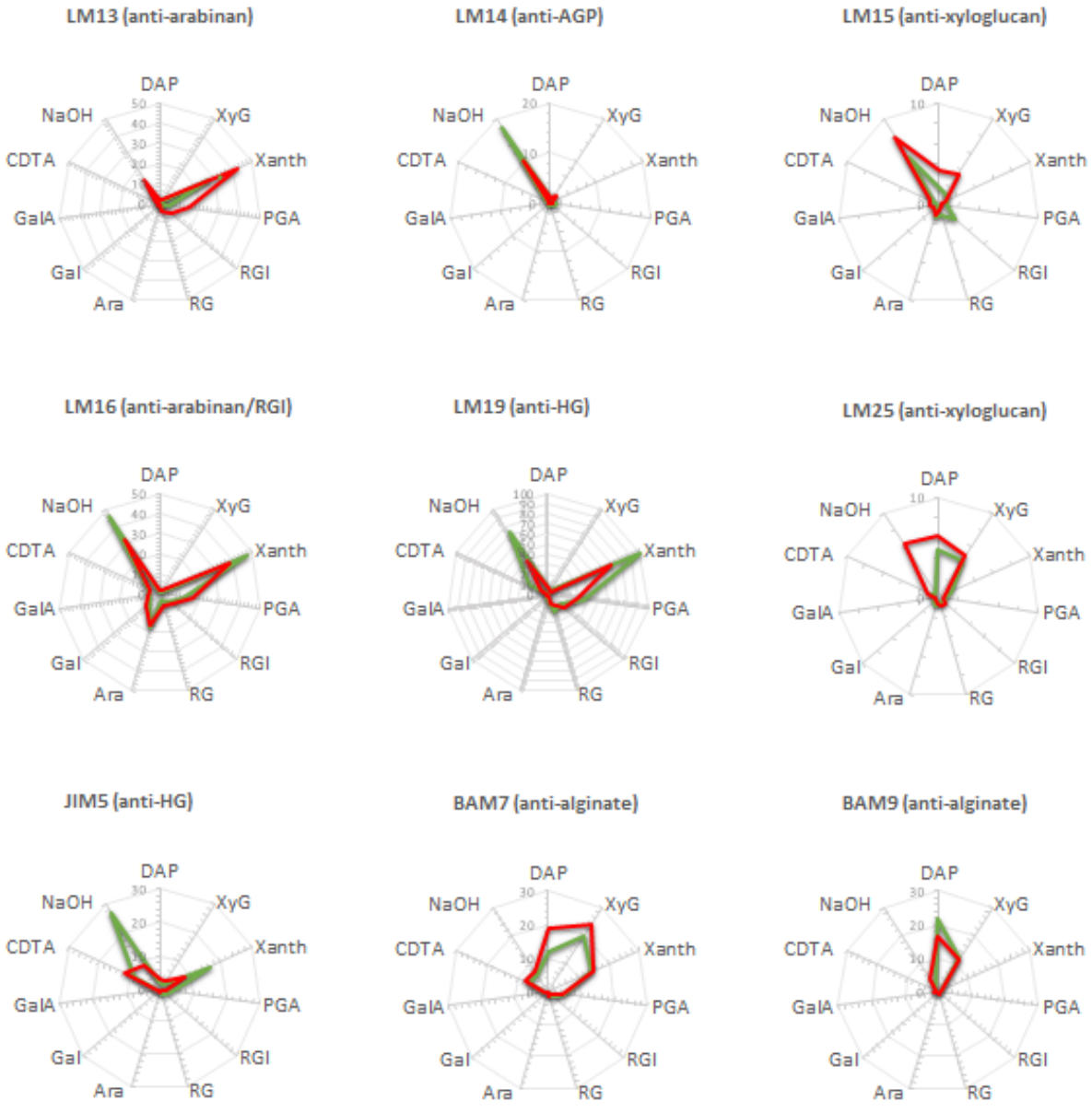

Figure 3.8. Data showing enzyme activity elicited by xyloglucan.
Radar charts showing monoclonal antibody binding values to multiple standard defined polysaccharides. This set of data was treated with supernatant, which contained **xyloglucan**, as a sole carbon source to culture *Pseudomonas savastanoi* (NCPPB 1957). Different lines represent the varying conditions, the inactivated boiled supernatant (red) and active enzymes untreated supernatant (green).

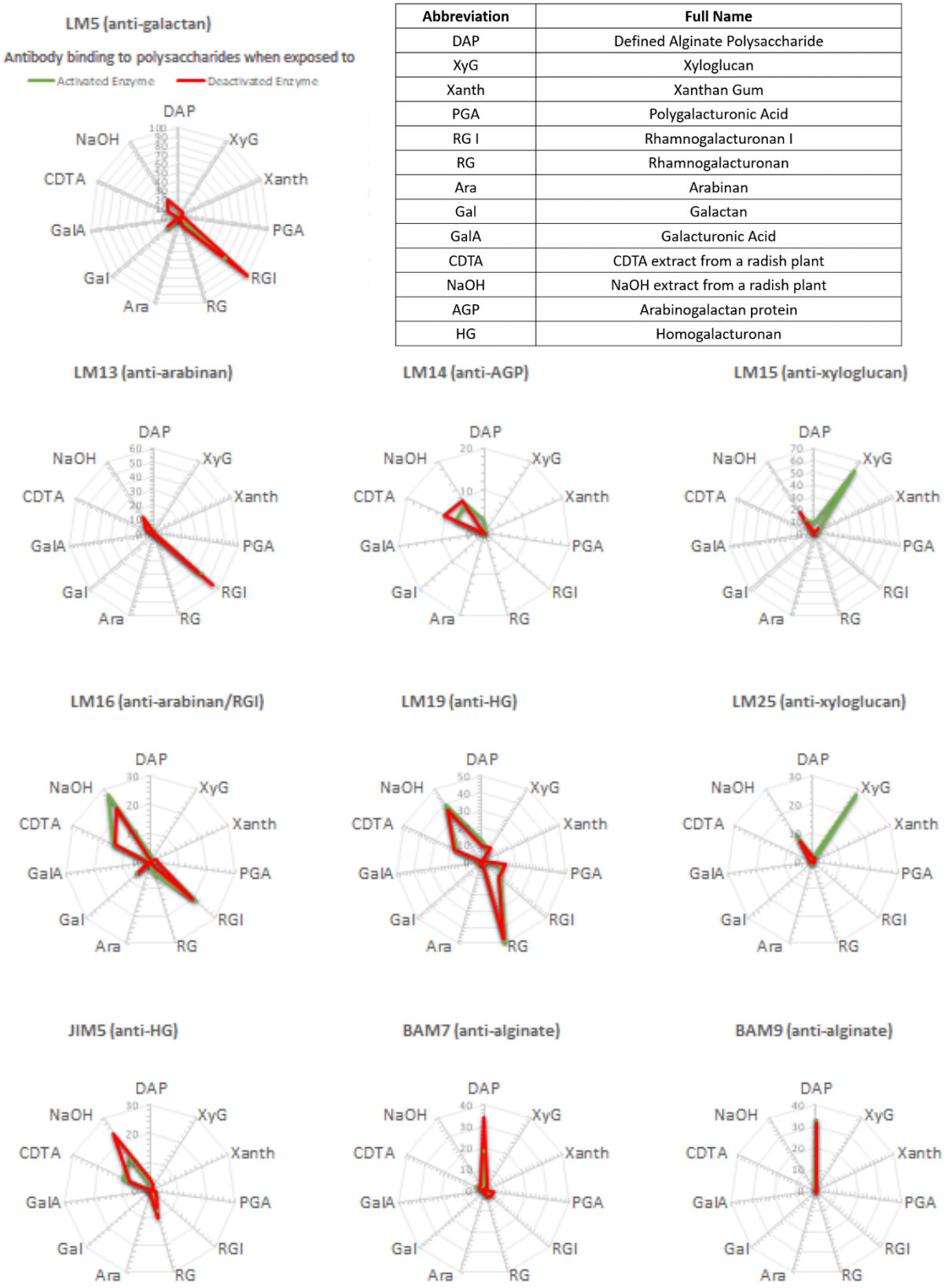

Abbreviation	Full Name
DAP	Defined Alginate Polysaccharide
XyG	Xyloglucan
Xanth	Xanthan Gum
PGA	Polygalacturonic Acid
RG I	Rhamnogalacturonan I
RG	Rhamnogalacturonan
Ara	Arabinan
Gal	Galactan
GalA	Galacturonic Acid
CDTA	CDTA extract from a radish plant
NaOH	NaOH extract from a radish plant
AGP	Arabinogalactan protein
HG	Homogalacturonan

Figure 3.9. Data showing enzyme activity elicited by glycerol. Radar charts showing monoclonal antibody binding values to multiple standard defined polysaccharides. This set of data was treated with supernatant, which contained **glycerol**, as a sole carbon source to culture *Pseudomonas savastanoi* (NCPPB 1957). Different lines represent the varying conditions, the inactivated boiled supernatant (red) and active enzymes untreated supernatant (green).

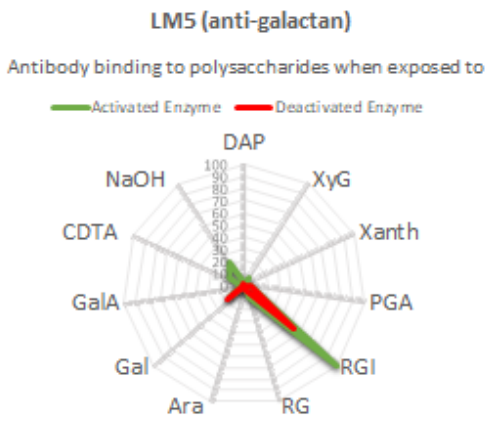

Abbreviation	Full Name
DAP	Defined Alginate Polysaccharide
XyG	Xyloglucan
Xanth	Xanthan Gum
PGA	Polygalacturonic Acid
RG I	Rhamnogalacturonan I
RG	Rhamnogalacturonan
Ara	Arabinan
Gal	Galactan
GalA	Galacturonic Acid
CDTA	CDTA extract from a radish plant
NaOH	NaOH extract from a radish plant
AGP	Arabinogalactan protein
HG	Homogalacturonan

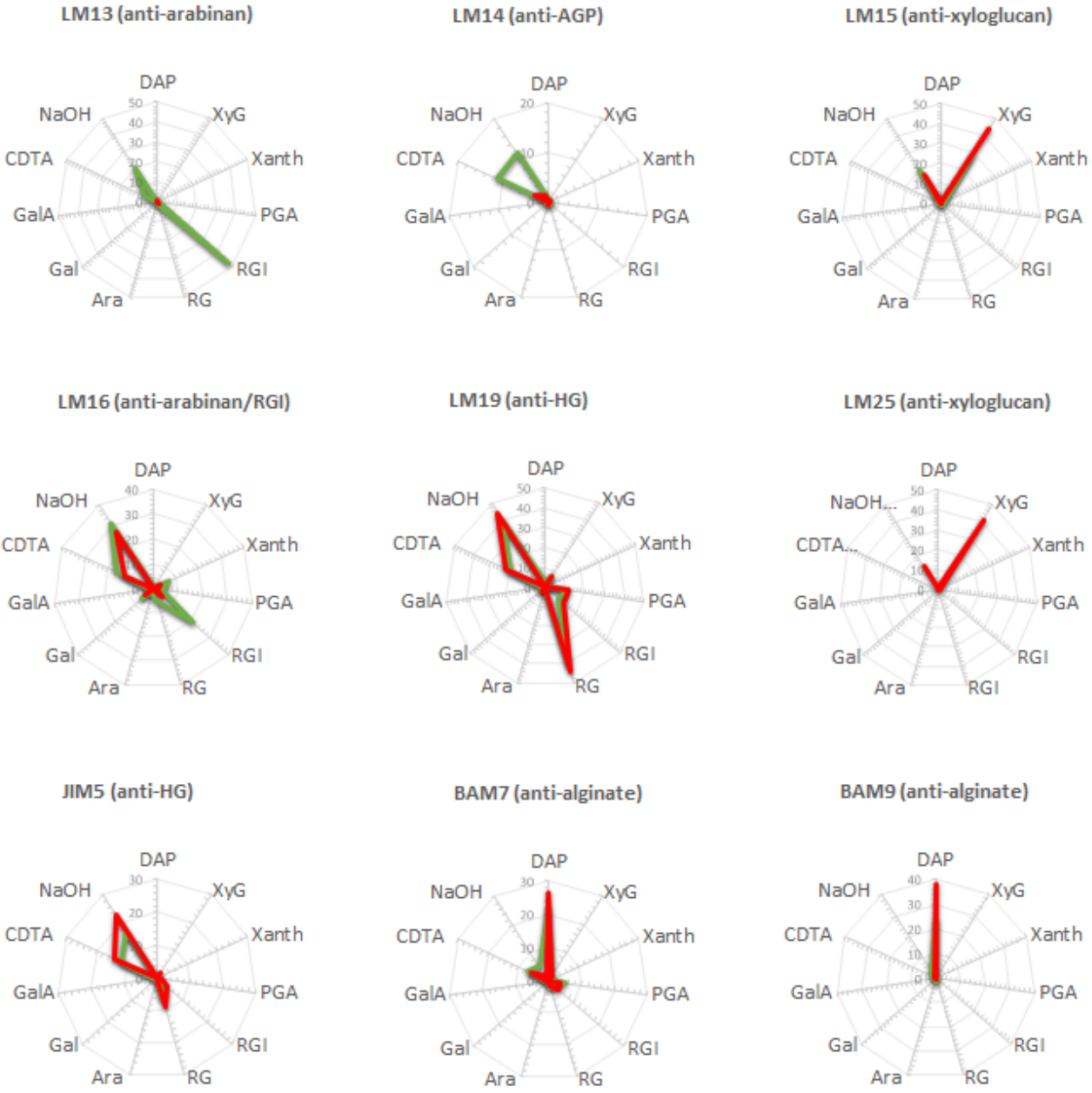

Figure 3.10. Data showing enzyme activity elicited by arabinan. Radar charts showing monoclonal antibody binding values to multiple standard defined polysaccharides. This set of data was treated with supernatant, which contained **arabinan**, as a sole carbon source to culture *Pseudomonas savastanoi* (NCPPB 1957). Different lines represent the varying conditions, the inactivated boiled supernatant (red) and active enzymes untreated supernatant (green).

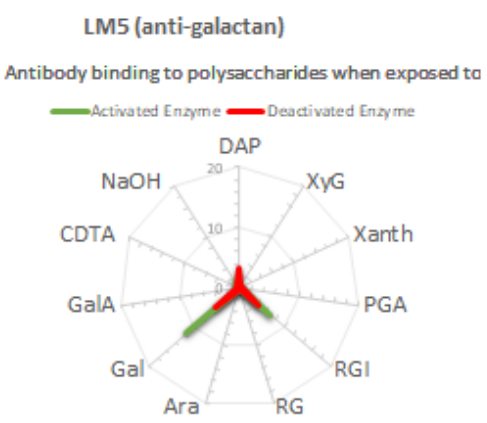

Abbreviation	Full Name
DAP	Defined Alginate Polysaccharide
XyG	Xyloglucan
Xanth	Xanthan Gum
PGA	Polygalacturonic Acid
RG I	Rhamnogalacturonan I
RG	Rhamnogalacturonan
Ara	Arabinan
Gal	Galactan
GalA	Galacturonic Acid
CDTA	CDTA extract from a radish plant
NaOH	NaOH extract from a radish plant
AGP	Arabinogalactan protein
HG	Homogalacturonan

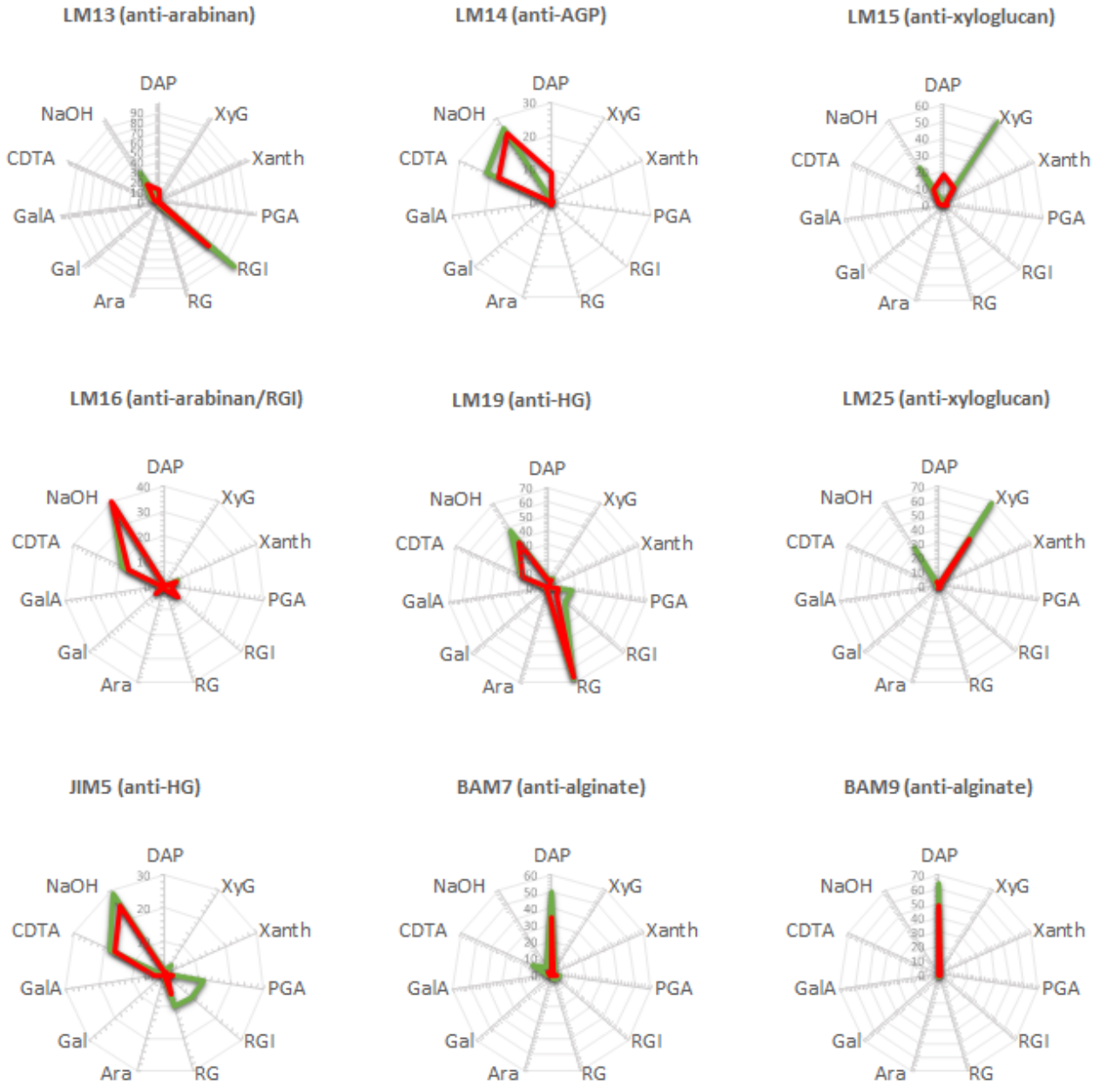

Figure 3.11. Data showing enzyme activity elicited by rhamnogalacturonan I. Radar charts showing monoclonal antibody binding values to multiple standard defined polysaccharides. This set of data was treated with supernatant, which contained **rhamnogalacturonan I**, as a sole carbon source to culture *Pseudomonas savastanoi* (NCPPB 1957). Different lines represent the varying conditions, the inactivated boiled supernatant (red) and active enzymes untreated supernatant (green).

Radar charts are able to highlight to the reader any major activity more easily compared to heatmaps. A sharp peak pointing inwards or outwards of the circular chart, signifies enzymatic activity that has changed antibody binding towards a particular defined polysaccharide. This method of presenting data offers an alternative to the heatmaps that are most commonly used to present carbohydrate microarray polymer profiling (CoMPP) data (Salmeán et al., 2018). The advantage of radar charts, is that both set of data are visible, control (inactive enzyme) and experimental (active enzyme). This provides additional insight in regard to antibody and defined polysaccharide binding and interactions. In some charts, i.e., BAM7 and BAM9 when induced by glycerol, both of the variables overlap and it's difficult to see activated enzyme value. Additional dots have been placed on top of the inactive enzyme reading to signify where the peak of the active enzyme reading is.

Despite radar charts allowing an alternative, they still have to be supplemented by data rich heat-maps. Heat-maps are able to provide exact values at one glance for this approach to epitope depletion.

3.4 Conclusion

Through method development and optimisation, a methodology has been created that can be used for enzyme characterisation. Though enzyme activity may be limited to extracellular enzymes, this methodology has many advantages; it is high-throughput, relatively low cost and generates a lot of data. With the large quantity of data generated across several defined polysaccharides of choice, as well as molecular probes, a lot of specific enzyme activity may be inferred. The simplicity of the methodology allows for adjustments to enzyme screening beyond polysaccharides. Microarray robots are capable of printing proteins, DNA, and other metabolites. By treating the arrays *in-situ* and with use of appropriate probes, tracking the changes of molecules printed is entirely possible. This methodology may be of great interest to industry, by providing alternative sources of enzymes. This may allow the production costs to be reduced and the process optimised.

Enzymatic activity related to polygalacturonic acid, xanthan gum, xyloglucan, CDTA and NaOH plant fractions. These activities were recorded by change of binding of molecular probes post crude enzyme extract treatment when compared to the control. Further work would be required in order to characterise the specific enzyme activity and mode of action.

3.5 Supplementary Figures

inducer	buffer	Substrate	Anti-AGP	Anti-galactan	Anti-arabinan	Anti-xylogalacturonan	Anti-galactan	Anti-xylan	Anti-xylan/arabinoxylan	Anti-arabinan/RGI	Anti-homogalacturonan	Anti-mannan	Anti-xyloglucan	Anti-xylan grass prep	Anti-glucuronoxylan	Anti-homogalacturoanan	Anti-homogalacturoanan	Anti-alginate	Anti-alginate	Anti-alginate	Anti-alginate
			LM2	LM5	LM6M	LM8	LM9	LM10	LM11	LM16	LM18	LM21	LM25	LM27	LM28	JIM5	JIM7	BAM4	BAM6	BAM7	BAM8
Glycerol	HEPPS	Xylan	7	18	16	0	0	-16	-8	9	0	25	2	0	-8	0	0	0	0	0	0
Glycerol	Succinate	Xylan	0	0	0	0	0	1	4	-2	0	0	0	0	3	0	0	0	9	0	14
Xylan	Succinate	Xylan	7	45	41	0	0	-22	-22	26	0	0	6	0	-25	0	0	0	0	0	0
Xylan	HEPPS	Xylan	0	0	0	0	0	2	23	5	0	0	0	0	19	0	0	0	0	0	0
			LM2	LM5	LM6M	LM8	LM9	LM10	LM11	LM16	LM18	LM21	LM25	LM27	LM28	JIM5	JIM7	BAM4	BAM6	BAM7	BAM8
Glycerol	HEPPS	Galactan	-2	-44	-25	0	0	17	45	-19	0	20	-4	0	44	0	0	0	0	0	0
Glycerol	Succinate	Galactan	2	14	-5	0	0	0	0	-10	0	0	0	0	4	0	0	0	2	0	0
Xylan	Succinate	Galactan	-7	-74	-55	0	0	18	40	-45	0	40	-5	0	39	0	0	0	0	0	0
Xylan	HEPPS	Galactan	4	-1	14	0	0	17	47	10	0	0	2	0	42	0	0	0	0	0	0
			LM2	LM5	LM6M	LM8	LM9	LM10	LM11	LM16	LM18	LM21	LM25	LM27	LM28	JIM5	JIM7	BAM4	BAM6	BAM7	BAM8
Glycerol	HEPPS	Galactomannan	0	0	0	0	0	16	41	1	0	-36	0	0	41	0	0	0	0	0	0
Glycerol	Succinate	Galactomannan	-5	5	6	0	0	0	0	1	-1	17	0	0	0	0	0	0	0	0	0
Xylan	Succinate	Galactomannan	-5	0	-1	0	0	17	42	0	-1	-29	0	0	44	0	0	0	0	0	0
Xylan	HEPPS	Galactomannan	4	2	4	0	0	18	40	1	0	2	0	0	39	0	0	0	0	0	0
			LM2	LM5	LM6M	LM8	LM9	LM10	LM11	LM16	LM18	LM21	LM25	LM27	LM28	JIM5	JIM7	BAM4	BAM6	BAM7	BAM8
Glycerol	HEPPS	β-glucan	0	0	0	0	0	17	46	3	0	0	0	0	47	0	0	0	0	0	0
Glycerol	Succinate	β-glucan	0	0	0	0	0	0	1	0	0	-4	0	0	1	0	0	0	0	0	0
Xylan	Succinate	β-glucan	0	0	0	0	0	11	31	2	0	-8	0	0	27	0	0	0	9	0	16
Xylan	HEPPS	β-glucan	0	0	0	0	0	17	42	0	0	7	0	0	44	0	0	0	0	0	0
			LM2	LM5	LM6M	LM8	LM9	LM10	LM11	LM16	LM18	LM21	LM25	LM27	LM28	JIM5	JIM7	BAM4	BAM6	BAM7	BAM8
Glycerol	HEPPS	pachyman	0	0	3	0	0	18	48	3	0	0	0	0	47	0	0	0	0	0	0
Glycerol	Succinate	pachyman	0	0	0	0	0	0	3	2	0	0	0	0	0	0	0	0	23	0	50
Xylan	Succinate	pachyman	0	0	5	0	0	0	0	0	0	0	0	0	0	0	0	0	14	0	20
Xylan	HEPPS	pachyman	0	0	0	0	0	16	41	1	0	0	0	0	39	0	0	0	0	0	0
			LM2	LM5	LM6M	LM8	LM9	LM10	LM11	LM16	LM18	LM21	LM25	LM27	LM28	JIM5	JIM7	BAM4	BAM6	BAM7	BAM8
Glycerol	HEPPS	Lichenan	0	0	0	0	0	0	4	-2	0	0	0	0	0	0	0	0	23	0	50
Glycerol	Succinate	Lichenan	0	0	7	0	0	0	0	-4	0	0	0	0	0	0	0	0	6	0	4
Xylan	Succinate	Lichenan	0	0	5	0	0	0	26	-4	0	0	0	0	3	0	0	0	11	0	15
Xylan	HEPPS	Lichenan	0	0	0	0	0	19	50	2	0	0	0	0	51	0	0	0	0	0	0
			LM2	LM5	LM6M	LM8	LM9	LM10	LM11	LM16	LM18	LM21	LM25	LM27	LM28	JIM5	JIM7	BAM4	BAM6	BAM7	BAM8
Glycerol	HEPPS	Arabinan	0	0	2	0	0	0	0	0	0	0	0	0	0	0	0	0	6	0	4
Glycerol	Succinate	Arabinan	0	-5	-2	0	0	0	36	0	0	0	0	0	4	0	0	0	17	0	22
Xylan	Succinate	Arabinan	0	-5	0	0	0	0	41	0	0	0	0	0	1	0	0	0	16	0	16
Xylan	HEPPS	Arabinan	0	3	1	0	0	13	37	3	1	1	1	0	34	0	0	0	0	1	0
			LM2	LM5	LM6M	LM8	LM9	LM10	LM11	LM16	LM18	LM21	LM25	LM27	LM28	JIM5	JIM7	BAM4	BAM6	BAM7	BAM8
Glycerol	HEPPS	Arabinoxylan (26% db)	0	3	3	0	0	3	7	2	2	1	1	0	3	0	0	0	9	1	9
Glycerol	Succinate	Arabinoxylan (26% db)	0	0	-5	0	0	0	-41	1	4	0	0	0	-5	0	0	3	12	2	13
Xylan	Succinate	Arabinoxylan (26% db)	0	5	1	0	0	0	-41	0	7	0	0	0	-5	0	0	0	32	4	63
Xylan	HEPPS	Arabinoxylan (26% db)	0	0	3	0	0	28	68	3	0	0	0	0	64	0	0	0	0	0	0
			LM2	LM5	LM6M	LM8	LM9	LM10	LM11	LM16	LM18	LM21	LM25	LM27	LM28	JIM5	JIM7	BAM4	BAM6	BAM7	BAM8
Glycerol	HEPPS	RG I	0	0	0	0	0	0	0	0	4	0	0	0	0	0	0	0	15	1	15
Glycerol	Succinate	RG I	0	7	8	0	0	0	0	0	6	0	0	0	0	0	0	0	44	5	85
Xylan	Succinate	RG I	0	29	32	0	0	0	0	20	32	0	24	0	0	0	0	0	28	22	28
Xylan	HEPPS	RG I	0	1	0	0	0	20	51	3	5	0	0	0	48	0	0	0	0	2	0
			LM2	LM5	LM6M	LM8	LM9	LM10	LM11	LM16	LM18	LM21	LM25	LM27	LM28	JIM5	JIM7	BAM4	BAM6	BAM7	BAM8
Glycerol	HEPPS	Rg mix	0	7	8	0	0	0	0	0	6	0	-2	0	0	0	-2	0	44	5	85
Glycerol	Succinate	Rg mix	1	41	46	0	0	0	0	30	47	0	34	0	0	0	0	0	14	31	2
Xylan	Succinate	Rg mix	1	13	15	0	0	23	47	14	16	0	10	0	43	0	0	0	2	11	1
Xylan	HEPPS	Rg mix	0	5	7	0	0	20	46	4	5	0	1	0	44	0	-2	0	0	1	0
			LM2	LM5	LM6M	LM8	LM9	LM10	LM11	LM16	LM18	LM21	LM25	LM27	LM28	JIM5	JIM7	BAM4	BAM6	BAM7	BAM8
Glycerol	HEPPS	PGA	1	5	-3	0	-2	0	0	-6	4	0	-5	0	0	0	0	0	15	3	2
Glycerol	Succinate	PGA	0	-45	-55	0	0	36	72	-25	-35	0	-38	0	66	0	0	0	0	-31	0
Xylan	Succinate	PGA	3	-17	-29	0	0	24	56	-10	-35	0	-34	0	51	0	0	0	0	-31	0
Xylan	HEPPS	PGA	1	-7	-9	0	-2	19	52	-8	-8	0	-10	0	53	0	0	0	0	-10	0

Figure 3.12. Full data set for results shown in Figure 3.3 - NCPPB 1957 was grown on either glycerol or xylan (inducer). The supernatant samples containing exogenous enzymes were mixed with buffers, succinate (pH 5) or HEPPS (pH 7.5).
The supernatant/buffer mixtures were incubated with substrates overnight. These were then printed and probed. Substrates were also printed onto nitrocellulose membrane, those were treated as controls, from which treatments (i.e., weather bacterium was raised on xylan or glycerol, mixed with succinate or HEPPs and substrate used e.g. Xylan) were subtracted.

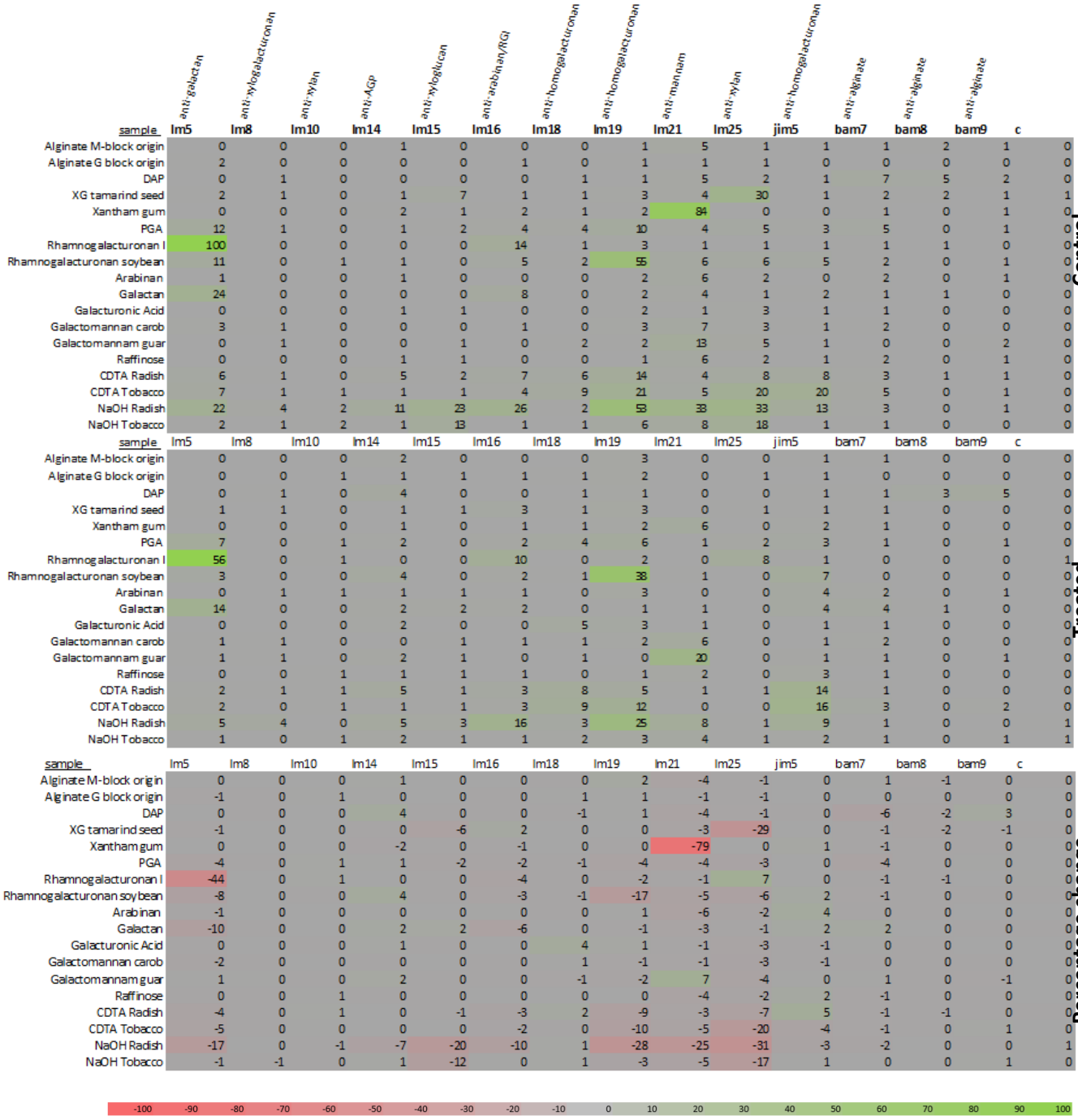

Figure 3.13. Full data set for Figure 3.7.
NCPPB 1957 was grown on 4 different carbon sources: glycerol, arabinan, xyloglucan and rhamnogalacturonan I. Control supernatant without any carbon sources was left to incubate for the same amount of time, then boiled but heating the tube until liquid reached 100°C. These carbon sources are referred to as inducers, at they are the factor that elicits different responses from the bacteria. A range of defined polysaccharides and plant extracts were printed onto nitrocellulose membrane. When normalising this data set, any values between -10 % and 10 % were excluded. “Control” and “Treated” heatmaps were produced using standard analysis method listed in chapter 1. Percentage change heatmap was produced by subtracting the control heatmap values from treated heatmap values.

4. Epitope depletion and structural changes observed in-situ with fluorescence microscopy.

Abstract

The aim of this study was to establish novel methodology for epitope depletion in situ, to provide insight into polysaccharide degrading enzymes secreted by plant pathogens. Investigating extracted polysaccharides offers limited insight, as plant polysaccharides form complex structures and play vital roles in plant growth and cell differentiation. By culturing a selection of Pseudomonas syringae pathovars from the national collection of plant pathogenic bacteria (NCPPB) were cultured on complex carbon sources, such as defined polysaccharide from plants, crude enzymatic extracts were prepared. These extracts were used to treat plant roots, which were then visualised with fluorescent molecular probes that bind to polysaccharides. By investigating the effects of crude bacterial enzymatic broths on plant root samples, it was possible to characterise enzymatic secretion from bacterial strains NCPPB 281, 1957 and 2716. A possible novel enzyme activity to *Pseudomonas syringae* pathovars has been observed as detected by anti-xyloglucan molecular probes (LM15 and LM25).

4.1 Introduction

4.1.1Polysaccharides in plants

Polysaccharides derived from plants, are a major component of the human diet. They are divided into two main categories, storage, and structure polysaccharides. Storage polysaccharides such as starch, phytoglycogen, and fructosans (e.g. inulin) are major sources of energy (Cammack and Attwood, 2008). Whereas cell wall polysaccharides, such as cellulose, pectins and hemicelluloses provide dietary fibre, with pectins being considered the predominant component of fibre (Lovegrove et al., 2015). Cellulose fibrils are produced by the plasma membrane, the matrix polysaccharides such as pectins are produced by the membrane bound enzymes in the Golgi apparatus. Structures of non-cellulosic polysaccharides are modified by apoplastic enzymes. Plants also produce proteins of structural importance, such as extensin and arabinogalactan protein (AGP) (Voiniciuc, Pauly and Usadel, 2018).

Plant cell walls are dynamic, as they can remodel during plant development and as a response to biotic and abiotic stress. Plants have the unique ability to elongate many times compared to their initial size. There are specific cells that are capable of such growth, they are surrounded by a thin primary cell wall (PCW). Primary plant cell walls use pectins and xyloglucans as the basic constituents, with hydrated pectin matrix filling up the space between cellulose microfibrils. In tissues undergoing growth, a plethora of enzymes are responsible for reuse and repurpose of polysaccharides in order to construct the elongating walls (Barnes and Anderson, 2018). Once elongation is finished, the cells deposit a thick secondary wall, that consist of additional polysaccharides, many of them containing lignin. Lignin is a complex and robust biopolymer that strengthens and waterproofs the secondary cell walls, aiding in stability in trees and long-distance water transport in xylem. Lignin self-aggregates to form hydrophobic and dynamically unique nanodomains that have extensive interactions with xylan (Kang et al., 2019).

Understanding the complex interactions and dynamics between plant cell walls and various polysaccharides has posed many challenges. Polysaccharides are structurally complex, with pectins incorporating up to 12 different sugars and 25 glycosidic linkages, which can have further methyl, acetyl or phenolic groups (Atmodjo, Hao and Mohnen, 2013). Analysis methods for extracted polysaccharides are well established, such as genetic sequencing (Carpita and McCann, 2015), gas chromatography-mass spectrometry (GC-MS) (Pettolino, Walsh, Fincher and Bacic, 2012) and carbohydrate microarray technology (Sørensen and

Willats, 2010). However, these techniques do not provide any insight as to what structures the polysaccharides contribute to, or their distribution within a plant. In the past Calcoflour White dye has been used to stain cell walls, it is a fluorescent dye that binds to cellulose and chitin (Herth and Schnepf, 1980), however it has been found to fluoresce in the presence of all β-glucan. Lack of specificity of Calcoflour White dye has resulted in a need for more specific probes for investigating plant cell walls and their structures.

4.1.2Molecular Probes

Carbohydrate-binding modules

Molecular probes, such as carbohydrate-binding modules (CBMs) and monoclonal antibodies have high specificity to structural epitopes. According to the CAZy classification system, CBMs are a large group of protein domains that are often discovered attached to glycoside hydrolase enzymes (Lombard et al., 2013). Despite CBMs not having any catalytic capabilities, they serve as substrate binding modules, and their removal has been proven to decrease enzymatic activity (Conway et al., 2016) and stability (Teo et al., 2019). Due to the CBMs having high specificity, they have been used to characterise polysaccharides (von Schantz et al., 2012).

Monoclonal antibodies

Monoclonal antibodies (mAbs) are a powerful research tool, widely used by many areas across biology and biotechnology due to their specificity and variety of assays they can be used in. Their production takes advantage of mammals' immune system differentiating foreign substances and / or organisms. By using crude enzyme extract from plant pathogens, and incubating them with plants, this study aims to identify novel enzyme activity, and provide additional information into how these enzymes may play a role in pathogenicity. Crude enzyme extract was successfully obtained and applied to microarrays in order to examine polysaccharide degrading enzymes in chapter 3. Similar methodology can be applied to plants, in order to assess complex relationships between plant polysaccharides and the enzymes that facilitate pathogenesis from *Pseudomonas syringae* strains. This chapter investigates the viability of using microscopy as a tool for identifying enzymatic activity from crude enzymatic extracts, with the use of molecular probes conjugates with fluorophores.

This chapter explores tracking polysaccharides changes on plant tissues caused by enzymatic bacterial broths. This is done by applying a modified version of techniques from chapter 3, and using fluorescent probes (CBMs and antibodies) in order to visualise the changes observed pre and post bacterial broth incubation. The change in fluorescence is quantified using ImageJ to prove difference in antibody binding.

4.2 Methods

4.2.1 Germinating seeds

Initially plant seeds were germinated in between 2 dampened filter papers placed in a parafilm sealed Petri dish. Due to a large number of seeds needed, the seeds would often intertwine, and would be damaged when trying to separate the samples. An alternative approach was designed where agarose powder (1 % v/w, 1 g) and Murashige and Skoog medium (0.43 g) were mixed with DiH_2O (100 mL), and heated until all of the powders dissolved and homogenous. The molten agarose mixture was then poured into an agarose gel tray with 3 combs put in place. The gel was left to set at room temperature. Once set it was placed in a 96-well plate lid, holes left by the agarose gel combs were used to wedge the seeds in (Figure 3.1.). The plate was covered with another plate lid and sealed with parafilm to keep it sealed and retain moisture. The incubation chamber was slowly elevated and placed into a plant growth incubator with day/night cycle. The plant incubator was set to 20 ^{o}C and had a 16-h day / 8-h night cycle. The seeds were left to grow until the roots reached approximately 2.5 cm in length for radish and 2 cm for tobacco. Plants much bigger than 2.5 cm would be difficult to manipulate and image. Using a smaller plant allowed for using a smaller volumes of antibodies.

Figure 4.1. Photo of set-up used for seed germination of radish plant (*Raphanus sativus*). Once seeds were put into wells and plate lids were sealed, they were places in a vertical position in a plant incubator. This set-up was used for both radish and tobacco plants (*Nicotiana alata*).

4.2.2 Preparing bacterial crude enzyme extract

Bacterial strains NCPPB 281, 1957 and 2716 were prepared according to methodology outlined in 3.2., overview of methodology can be seen in Figure 3.2.

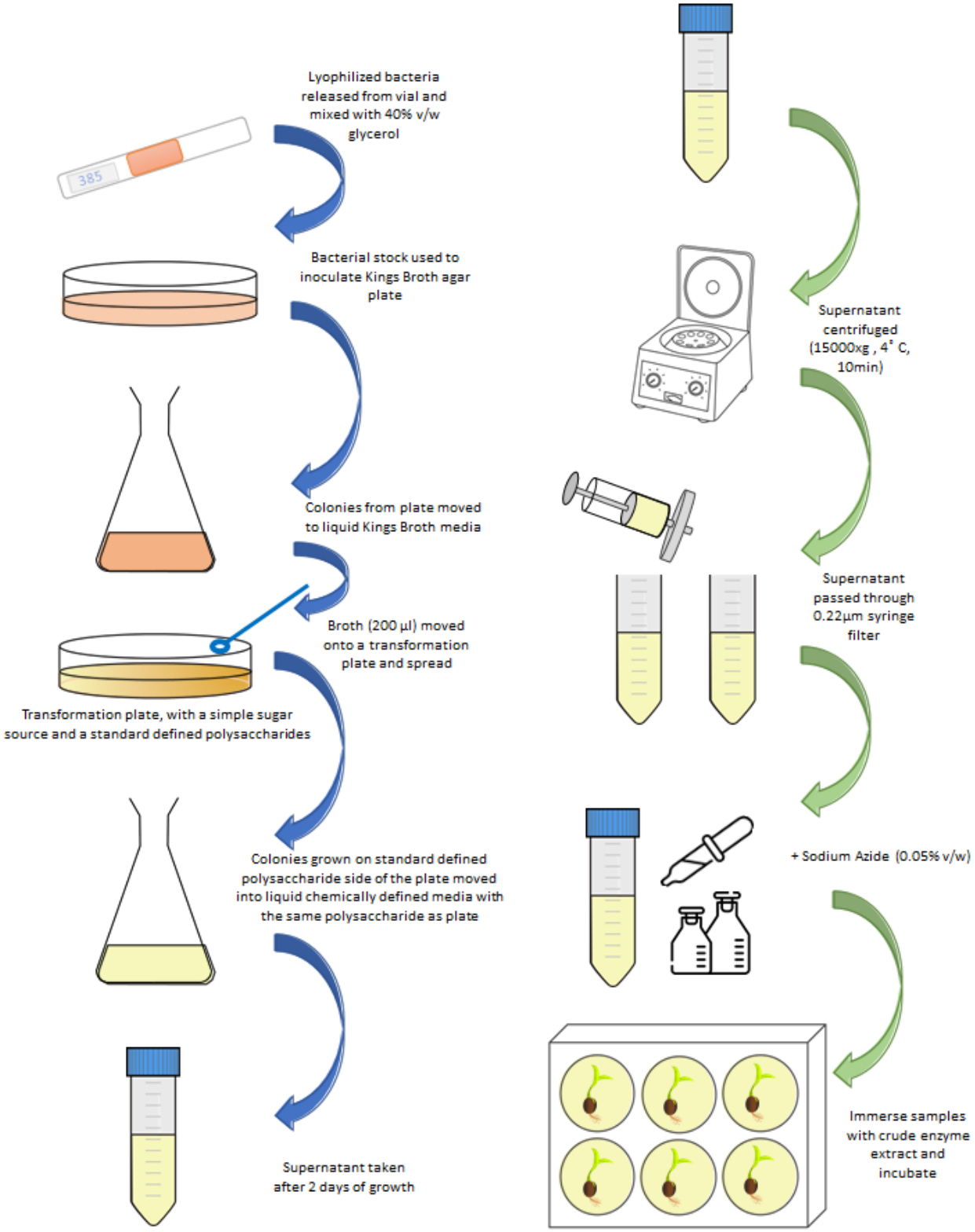

Figure 4.2. Methodology overview used for preparation of crude bacterial extract used for in-situ epitope depletion investigations.

Vial with bacteria lyophilised onto filter paper was opened and filled with 40 % v/w glycerol solution, in order to resuspend the bacteria. The liquid with resuspended bacteria was used to inoculate a Petri dish filled with Kings Broth media, and left to incubate (28 ^{o}C, 48 hrs). A colony was taken from the plate and used to inoculate a flask with Kings Broth media, then left to incubate (28 ^{o}C, 48 hrs). An aliquot was taken from the flask, and spread onto the surface of a transformation plate, where there were two sugar sources present. Half of the plate was filled with minimal media mixed with glycerol (a sugar source used in Kings Broth media), and a defined polysaccharide of choice (galactan, xyloglucan). This plate was used to ensure the bacteria selected would be able to grow in liquid media, where a defined polysaccharide is the sole carbon source, unlike Kings Broth media which contains peptone. Plate was incubated (28 ^{o}C, 48 hrs), and colonies growing on the plate where a defined polysaccharide was, were taken to inoculate a flask with minimal media and defined polysaccharide standard that bacteria has grown on. The flask was left to incubate (28 ^{o}C, 48 hrs), and supernatant was taken in order to prepare a crude enzyme extract. The extract was prepared by centrifugation, in order to pellet the bacteria, the liquid was decanted and passed through a 2 µm filter, then an addition of sodium azide was made to ensure no further bacterial growth. Lack of bacteria within the sample is crucial, as enzymes present in the media were secreted as a response to defined polysaccharides, if there were any bacteria present, they would produce a complex enzymatic response towards the plant they are incubated with. This crude enzymatic extract was used to incubate the plant samples in (28 ^{o}C, 24 hrs).

4.2.3 Incubation of plants in crude enzyme extract

Once plant roots reach desired length, they are placed in 6-well plates and submerged in relevant crude bacterial enzyme extract (4 mL). The plates are then sealed with parafilm and left to incubate overnight, gently agitated (20 rpm) at 28 ^{o}C . Control plants are submerged in control bacterial broth that has no carbon source in it. Bacterial broth with no carbon sources was used as a negative control as it accounts for enzymatic changes that the bacteria produced in response to carbon source, while keeping all other variables constant. This bacterial broth after incubation (28 ^{o}Cm 48 hrs) was streaked onto Kings Broth media plates, and no growth was observed. After incubation in set conditions, the samples were rinsed in diH_2O, 2 times over 30 mins.

4.2.4 Probing of plants

Probing with CBM

Carbohydrate-binding module CBM61A-GFP (anti-galactan) was used for probing. CBM61A-GFP is conjugated to green fluorescent protein (GFP), therefore no secondary antibody was used.

The plant was submerged and incubated in a blocking solution for 1 h (5 % w/v milk protein in TBST; 20 mM Tris-HCl, 140 mM NaCl, pH 7.5 and 0.1 % Tween-20, v/v). Volume used was dependent on the size of well used and plant size. The plants were incubated in the dark, in order prevent further growth, for 1.5 h in the blocking solution with CBM61A (5 µg/mL). The plants were then washed thoroughly in TBST, 4 times over the course of 1h. Whilst probed and washed, the 6 well plates were wrapped in aluminium foil to avoid CBM-fluorophore exposure to light.

Probing with primary and secondary antibodies

For probing with monoclonal antibodies, methodology outlined in 2.2 was used until secondary antibody probing step. The following changes were made to secondary antibody probing step.

The volume used was dependent on the size of well used and plant size. The plants were incubated in the dark for 1.5 h in the blocking solution with either: Goat anti-Rat IgG (H+L) Cross-adsorbed secondary antibody conjugated with Alexa Fluor 488 (Invitrogen), or goat anti-Rat IgG (H+L) Cross-Adsorbed Secondary Antibody, Texas Red-X (Invitrogen). For both of these antibodies a concentration of 4 µg/mL was used (1:500 dilution). The plants were then washed thoroughly in TBST, 4 times over the course of 1 h. Whilst probed and washed, the 6 well plates were wrapped in aluminium foil to avoid fluorophore exposure to light.

4.2.5 Microscopy

Once washed, the plant roots were mounted onto glass microscope slides using a 5cm gene frame, covered with AF1 mounting solution and sealed. The microscope slides were labelled with treatment each plant underwent, e.g., bacterial strain used, carbohydrate media inducer and molecular probe used.

The samples were imaged in a dark room using widefield epifluorescence microscopy (Leica DMC4500). Optimal exposure settings for fluorophore channel emittance 488 was set for the experiment, by comparing signals from probed and non-probed samples was obtained to limit

background autofluorescence whilst obtaining adequate fluorescence from probes on one sample, the same settings were used for visualising the rest of the sample set.

Once images were taken, they were saved in session files with all parameters that were used when taking the image. Image files were exported in .jpeg format. These files were compiled and analysed in ImageJ.

4.2.6 Analysis of microscopy images

Images were uploaded into ImageJ. By using the draw tool, general area of the root was circled using freeform. The "set measurements" option was selected from analysis menu, where area integrated intensity and mean grey value were ticked. Analysis was carried out by the software once "measure" was clicked, and a results window popped up. This was repeated for area of the image that had no fluorescence, i.e., the background.

Following equation was used for corrected total cell fluorescence (CTCF).

$$CTCF = Integrated\ Density - (Area\ of\ Selected\ Cell\ x\ Fluorescence\ of\ Background)$$

A bar chart was produced in excel, where integrated area density was plotted with CTCF. The integrated area density being a measure of brightness within selected area, and CTCF being a value accounting for background within the integrated area density (Fitzpatrick, 2014).

4.3 Results and Discussion

Enzymatic activity produced by strains, 1957 and 2716 towards pectins and galactan as detected by LM5 were noted (chapter 3). Previously published research by Sergeeva and Vreugdenhil (2002) has highlighted that using plant tissue allowed for localising enzyme activity in situ. By applying the same principles, it was possible to study unknown enzymes and highlight their activity using complex plant physiological structures (cell walls of roots, leaf, stem). Proving that in-situ enzyme treatment paired with imaging can be a powerful tool for characterising enzyme activity.

The methodology used for probing microarrays described in chapters 2 and 3 were adapted. Similar to probing microarrays, samples (roots) were incubated with primary and secondary mAbs. A modification of the microarray probing protocol was to extend the duration of washes duration after incubation with primary and secondary antibodies, due to larger and more complex surface area of the root sample that was being probed.

CBMs are co-localised with carbohydrate-hydrolysing enzymes that are thought to have evolved in microbial systems to enhance the ability for bacteria to localise and metabolise carbohydrate. Thus, they tend to be structurally specific to the enzyme that they are co-localised to.

The CBM used in this study was conjugated to a fluorophore, meaning that the use of a secondary antibody was not needed for detection of CBM binding, allowing for a shorted methodology, which helps to retain integrity of the sample. It is worth noting that CBM's can be conjugated to a variety of molecules, making them a versatile diagnostic tool.

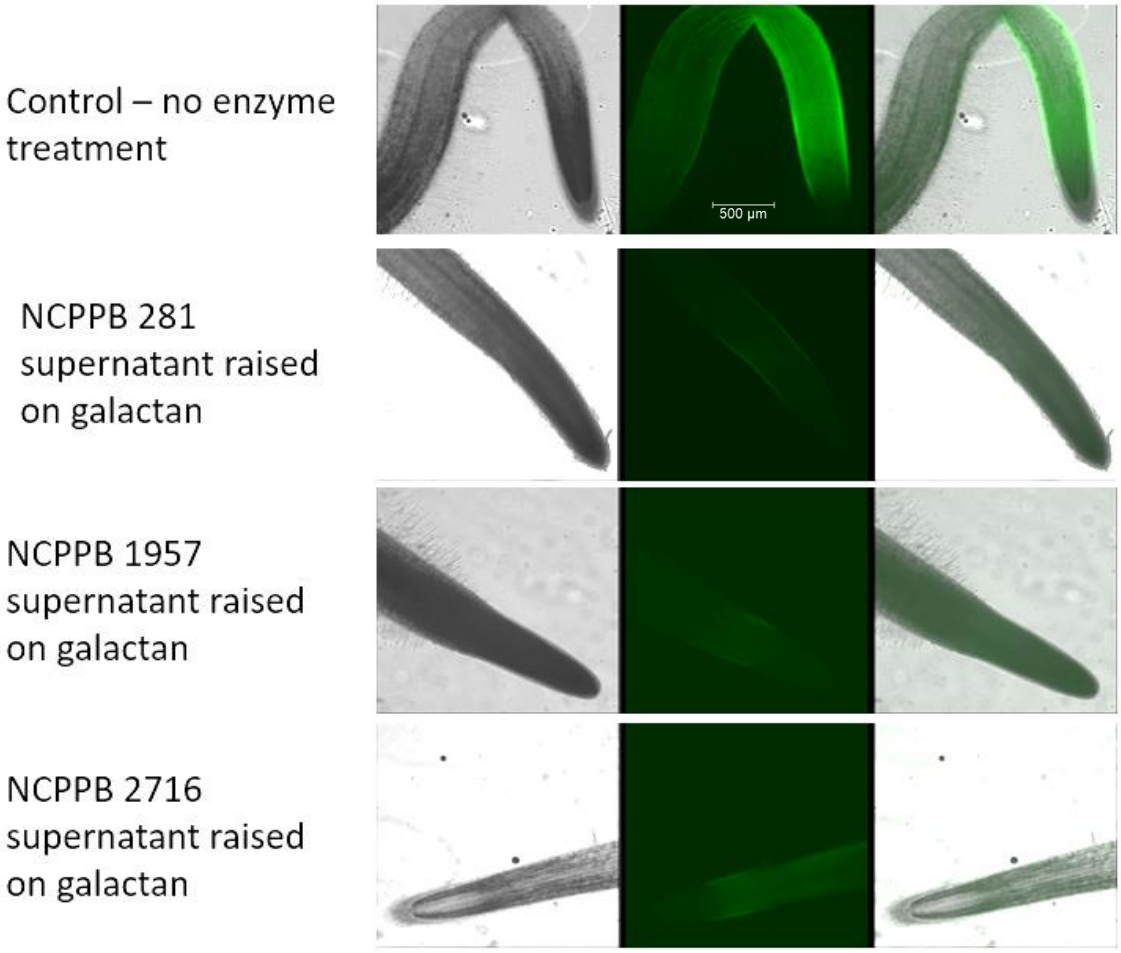

Figure 4.3. NCPPB 281, 1957 and 2716 were raised on galactan (lupin). Crude enzyme extract was prepared from the supernatant and was used to incubate the radish plant samples overnight, alongside a control. The plants were then probed with CBM61A-GFP (anti-galactan). Once labelled fluorescently the samples were imaging with widefield epifluorescence(Leica DMC4500) and images were taken of the tip and elongation zones of the radish root. The first column shows a grayfield image of the plant root tip, middle column shows an image taken under the fluorescent channel emittance set to 488, which corresponds to GFP. The final column shown an overlay of the two images. Scale bar can be seen in the 2nd image of the first row.

NCPPB 281, 1957 and 2716 were all raised on galactan (extracted from lupin) being the only carbon source, therefore their growth could be inferred as their ability to degrade galactan. The control flasks that were inoculated and contained no carbon source were streaked onto plates and incubated to check for growth. The controls never exhibited any growth, making them sterile controls that further supported galactan degrading ability of the strains. Degradation of galactan into simpler sugar molecules, monomers, would require hydrolytic enzyme activity, such as galactanase. The CBM used, CBM61A-GFP (Enzytech) has specific binding site of beta-1,4-galactan (Cid et al., 2010), indicating that a site on this structure on the root surface was cleaved by strains 281, 1957 and 2716, causing a depletion of fluorescence

signal emitted by CBM61A-GFP after radish roots were treated with crude bacterial enzyme extracts (Figure 4.3). CBM61A-GFP was observed to bind to the elongation zone of the radish root. In Arabidopsis, β-1,4-galactan has been highlighted in having a vital role in cell remodelling during elongation. β-1,4-galactan is one of the main side chains of the pectin, rhamnogalacturonan I, which plays a key role in structure of plants. It is speculated that β-1,4-galactan is involved in xyloglucan structure, and therefore the interaction between cellulose and xyloglucan (Moneo-Sánchez et al., 2018).

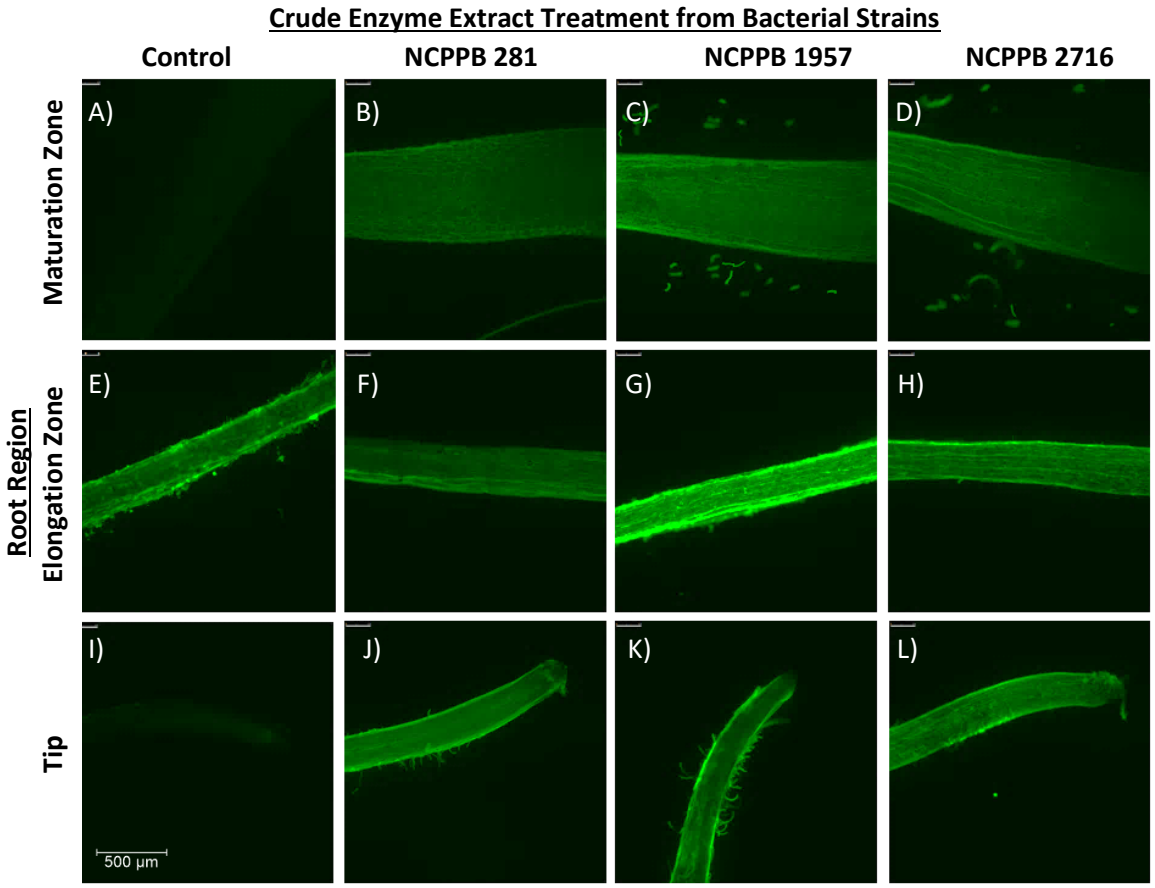

Figure 4.4. NCPPB 281, 1957 and 2716 were raised on galactan (lupin). Crude enzyme extract was prepared from the supernatant and was used to incubate the radish plant samples overnight, alongside a control. The radish plants were then probed with **JIM5** (anti-homogalacturonan). Once labelled fluorescently the samples were imaging with widefield epifluorescence (Leica DMC4500) and images were taken of the tip, elongation and maturation zones of the radish root. Scale bar can be seen in the control image of the plant root tip.

JIM5 is a monoclonal antibody that binds to homogalacturonan, it has the ability to recognise this pectic polysaccharide in several species. It specifically binds to methyl-esterified epitopes of homogalacturonan, but it can also bind to un-esterified homogalacturonan in a lesser capacity (Verhertbruggen et al., 2009). JIM5 is often used as a tool to identify extent of methyl-esterification of homogalacturonan (Clausen, Willats and Knox, 2003). Epitope depletion is not the only indicator of enzymatic activity, an increase in fluorescence is also an indicator of enzymatic activity. Images in Figure 4.6. where radish root tip is treated with enzymes from NCPPB 281, 1957 and 2716, the tip appears to fluoresce more than the control, this is most likely due to epitope unmasking. Epitope masking is thought to be an evolutionary adaptation of the plant, were polysaccharides such as xyloglucan, xylan and mannan have their epitopes hidden by pectic-HG in order to limit interactions with proteins or enzymes. Removal of the pectic-HG can result in epitope unmasking (Lee, Marcus and Knox, 2011). The phenomenon of epitope unmasking has been observed in several studies, a removal or degradation of e.g., pectic homogalacturonans unmasked xyloglucan epitopes in pea stems (Marcus et al., 2008). It is also likely that bacteria were able to produce pectinesterases, which is an abundant cell-wall-associated enzyme that facilitates plant cell wall modification followed by breakdown. Pectinesterase catalyses the de-esterification of pectin into methanol and pectate (Fries et al., 2007). Methyl esterification of pectin would increase the binding of JIM5, therefore increasing the fluorescence observed on the radish roots after they were treated with crude microbial enzyme extract.

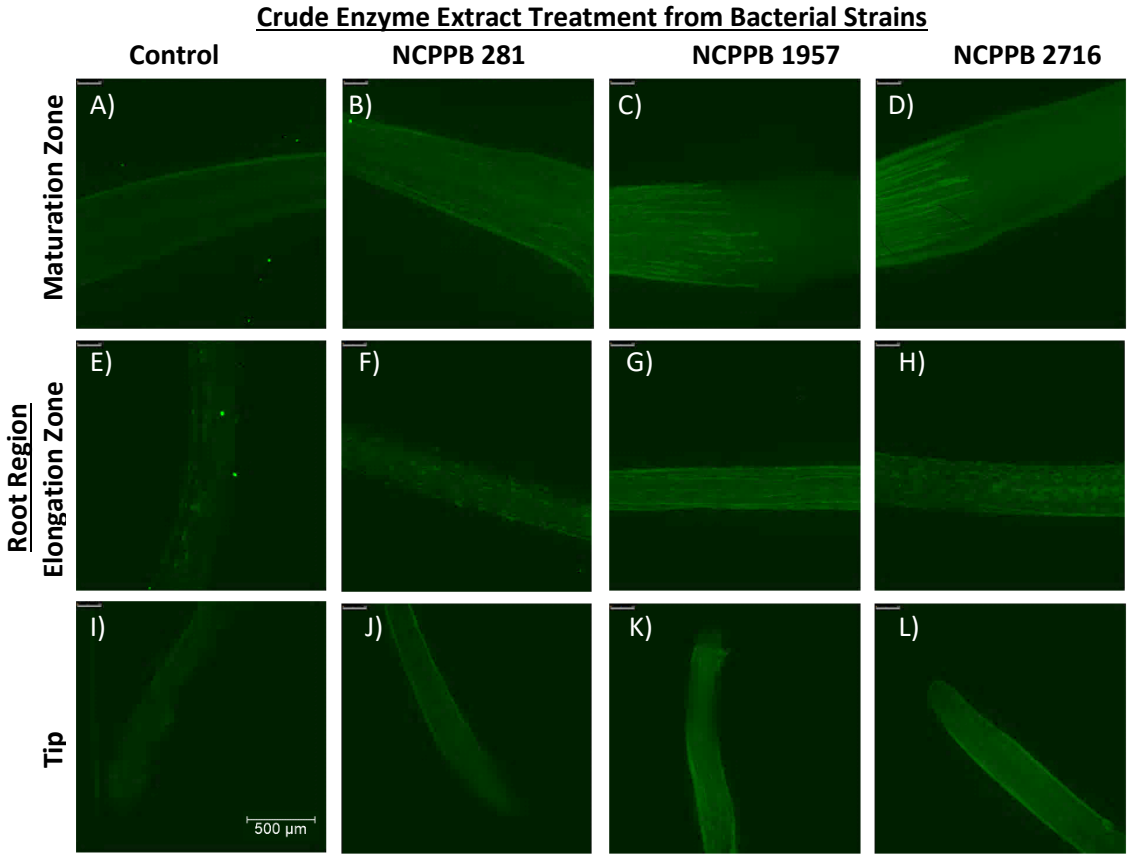

Figure 4.5. NCPPB 281, 1957 and 2716 were raised on galactan (lupin). Crude enzyme extract was prepared from the supernatant and was used to incubate the radish plant samples overnight, alongside a control. The radish plants were then probed with **LM8** (anti-xylogalacturonan). Once labelled fluorescently the samples were imaging with widefield epifluorescence (Leica DMC4500) and images were taken of the tip, elongation and maturation zones of the radish root. Scale bar can be seen in the control image of the plant root tip.

LM8 is an antibody that was raised against xylogalacturonan isolated from pea testae (Le Goff, Renard, Bonnin and Thibault, 2001) . Xylogalacturonan is a class of pectin polysaccharides found in plant cell walls. The xylogalacturonan domain is substituted homogalacturonan present in pectic polysaccharides. It is estimated that a proportion of xylogalacturonan in Arabidopsis varies from 2.5 to 7 %, depending on location and organ of the plant (Harris, 2009). Though there is no research on xylogalacturonan in radish, it's expected to be present in small quantities, similar to Arabidopsis, as they are both dicots. Dicots are one of the two groups into which flowering plants have been divided into, the other group is monocots. Dicots are typically characterised by having a seed that has two embryonic leaves, whereas monocots have just one (Fey and Maréchal-Drouard, 1999).

Work on characterising LM8 has shown binding activity to intracellular regions, cell walls and root cap mucigel. In all cases it has been associated with detached cells, or cell that will be

getting detached shortly (Willats et al., 2003). The binding intensity of LM8 was increased to the radish root after crude enzyme treatment, indicating that degradation of root surface may cause shedding of cell, which is observed by LM8. Specifically, linear pattern observed at the top of the root and the elongation zone, this is most apparent when the root was treated with crude enzyme extract from NCPPB 1957 and 2716.

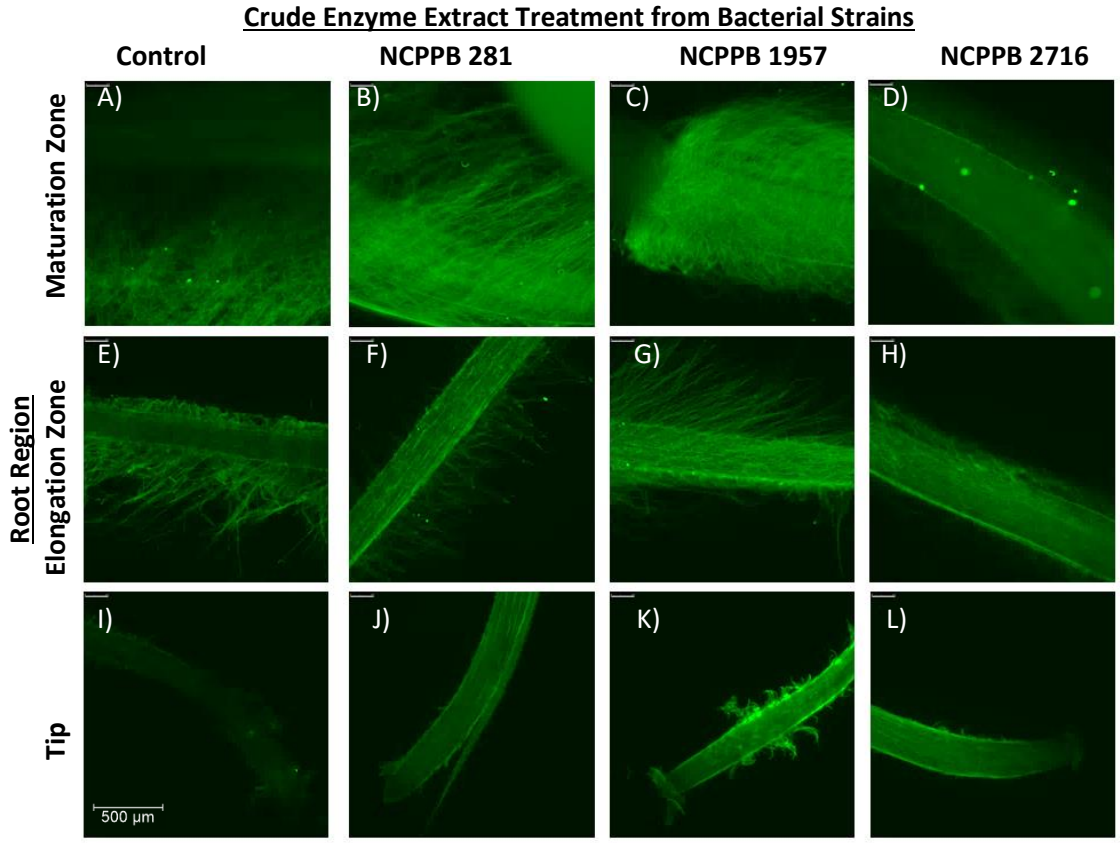

Figure 4.6. NCPPB 281, 1957 and 2716 were raised on galactan (lupin). Crude enzyme extract was prepared from the supernatant and was used to incubate the radish plant samples overnight, alongside a control. The radish plants were then probed with **LM15** (anti-xyloglucan). Once labelled fluorescently the samples were imaging with widefield epifluorescence (Leica DMC4500) and images were taken of the tip, elongation and maturation zones of the radish root. Scale bar can be seen in the control image of the plant root tip.

When initially germinating plants between dampened filter paper in a Petri dish, the plant roots would often tangle together and damage root hairs. As root hairs were providing additional insight, and are structurally of major importance, a new set up for germinating and growing the plant samples was designed (Figure 4.1.).

Xyloglucan is a complex polysaccharide, that is an abundant component of primary plant cell walls of higher plants (Kim et al., 2020). It consists of a glucose backbone and has sidechains containing xylose, galactose, and fucose (Figure 4.7).

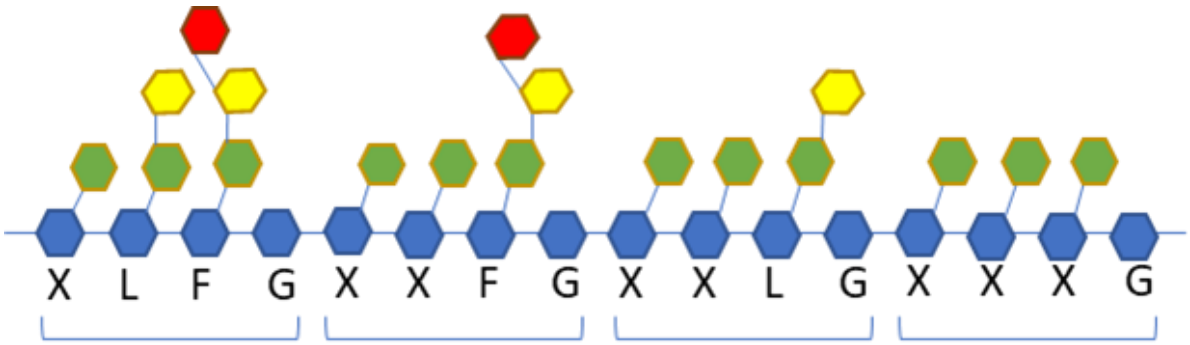

Figure 4.7. A diagram showing the structure of xyloglucan from cotton. Backbone made up of glucose monomers (blue), linked with B-1,4 linkages. The backbone often has xylose chains (green), with additional side chains of galactose (yellow) and fucose (red).

Xyloglucan biosynthesis occurs in Golgi apparatus, before it is transported to the cell surface where is it integrated into the wall matrix (Kim and Brandizzi, 2016). Primary cell walls are thin and extensible, they play a major role in plant cell growth (Wilson and Hunt, 2002), hence why xyloglucan is a significant polysaccharide.

A clear decrease in antibody binding can be observed in radish plant treated with crude enzyme extract from NCPPB 2716. In the control there is clear binding of LM15 (anti-xyloglucan) (Marcus et al., 2008) to plant root hairs, when looking at Figure 4.6, top of radish root treated with extract from strain 2716, there is a shadow of where the plant root hair cells are, but no fluorescence. This is an indication of enzyme activity that disrupts binding of LM15 to its preferred epitope activity produced specifically by NCPPB 2716.

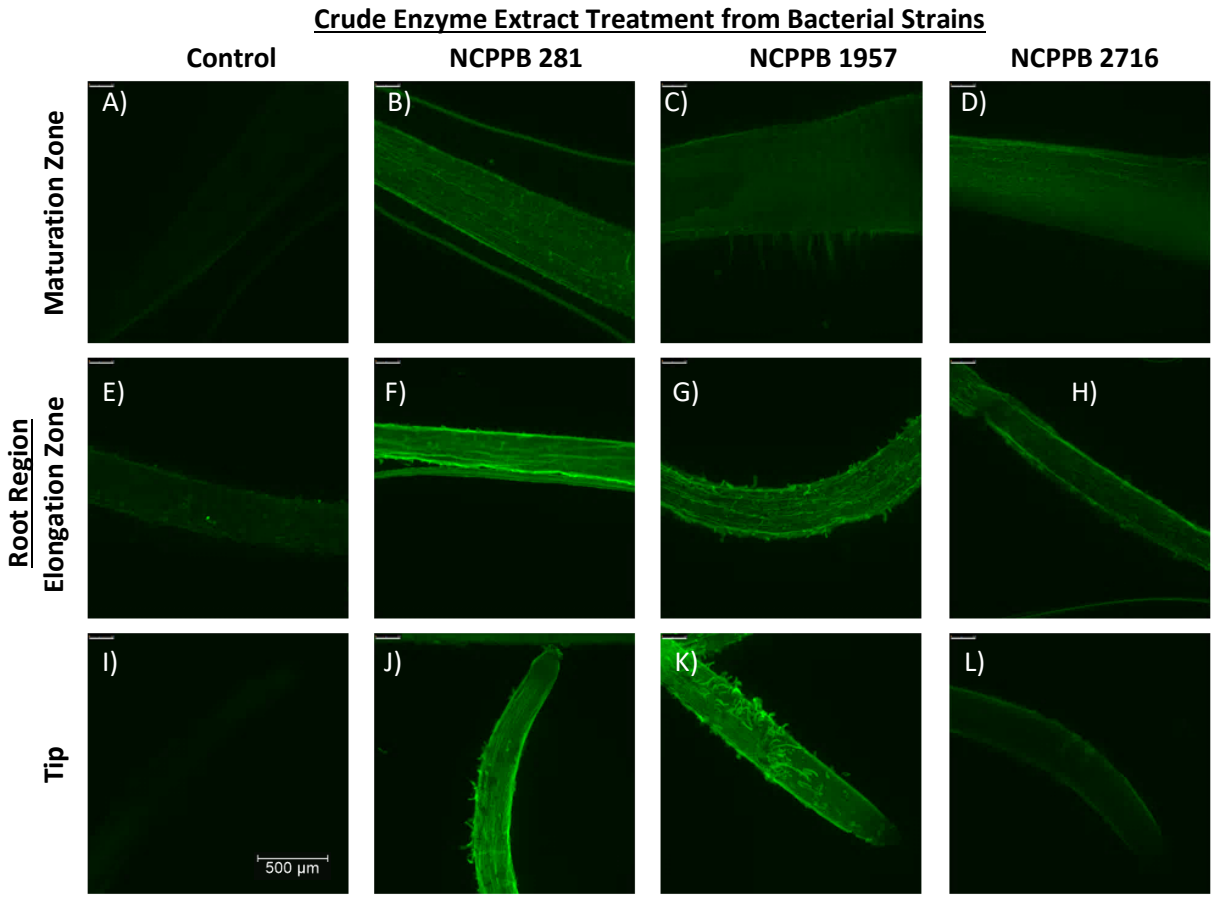

Figure 4.8. NCPPB 281, 1957 and 2716 were raised on galactan (lupin). Crude enzyme extract was prepared from the supernatant and was used to incubate the radish plant samples overnight, alongside a control. The radish plants were then probed with **LM18** (anti-homogalacturonan). Once labelled fluorescently the samples were imaging with widefield epifluorescence (Leica DMC4500) and images were taken of the tip, elongation and maturation zones of the radish root. Scale bar can be seen in the control image of the plant root tip.

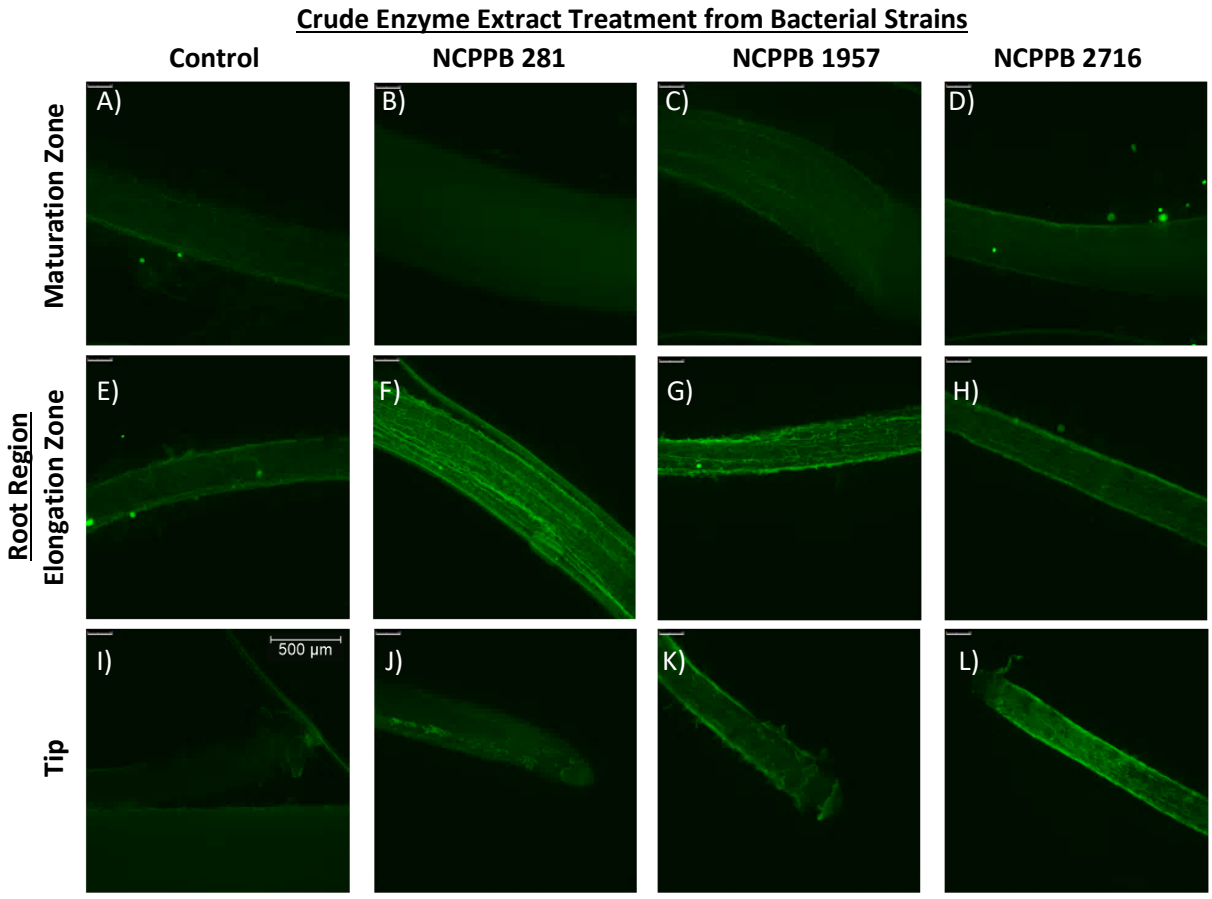

Figure 4.9. NCPPB 281, 1957 and 2716 were raised on galactan (lupin). Crude enzyme extract was prepared from the supernatant and was used to incubate the radish plant samples overnight, alongside a control. The radish plants were then probed with **LM19** (anti-homogalacturonan). Once labelled fluorescently the samples were imaging with widefield epifluorescence(Leica DMC4500) and images were taken of the tip, elongation and maturation zones of the radish root. Scale bar can be seen in the control image of the plant root tip.

LM18 antibody recognises homogalacturonan epitopes, though it has the capacity to bind to un-esterified homogalacturonan too. LM19 has similar binding properties to JIM5, however LM19 binds more effectively to unesterified homogalacturonan (Verhertbruggen et al., 2009). With these 3 molecular probes having an overlap in recognised epitopes, it is important to include all 3 in order to achieve good insight into enzymatic action, and how it affects the binding intensities of these 3 probes. JIM5 (Figure 4.4), shows the most drastic change in fluorescence levels. Though LM18 (Figure 4.8), shows clear degradation of plant cell wall surface, with layers having holes and starting to peel off in images of plant root tip when treated with enzymatic extracts from NCPPB 281 and 1957.

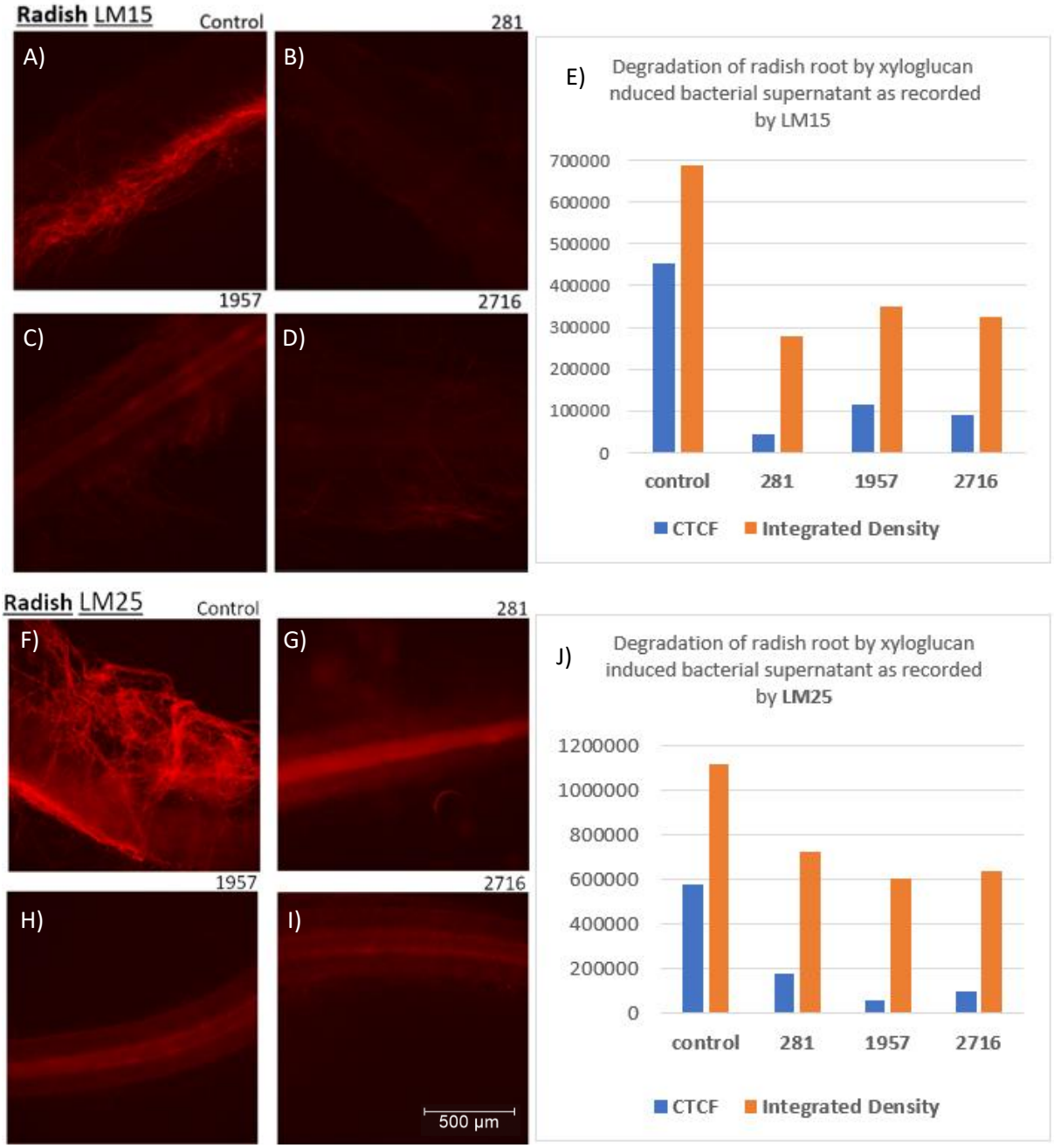

Figure 4.10. NCPPB 281 (B, G) , 1957 (C, H) and 2716 (D, I) were raised on xyloglucan. Crude enzyme extract was prepared from the supernatant and was used to incubate the radish plant samples overnight, alongside a control that contained no carbon source (A, F). The plants were then probed with LM15 (A-D) and LM25 (F-I) (both anti-xyloglucan). Once labelled fluorescently the samples were imaging with widefield epifluorescence(Leica DMC4500) and images were taken of radish plant hair root cells. Images were analysed using ImageJ to produce integrated density and corrected total cell fluorescence (CTCF) values. CTCF value accounts for area of the image, making it a more accurate and reliable method of quantification of fluorescence. Bar charts were produced displaying the quantified fluorescence as recorded by LM15 (E) and LM25 (J).

There is a significant difference in antibody binding of LM15 (anti-xyloglucan) and LM25 (anti-xyloglucan) after the radish plants were treated with crude enzymatic extract from microbial broth. All of the bacterial strains are capable of producing xyloglucanases activity that is specific to LM15 and LM25. Xyloglucanase enzymes have not been noted on the CAZY database for *Pseudomonas syringae*, meaning this may be novel enzyme activity seen in these strains (Lombard et al., 2010). Texas red fluorophore was used to ensure results were not due to autofluorescence produced by the plant.

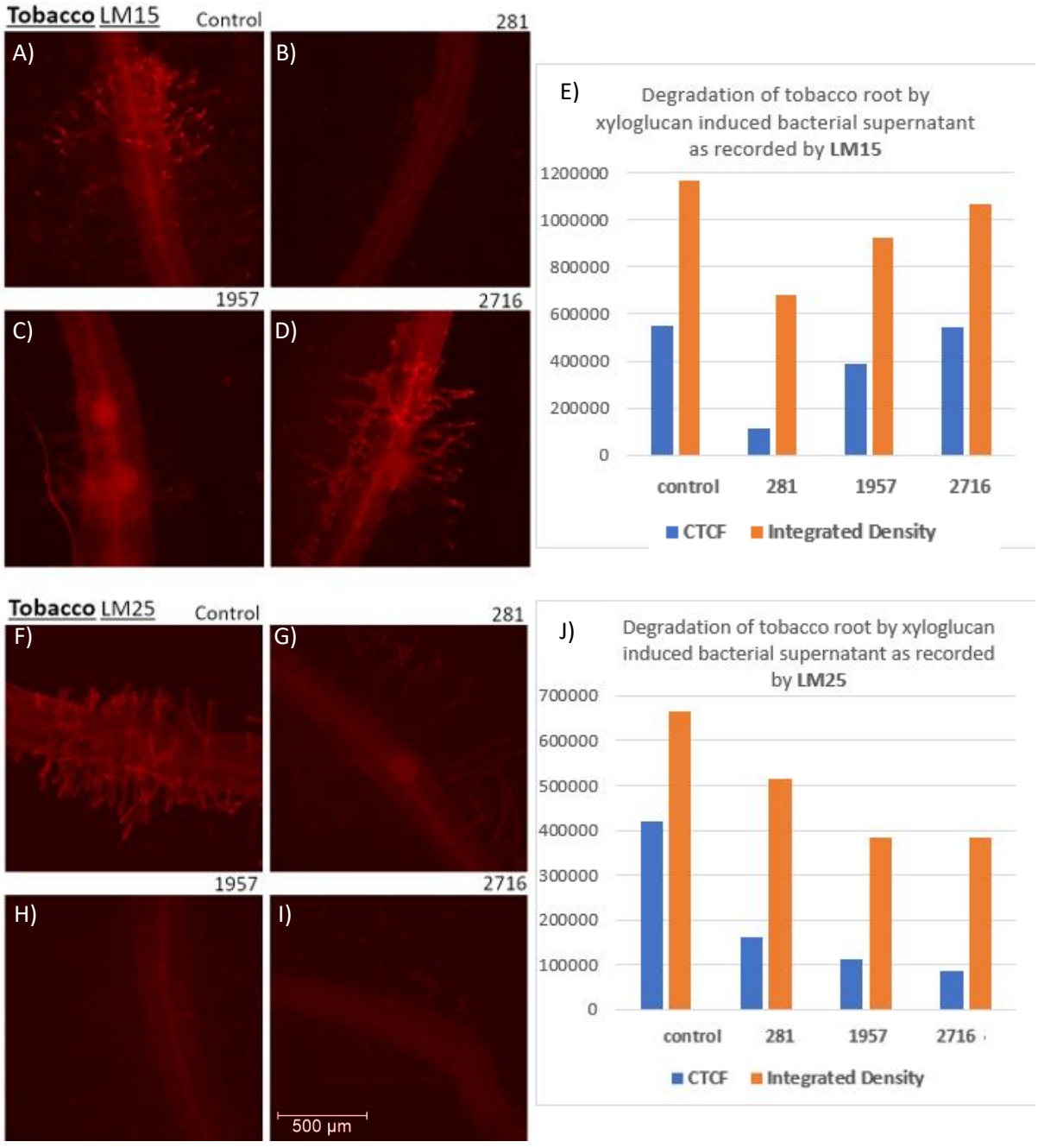

Figure 4.11. NCPPB 281 (B, G) , 1957 (C, H) and 2716 (D, I) were raised on xyloglucan. Crude enzyme extract was prepared from the supernatant and was used to incubate the radish plant samples overnight, alongside a control that contained no carbon source (A, F). The plants were then probed with LM15 (A-D) and LM25 (F-I) (both anti-xyloglucan). Once labelled fluorescently the samples were imaging with widefield epifluorescence(Leica DMC4500) and images were taken of tobacco plant hair root cells. Images were analysed using ImageJ to produce integrated density and corrected total cell fluorescence (CTCF) values. CTCF value accounts for area of the image, making it a more accurate and reliable method of quantification of fluorescence. Bar charts were produced displaying the quantified fluorescence as recorded by LM15 (E) and LM25 (J).

The findings showing xyloglucanase activity as shown by epitope depletion with molecular probes, LM15 and LM25 were significant in radish plant. Tobacco is considered a model plant (Ganapathi et al., 2004), due to its use in culture cultivation and genetic engineering over the years. Plant root hair cells also play a significant role in plant cell growth and are considered the model system to study it (Peña, Kong, York and O'Neill, 2012).

Similar activity was observed in Figure 4.6, with strain 2716 causing a significant depletion of LM15 binding to radish root hair cells observed near the top of the plant root. By growing the bacteria with xyloglucan as the sole carbon source, it was possible to induce a similar enzymatic response in strains 281, 1957 and 2716. Though the decrease of fluorescence is more significant in radish, it was also observed in tobacco plant. This shows that this versatile methodology can be applied to a variety of samples.

Bar charts showing fluorescence and CTCF were only made for Figure 4.10 and 4.11, this was done due to plant samples being physiologically similar. Plant samples used in 4.4-4.9 (excluding 4.7), varied a lot in root hair density and root thickness. Providing fluorescence measurement for them would not be representative.

A further study was carried out where NCPPB. 2716 was grown up on a mixture of arabinan and rhamnogalacturonan I, a more complex mixture of pectin related carbohydrates in order to induce a more complex enzymatic response (Figure 4.12).

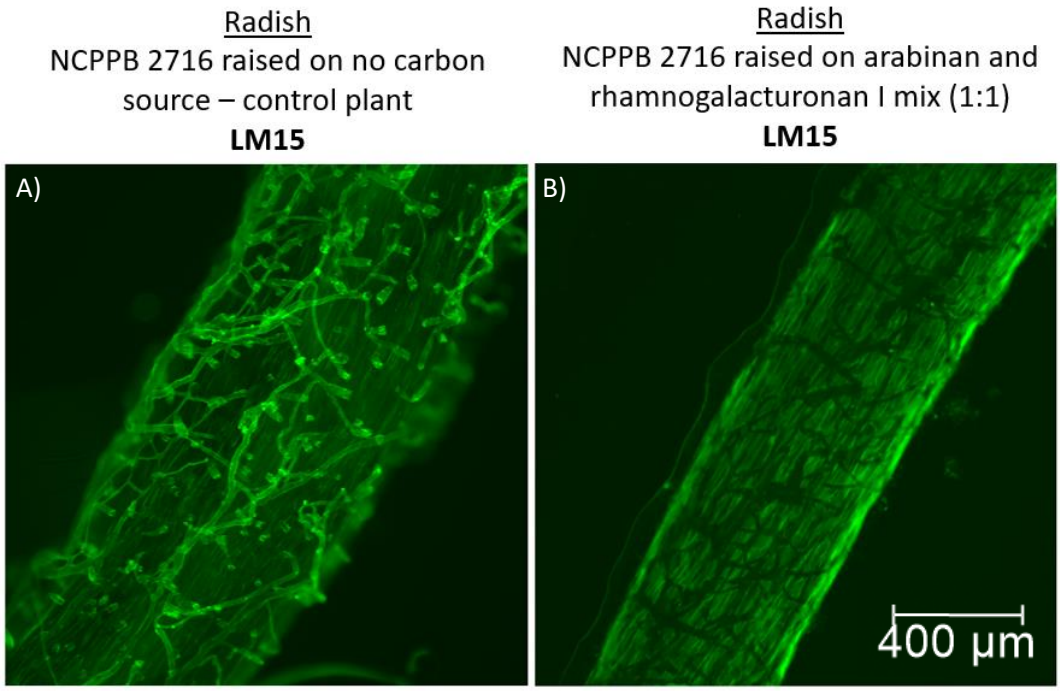

Figure 4.12. NCPPB 2716 was raised on arabinan and rhamnogalacturonan I (1:1 ratio). Crude enzyme extract was prepared from the supernatant and was used to incubate the radish plant samples overnight, alongside a control. The plants were then probed with LM15 Once labelled fluorescently the samples were imaging with widefield epifluorescence(Leica DMC4500) and images were taken of radish plant root hair cells.

Findings presented in Figure 4.12 confirm production of hydrolytic enzymes that cause degradation of epitopes recognised by LM15. In images there is apparent disappearance of clearly defines plant root hair cells in plant treated with NCPPB 2716 supernatant (4.12.B). In the image on the right, there is lack of binding observed where hair root would be extected to be present, meaning that most likely the root hair cells were depleted of epitopes recognised by LM15 (anti-xyloglucan).

Despite best efforts of picking out plant roots of similar width and length, there were many differences between each specimen. It is most apparent in Figure 4.6, with each specimen having a different amount and density of root hairs. Each plant behaves and grows differently despite growing in the same conditions, this can be seen by differences in elongation zones of the radish plants, some would be much longer than others (Figure 4.7). Quantifying fluorescence was not appropriate for some samples due to their physiological differences. Qualitative data best is the better choice for Figures 4.4-6, 4.8 and 4.12, as it focuses on specific structures, rather than overall fluorescence which greatly varied due to plant physiology. Though providing images of each of the key areas offers a lot of insight, it also produces an overwhelming amount of data.

4.5 Conclusion

Investigating extracted polysaccharides provides insight into complexity of plant structured and the range of polysaccharide present in samples. We extract them using sequential series of solvents recognised to pull apart different classes of polysaccharides, which can simply the cocktail of polysaccharides present in each fraction that is printed as spots on microarrays. In doing so, we lose information on how polysaccharides are arranged in-situ in the cell wall, on the surface of plant structures such as roots, which are accessible to microbes inhabiting the root zone. By treating plants with crude enzyme extracts (prepared from known plant root pathogens / opportunists) and in-situ labelling using molecular probes, it was possible to investigate how enzymes affect structures on the surface of plant roots. With tools available to quantify fluorescence, it was possible to measure activity of the enzymes, when produced by different microbial strains, as detected by molecular probes (LM15 and LM25). Despite selecting plant samples with similar physiology between radish plants, there were clear differences visible under the microscope, with root hair densities, position and length of the elongation zone, and thickness of the root. These physiological differences would skew the quantification of the fluorescence. Data obtained from plant samples is still valuable, as it offers insight into how the enzymes degrade specific structured within the plant root, such as plant root hair cells, as observed by LM15 (Figure 4.11). Xyloglucanase activity would be considered novel activity to *Pseudomonas syringae* pathovars (NCPPB 281, 1957 and 2716), as this enzymatic group has not been noted in literature, neither has it been inferred from homology on the CaZY catalogue. Activity observed may also be due to xylosidase, however additional characterisation is necessary in order to confirm exact enzyme activity. LM15 and LM25 recognise the XXXG epitope (Figure 4.7), so activity observed it unlikely to be caused by fucosidase or galactosidase. This methodology can be used to identify potential enzymatic activity; however, it will require additional analysis with methods such as high-performance-liquid-chromatography in order to characterise its action.

4.6 Supplementary Figures

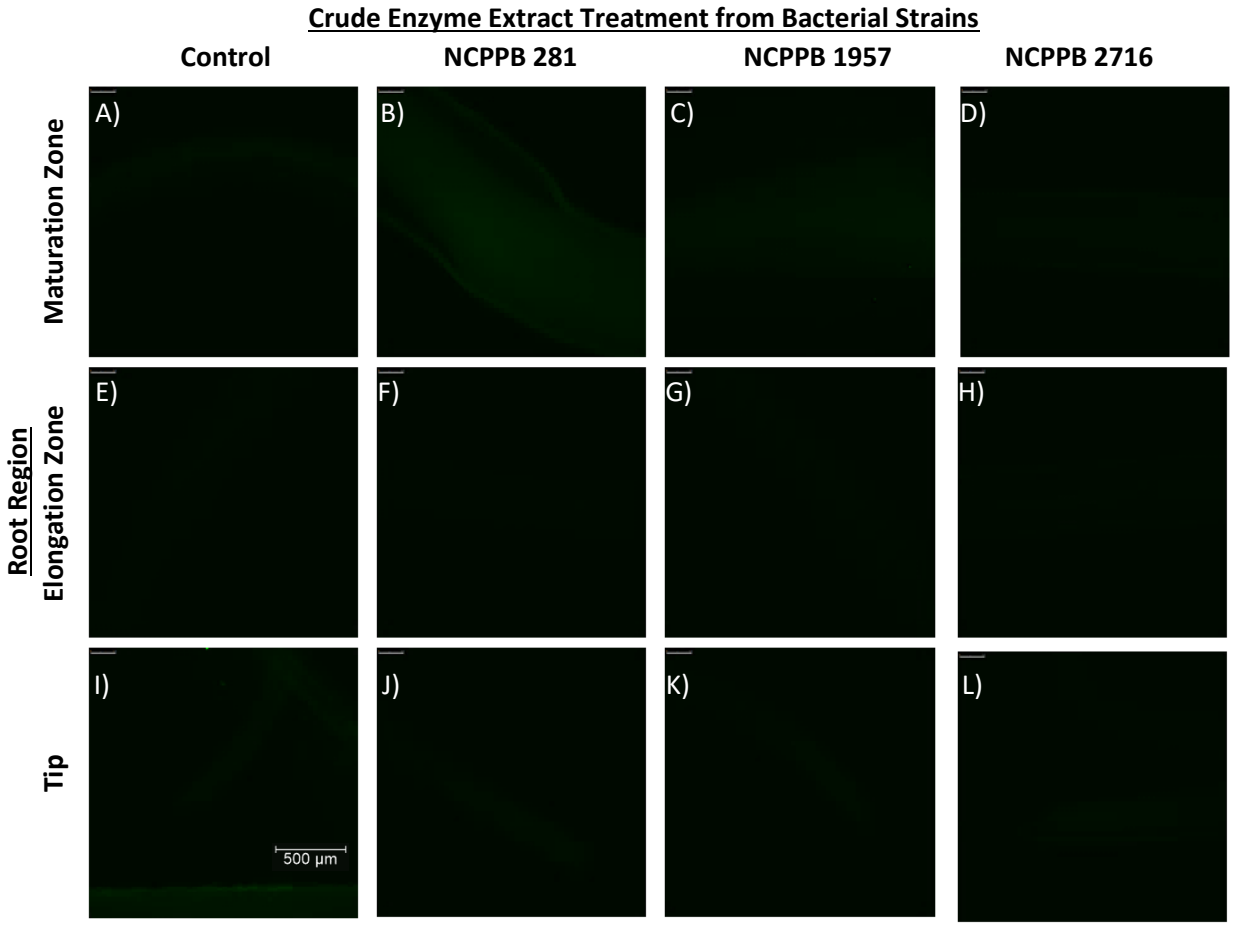

Figure 4.13 Images taken of the no primary antibody controls. NCPPB 281, 1957 and 2716 were raised on minimal media with no carbon source. Crude enzyme extract was prepared from the supernatant and was used to incubate the radish plant samples overnight, alongside a control. The radish plants were then probed with secondary antibody only. Once labelled fluorescently the samples were imaging with widefield epifluorescence (Leica DMC4500) and images were taken of the tip, elongation and maturation zones of the radish root. These controls account for any naturally occurring autofluorescence in the plant. Scale bar can be seen in the control image of the plant root tip.

5. Utilising microarray technology to investigate the alginate production and degradation ability of *Pseudomonas syringae* pathovars.

Abstract

Biofilms are a matrix produced by fungi and bacteria that allow for surface adhesion, and aid in proliferation and spread of infection. Current methodologies of identifying these biofilms rely heavily of cultures, however by utilising sensitive molecular probes it may be possible to consider comprehensive microarray polymer profiling (CoMPP) as a means of detection and partial characterisation of bacterial biofilms. The aim of this experiment is evaluation of microarray technology as suitable tool for the detection of bacterial biofilm production, and the growth thereof. Bacterial biofilm production is inferred from detection of alginate with relevant molecular probes. Bacterial biofilms contain alginate, which is rich mannuronic acid. Multiple molecular probes (LM7, BAM6, BAM8, BAM9, BAM10) detected presence of mannuronic rich alginate in liquid culture and solid media plates of *Pseudomonas syringae van Hall 1902* (NCPPB 365) and Pseudomonas *tolaasii* (NCPPB 1957).

5.1 Introduction

5.1.1 Biofilms

Biofilms were first discovered by Antoni van Leeuwenhoek in 1683, whilst examining matter from his teeth under a microscope. It wasn't until 1970s that scientists had taken interest in biofilms, when Nils Høiby noted a correlation in cystic fibrosis patients, between the aetiology of an infection and aggregates of bacteria (Høiby, 2017).

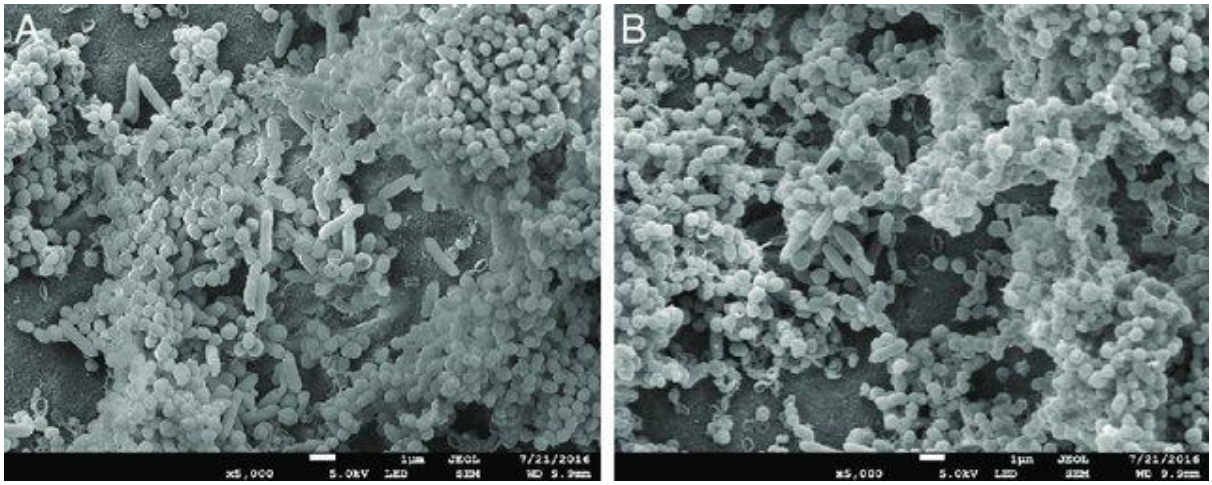

Figure 5.1. Image from a scanning electron microscope of 3-week-old bacterial biofilms formed on dentin surfaces, showing the complex bacterial community adhering to each other, covered in biofilm. (A) - Biofilm formed by bacteria obtained from an infected root canal of a mature tooth with necrotic pulp. (B) Biofilm formed by bacteria obtained from an infected root canal of an immature tooth with necrotic pulp (Jacobs et al., 2017). Photo credit Ghaeth Yassen, 2017.

Biofilms been found to be the root cause of biofouling in a lot of industrial processes. Polysaccharides present in biofilms have various properties, that allow them to bind to surfaces which would normally be considered a difficult environment for bacteria to survive on, such as metal and glass surfaces. Bacterial biofilms affect medical industry significantly, with implanted medical devices providing a surface for biofilms to attach to and cause infection for the patient (Mittelman, 2000).

The build-up of biofilms means that bacteria can survive even longer periods of time in water, animal manure, soil and on plant surfaces. This accumulation affects the heat flow across surfaces and increases likelihood of corrosion of on-site machinery, resulting in loss of energy and an overall loss of product (Kumar and Anand, 1998). The biofilms have a detrimental economic impact. They have been found to be a source of an estimated 80 % of bacterial

infections in the United States by CDC (Centre for Disease Control and Prevention) (Srey, Jahid and Ha, 2013).

A high proportion of microorganisms survive by attaching and growing on a surface of a living organism, or inanimate surfaces. The formation of biofilm is an adaptation and survival strategy developed by bacteria and/or fungi in order to ease surface attachment (Donlan, 2001). Bacterial biofilms are clusters of bacteria that are attached to a surface or each other (Figure 5.1), embedded in a secreted matrix. The matrix consists of proteins, polysaccharides and eDNA (environmental DNA). Biofilms allow bacteria to evade host immune response by employing survival strategies. Adaption to environmental stress is performed by all microorganisms. There are different strategies, with biofilm production being one of them. Bacteria adapt to environmental anoxia and limited nutrients by altering metabolic processes, gene expression and protein production. These survival strategies lead to a lower metabolic rate, and therefore a lower rate of cell division (Donlan and Costerton, 2002). The biofilm later allows the bacteria to withstand biotic and abiotic conditions in the environment (Chew and Yang, 2016).

5.1.2 *Pseudomonas Syringae* Biofilm

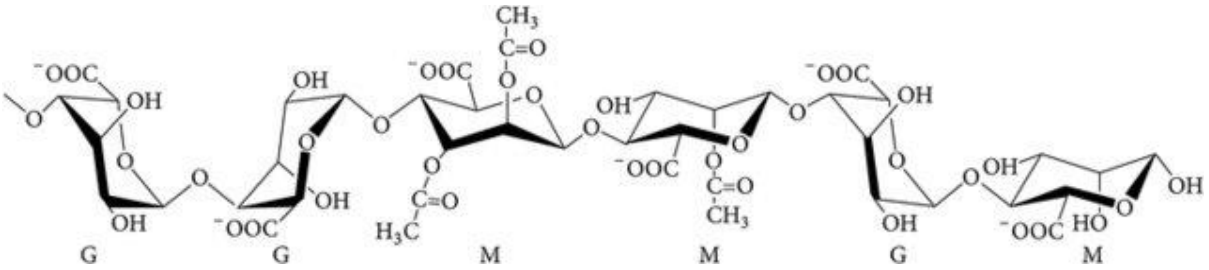

Figure 5.2. Chemical structure of bacterial alginate, a copolymer made up of mannuronic acid (M) and guluronic acid (G) residues. The composition and molecular weight of alginates are known to have effects on their property of alginate (Urtuvia et al., 2017).

Pseudomonas syringae is a plant pathogen that infects more than 50 plant species in the world. *P. syringae* is considered a model plant pathogen, which has been studied in order to establish type 3 secretion system mechanism (Xie, Shao and Deng, 2019). Majority of *Pseudomonas* species synthesise exopolysaccharides, with the most important one for biofilm production being alginate (Shao, Xie, Zhang and Deng, 2019).

Alginate produced by *P. syringae* is an important polymer for *P. syringae* biofilm formation and contributes to its virulence and fitness, indicating its importance in plant-pathogen interaction (Preston, Bender and Schiller, 2001; Engl et al., 2014). There are three main stages involved with biofilm development in bacteria, adherence, proliferation, and dispersion. Each stage involves reinforcement or modulation of the extracellular matrix (Mann and Wozniak, 2012). The formation of *P. syringae* and *P. fluorescens* biofilms can also be measured using crystal violet staining in microwell plates (Carezzano et al., 2017; Patange et al., 2019).

5.1.3 Utilisation of bacterial biofilms

Despite many issues that biofilms pose in several fields, they can also be utilised constructively. With an estimated 40-80 % of bacteria being able to produce biofilms, the scientific community and industry have started finding applications for them in: food fermentation, biofertilizer, filtration, biofouling, prevention of corrosion, antimicrobial agents, wastewater treatment, bioremediation, and microbial fuel cells (Ünal Turhan, Erginkaya, Korukluoğlu and Konuray, 2019). Biofilms have been utilised in sewage treatment plants, for secondary water treatment, where water is passed over biofilms that digest organic compounds. Bacteria in these biofilms are often used for removal of organic matter (Zhao et al., 2019).

More recently biofilms have been utilised in microbial fuel cells, where they generate electricity from complex organic waste and renewable biomass (Wang et al., 2013). Biofilms are versatile and with so many applications, additional means of their detection are needed.

This chapter aims to develop methodology for identifying alginate produced by different bacterial strains. By applying CoMPP alginate was identified in bacterial broths at different quantities in previous chapters (figure 3.12). This chapter developed a methodology for identifying different alginate growth patterns as indicated by antibody binding. This was done by exploring different media types (solid and liquid) affecting alginate production, and developing methodology further based on using liquid media.

5.2 Methods

5.2.1 Preparation of samples

Preparation of media

The Kings broth was prepared according to methodology outlined in 2.2.

Minimal media was prepared according to methodology outlined in 2.2.

Solid version of the media was made by addition of 1 % [v/w] of microbiology agar powder prior to autoclaving.

Culturing of Bacterial Strains

The bacterial strains were cultured following methodology outlined in 2.2.

Table 5.1. Table containing a list of bacterial strains from NCPPB catalogue use for biofilm production analysis. Data taken from NCPPB catalogue (NCPPB, 2021).

NCPPB catalogue number	Catalogue Name	Name as Received	Host Plant
281	*Pseudomonas syringae* pv. *syringae* van Hall 1902	*Pseudomonas syringae*	*Syringa vulgaris*
365	*Pseudomonas syringae* van Hall 1902	*Pseudomonas syringae* van Hall 1902	*Forsythia suspensa*
385	*Pseudomonas syringae* van Hall 1902	*Pseudomonas syringae* van Hall 1902	*Magnolia sp.*
1957	*Pseudomonas tolaasii* Paine 1919	*Pseudomonas tolaasii*	*Agaricus bisporus*
2716	*Pseudomonas savastanoi pv. fraxini* (Janse 1982) Young et al. 1996	*Pseudomonas savastanoi*	*Fraxinus excelsior*
3768	*Pseudomonas syringae* van Hall 1902	*Pseudomonas syringae* van Hall 1902	*Rosa hybrid*

Sampling bacteria at multiple time points

The bacterial strains grow in liquid culture, were taken to microbial safety cabinets, where 1 mL of liquid culture (culture) was taken and kept in a freezer (-20 ^{o}C) until sample set was ready for printing with the microarray robot.

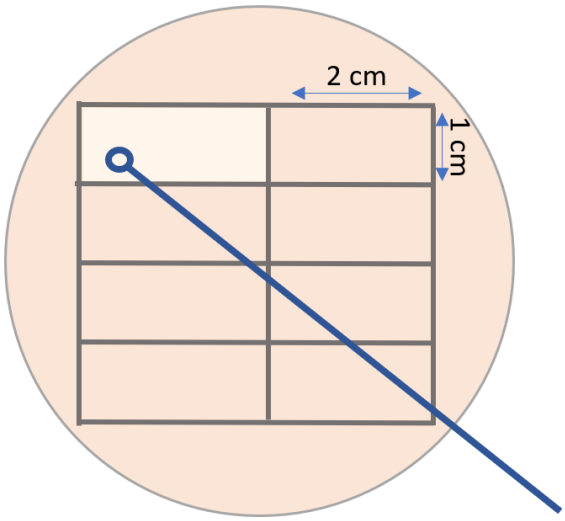

Figure 5.3. A diagram of a grid drawn on the back of a Petri dish that bacteria was grown on. A thick black marker is visible from the front of the plate, allowing to take 1cm by 1cm sections of bacterial growth from the surface of the media, by using an inoculating loop.

Bacterial strains grown on plates, were taken to microbial safety cabinets, where grids were drawn on the back of the plate, as seen in Figure 5.3. The small, 2 cm x 1 cm sections of bacterial growth were scraped off with an inoculating loop and mixed with SDW (0.1 mL) for each time point. The samples were kept in a freezer (-20 ^{o}C) until sample set was ready for printing with the microarray robot.

5.2.2 Microarray Technology

Printing samples with microarray robot

The samples were printed following methodology outlined in 2.2.

The dilution of the bacterial samples was altered for printing, due to a lower sample concentration when comparing to defined polysaccharide standards. The first dilution contained 30ul of system buffer and 20ul of the sample.

DAP (defined alginate polysaccharide) stock (1 % v/w) was diluted following standard methodology outlined in 2.2.

Probing

The arrays were probed following methodology outlined in 2.2., with a different selection of monoclonal antibodies (Table 5.2). The same secondary antibody was used as in 2.2.

LM25 was used as a negative control, to ensure there was no non-specific antibody binding.

Table 5.2. Table showing a list of antibodies used in this chapter, with corresponding epitopes (Torode et al., 2016; Torode et al., 2016).

mAb Code	Epitope Recognised
BAM1	un-sulfated epitope present in sulfated fucan/fucoidan preparations
BAM2	sulfated epitope present in sulfated fucan/fucoidan preparations
BAM3	sulfated epitope present in fucan/fucoidan preparations
BAM4	sulfated epitope present in fucan/fucoidan preparations
BAM6	mannuronate-rich epitope
BAM7	mannuronate-guluronate
BAM8	mannuronate-guluronate
BAM9	mannuronate-guluronate
BAM10	mannuronate-guluronate
BAM11	~ 7 guluronate residues
LM7	HG/Alginate
LM18	HG partially/de-esterified
LM19	HG partially/de-esterified
LM20	HG partially/de-esterified
JIM5	HG partially/de-esterified
JIM7	HG partially/de-esterified
LM25	Xyloglucan / unsubstituted β-D-glucan
LM16	Processed arabinan

The arrays were analysed following the methodology outlined in 2.2.

5.3 Results and Discussion

A small selection of bacterial strains was selected for a small-scale study, to test viability of applying microarray technology for alginate detection across two different growth conditions. Methodology was altered when printing crude samples, to increase concentration of the sample in each well. The standard methodology was designed for COMMP of extracTable plant polysaccharides that are quite abundant and relatively easy to successfully extract (Chialva et al., 2019).

Culture or Plate (C/P)	Bacterial Strain (NCPPB)	Anti-Mannuronate-rich BAM6	Anti-Mannuronate-rich BAM7	Anti-Mannuronate-rich BAM8	Anti-Mannuronate-rich BAM9	Anti-Mannuronate-guluronate* BAM10	Anti-HG LM7
Culture	281	0	0	0	0	0	0
Culture	365	0	0	0	0	0	0
Culture	385	0	0	0	0	0	0
Culture	1957	78	23	80	100	67	0
Culture	2716	0	0	0	0	0	0
Culture	3268	0	0	0	0	0	0
Plate	281	0	0	0	0	0	0
Plate	365	0	0	0	0	0	0
Plate	385	36	10	24	38	22	0
Plate	1957	42	13	37	56	35	6
Plate	2716	0	0	7	5	0	0
Plate	3768	0	0	0	0	0	0

Figure 5.4. Heatmap showing production of alginate related polysaccharides by 6 different *Pseudomonas spp.,* when grown on King B media, in liquid culture (culture), or on a solid media in a Petri dish (plate) for 72h. The production of alginate related polysaccharides is detected by a range of mAbs – BAM1, BAM2, BAM3, BAM4, BAM6, BAM7, BAM8, BAM9, BAM10, BAM11, LM7, LM18, LM19, LM20, JIM5, JIM7 and LM25. The opacity of colour green represents a higher binding intensity, and grey represents lack of it. The Figure shows 6 antibodies. The full set is available in supplementary Figure 5.10.

Alginate is a main component of bacterial biofilms; it is a copolymer of α-l-guluronate residues (G-block) and β-d-mannuronate residues (M-block) linked by β-1-4 glycosidic bonds. The structure of alginate depends on its' source, as it can originate from algae, *Pseudomonas* or *Azotobacter.* Algal alginate contains blocks of repeating G-block, whereas G-blocks are not found in alginate produced by *Pseudomonas* species (Fabich et al., 2012). Binding observed in Figure 5.4 shows presence of M-blocks within sample, confirming presence of alginate and therefore biofilm produced by NCPPB1957 and 385. NCPPB 1957 produced high levels of

alginate in liquid culture and on plates (solid media), whereas NCPPB 385 was only able to produce detectable levels of alginate on solid media.

Going forward, three bacterial strains were selected for a longer-term study, monitoring the alginate production over the course of 7 days. NCPPB 1957 and 385 were selected as they both exhibited abilities to produce detectable levels of alginate under laboratory conditions. NCPPB 365 was selected due to its close homology to 385, it is possible that it would produce alginate after 48h period.

			Anti-Mannuronate-rich	Anti-Mannuronate-rich	Anti-Mannuronate-rich	Anti-Mannuronate-rich	Anti-Mannuronate-guluronate*	Anti-HG
Culture or Plate (C/P)	**Bacterial Strain (NCPPB)**	**Day**	**BAM6**	**BAM7**	**BAM8**	**BAM9**	**BAM10**	**LM7**
Starter culture	365	0	1	0	0	0	0	0
Culture	365	1	0	0	0	0	1	0
Culture	365	2	0	0	1	0	0	1
Culture	365	3	0	0	0	0	0	0
Culture	365	4	0	0	0	0	0	0
Culture	365	5	0	0	0	0	0	1
Culture	365	6	0	0	0	1	0	0
Defined Alginate PS (DAP)			16	22	31	48	20	45
Culture or Plate (C/P)	**Bacterial Strain (NCPPB)**	**Day**	**BAM6**	**BAM7**	**BAM8**	**BAM9**	**BAM10**	**LM7**
Starter culture	385	0	0	0	0	0	0	0
Culture	385	1	0	0	0	1	0	1
Culture	385	2	1	1	0	0	0	0
Culture	385	3	0	0	0	0	0	0
Culture	385	4	1	1	1	1	0	1
Culture	385	5	1	1	1	1	0	0
Culture	385	6	3	6	5	8	2	7
Defined Alginate PS (DAP)			16	22	31	48	20	45
Culture or Plate (C/P)	**Bacterial Strain (NCPPB)**	**Day**	**BAM6**	**BAM7**	**BAM8**	**BAM9**	**BAM10**	**LM7**
Starter culture	1957	0	0	0	1	0	0	0
Culture	1957	1	1	0	1	0	0	1
Culture	1957	2	1	0	1	1	1	0
Culture	1957	3	3	1	3	4	0	0
Culture	1957	4	24	2	24	37	0	2
Culture	1957	5	41	5	41	63	2	5
Culture	1957	6	48	8	49	71	2	8
Defined Alginate PS (DAP)			16	22	31	48	20	45

0	10	20	30	40	50	60	70	80	90	100

Figure 5.5. Heatmap showing production of alginate polysaccharides from three *Pseudomonas spp.* (NCPPB 365, 385 and 1957) grown in liquid culture (Kings broth) over the course of a week. The alginate production was detected by BAM6, BAM7, BAM8, BAM9, BAM10 and LM7. DAP was printed alongside this sample set as a positive control. The opacity of colour green represents a higher binding intensity, and grey represents lack of it. The opacity of colour green represents a higher binding intensity, and grey represents lack of it. The Figure shows 6 antibodies. The full set is available in supplementary Figure 5.11.

After culturing the three strains for a week, the only one that was able to produce detectable levels of alginate in liquid culture was only NCPPB 1957. A positive control, DAP was included in the experiment to act as a positive control and to provide comparability to a defined polysaccharide. Though there are low values detected by BAM9 in day 6 of culturing NCPPB 385, they are not substantial enough to infer a satisfactory level of growth.

			Anti-Mannuronate-rich	Anti-Mannuronate-rich	Anti-Mannuronate-rich	Anti-Mannuronate-rich	Anti-Mannuronate-guluronate*	Anti-HG
Culture or Plate (C/P)	**Bacterial Strain (NCPPB)**	**Day**	**BAM6**	**BAM7**	**BAM8**	**BAM9**	**BAM10**	**LM7**
Starter culture	365	0	1	0	0	0	0	0
Plate	365	1	5	0	2	2	1	0
Plate	365	2	7	1	4	4	1	0
Plate	365	3	5	1	3	3	2	1
Plate	365	4	5	2	3	4	3	2
Plate	365	5	6	1	2	3	3	1
Plate	365	6	5	2	6	6	5	5
Defined Alginate PS (DAP)			16	22	31	48	20	45
Culture or Plate (C/P)	**Bacterial Strain (NCPPB)**	**Day**	**BAM6**	**BAM7**	**BAM8**	**BAM9**	**BAM10**	**LM7**
Starter culture	385	0	0	0	0	0	0	0
Plate	385	1	36	3	27	31	4	2
Plate	385	2	34	4	33	36	12	2
Plate	385	3	43	3	36	39	21	2
Plate	385	4	42	2	35	38	23	2
Plate	385	5	80	12	87	100	67	9
Plate	385	6	28	3	20	26	13	3
Defined Alginate PS (DAP)			16	22	31	48	20	45
Culture or Plate (C/P)	**Bacterial Strain (NCPPB)**	**Day**	**BAM6**	**BAM7**	**BAM8**	**BAM9**	**BAM10**	**LM7**
Starter culture	1957	0	0	0	1	0	0	0
Plate	1957	1	23	2	19	21	5	2
Plate	1957	2	31	4	25	30	18	3
Plate	1957	3	42	8	32	38	30	7
Plate	1957	4	63	11	51	60	67	13
Plate	1957	5	61	7	56	75	46	10
Plate	1957	6	38	11	45	54	36	14
Defined Alginate PS (DAP)			16	22	31	48	20	45

Figure 5.6. Heatmap showing production of alginate polysaccharides from three *Pseudomonas spp.* (NCPPB 365, 385 and 1957) grown on Kings broth solid media (plate) over the course of a week. The alginate production was detected by BAM6, BAM7, BAM8, BAM9, BAM10 and LM7. DAP was printed alongside this sample set as a positive control. The opacity of colour green represents a higher binding intensity, and grey represents lack of it. The Figure shows 6 antibodies. The full set is available in supplementary Figure 5.11.

Heatmap showing detectable levels of alginate as produced by NCPPB 1957 and 385 (Figure 5.6.). NCPPB 385 secreted higher levels of alginate than 1957 across the whole timeline, with alginate quantity declining after day 5 for both bacteria. Bacterial biofilm dispersal is a key mechanism that plays a role in cross-host transmission and spread of infection. A basic

mechanism of bacterial biofilm dispersal involves extracellular enzymes, that degrade the matrix of the biofilm, enabling the cells to detach from the colony (Kaplan, 2010).

It is possible that the decline in detection of alginate is due to the methodology used. Despite a drawn-on grid to consistently sample bacteria from the plate, it was not an entirely accurate methodology, as it did not account for variability in colony thickness across the plate. Though the bacteria inoculant was spread onto the plate as equally as possible, and grew in a uniform layer, it was possible the distribution of bacteria and alginate was uneven. The data was assessed for variability between the biological triplicates, to assess the reliability of the methodologies used (Figures 5.7.,5.8).

There is a high level of variability in the data from solid media plates, which is seen in Figure 5.8. as standard error bars have increased in size in NCPPB 1957 when compared to liquid culture (Figure 5.7.). High level of variability means significant differences between biological replicates taken from the plates. As mentioned previously, this is most likely due to methodology used not being precise and reliable enough. With such a big data spread, data obtained from solid plates should be treated as binary, i.e., presence or lack of alginate detected. Any further interpretation from this data set would be unreliable and not representative.

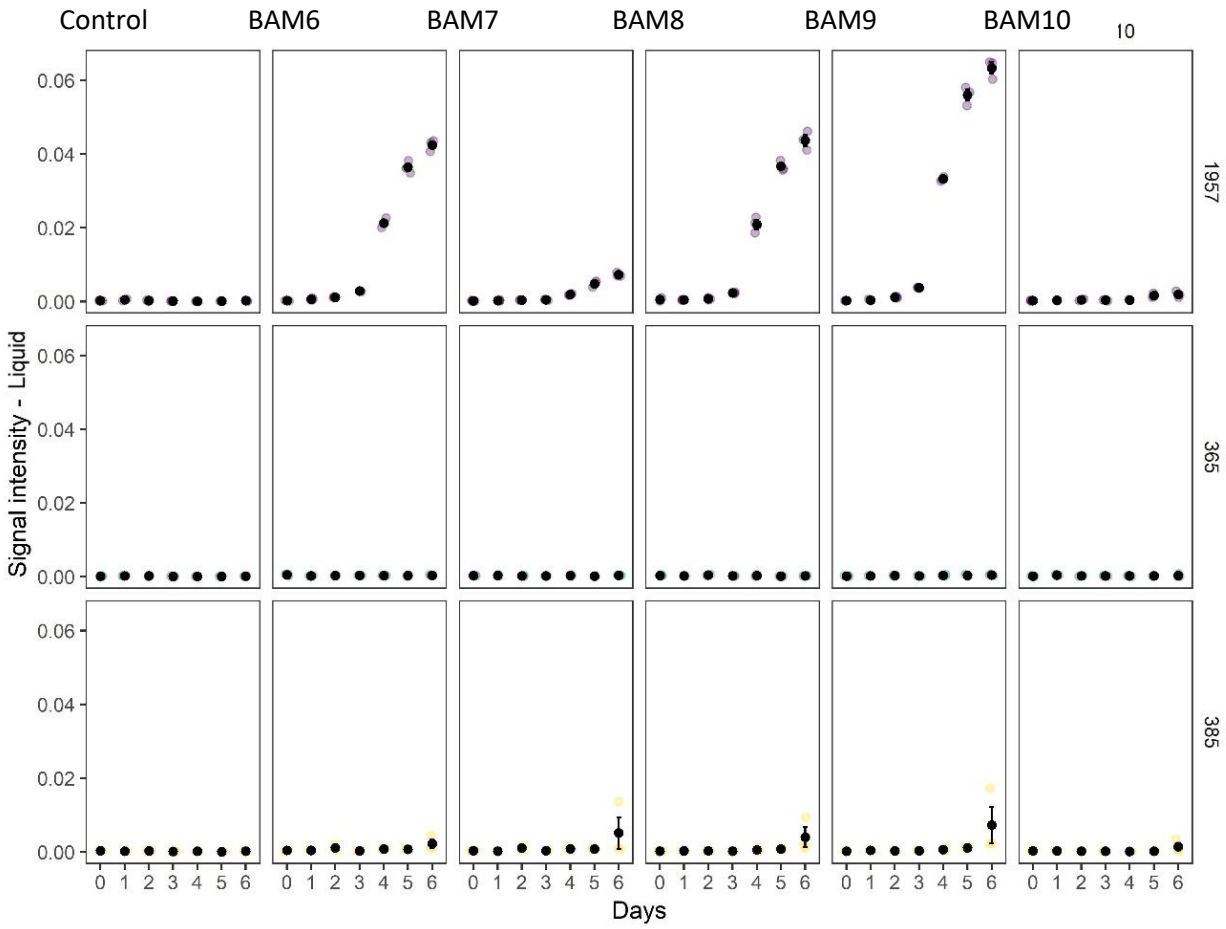

Figure 5.7. Jitter plots produced in R, assessing variability of detected alginate production between biological triplicates across 7-day period in liquid culture (Kings broth).
The jitter plot presents all biological replicates as coloured dots. Each biological replicate is the mean of 3 technical replicates. Black dot represents the mean of all three biological replicates, with whiskers attached to the dot, showing the standard error.

Jitter plots are a variant of strip plots. Strip plots are a single-axis scatter plots that visualise the distribution of one-dimensional values (signal intensity). Jitter plots offer a better view of overlapping data points, allowing the dots not to overlap. Standard error bars were added onto the jitter plot (Figure 5.7., 5.8.). Overlapping of standard error bars signifies that data is not statistically significant (Krzywinski and Altman, 2013).

Data obtained from liquid culture has very small standard error bars for NCPPB 1957. NCPPB 385 shows a higher degree of statistical variation due to lower values recorded by mAbs, making differences seem proportionally higher. This jitter plot confirms the reliability of sample set obtained from liquid culture (Figure 5.5.).

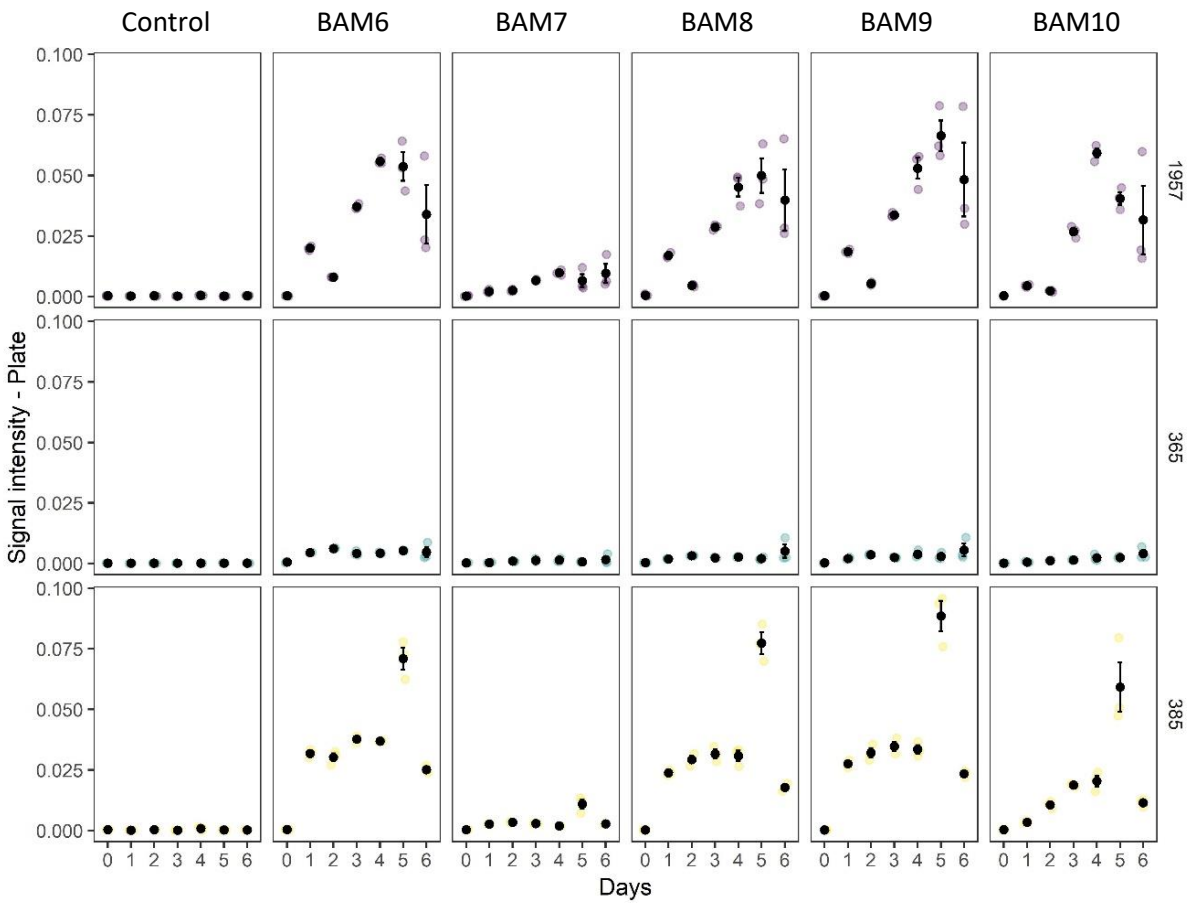

Figure 5.8. Jitter plots produced in R, assessing variability of detected alginate production between biological triplicates across 7-day period in solid media plates (Kings broth).
The jitter plot presents all biological replicates as coloured dots. Each biological replicate is the mean of 3 technical replicates. Black dot represents the mean of all three biological replicates, with whiskers attached to the dot, showing the standard error.

Jitter plots were made for data obtained from solid media plates; however, they confirmed the flow within sampling methodology. There are many instanced of standard error bars overlapping in NCPPB 1957, making the data not statistically significant. NCPPB 385 shows an outlier on day 5, that does not fall into the trend, signifying issues with sampling on that day. Despite NCPPB 385 not showing significant alginate production in liquid culture, it appears to be much more prevalent in solid media plates.

A further investigation into NCPPB 385 and 1957 was carried out, monitoring their alginate production over the course of 10 days in liquid media. An alternate sampling technique for solid media plates would require single colony counting, which goes against what biofilms are, making the sampling method also not viable for alginate relative quantification.

Bacterial Strain (NCPPB)	Media Type	Day	Anti-HG/alginate LM7	Anti-HG partially/de-esterified JIM5	Anti-HG partially/de-esterified JIM7	Anti-mannuronate-guluronate BAM7	Anti-mannuronate-guluronate BAM8	Anti-mannuronate-guluronate BAM9	Anti-mannuronate-guluronate BAM10	Anti-HG partially/de-esterified LM18	Anti-HG partially/de-esterified LM19	Anti-6'-β-D-galactosyl-β-(1->4)-D-galactotriose LM16
385	KB	0	0	0	10	0	0	7	8	0	9	9
385	KB	1	0	0	8	0	0	0	11	0	0	0
385	KB	2	0	0	6	0	0	0	0	0	0	0
385	KB	3	0	0	0	0	0	0	0	0	0	0
385	KB	4	5	0	0	0	0	5	13	0	0	0
385	KB	5	0	18	0	0	0	0	10	0	0	0
385	KB	6	0	0	0	19	10	6	15	0	6	0
385	KB	7	0	16	0	26	6	0	21	0	17	0
385	KB	8	0	12	8	50	9	14	46	9	43	0
385	KB	9	14	0	8	72	16	29	100	16	68	0
385	MM	0	9	0	9	0	0	0	0	0	0	0
385	MM	1	10	0	0	0	0	0	0	5	0	0
385	MM	2	0	0	18	0	0	0	0	0	0	0
385	MM	3	0	0	0	0	0	0	5	0	0	0
385	MM	4	0	0	0	0	0	0	0	0	0	0
385	MM	5	0	0	6	0	0	0	10	0	0	0
385	MM	6	0	5	0	13	0	0	6	0	0	0
385	MM	7	0	7	0	13	5	11	23	0	0	0
385	MM	8	0	10	0	9	0	7	24	0	7	0
385	MM	9	6	0	8	10	7	0	17	0	6	6
1957	KB	0	0	0	11	6	0	0	7	0	0	0
1957	KB	1	0	0	0	0	0	0	8	0	0	0
1957	KB	2	6	0	0	0	0	5	8	0	0	0
1957	KB	3	7	0	0	0	0	0	0	0	0	0
1957	KB	4	8	0	0	0	8	6	37	6	0	6
1957	KB	5	21	0	0	12	0	11	38	0	8	9
1957	KB	6	0	0	0	31	7	9	30	0	0	13
1957	KB	7	0	14	0	24	6	9	46	0	0	7
1957	KB	8	0	6	0	18	11	14	57	6	6	7
1957	KB	9	6	0	9	32	15	11	32	0	13	8
1957	MM	0	7	0	17	0	0	0	0	0	0	0
1957	MM	1	6	0	0	5	0	8	0	0	0	0
1957	MM	2	0	0	0	0	0	0	0	0	0	0
1957	MM	3	0	0	0	0	0	0	0	0	0	0
1957	MM	4	0	0	5	0	0	0	7	0	0	0
1957	MM	5	0	0	0	0	0	0	0	0	0	0
1957	MM	6	0	7	0	0	0	0	7	0	0	0
1957	MM	7	0	0	0	0	0	0	18	0	5	0
1957	MM	8	0	0	0	6	0	0	18	0	0	0
1957	MM	9	0	0	0	9	0	8	15	0	0	10

Figure 5.9 Heatmap showing production of alginate polysaccharides from two *Pseudomonas spp.* (NCPPB 365 and 1957) grown on rich media (Kings broth – KB) and minimal media (MM) over the course of 10 days, as detected by a selection of anti-alginate and anti-homogalacturonan mAbs.
The alginate production was detected by LM7, JIM5, JIM7, BAM7, BAM8, BAM9, BAM10, LM18, LM19 and LM16 (see Table 5.2. for epitope specificities). The media flasks (250 mL) were inoculated, and an aliquot was then taken at day 0, as a base reading. Subsequent aliquots were taken at the same time for the next 9 days. Once taken, the aliquots were stored in a freezer (-20 °C), until they were printed using a microarray robot. The samples were printed using an altered methodology, to increase the proportion of sample to system buffer, in order to maximise detection of alginate from the sample.

As reported previously in Figures 5.4. - 5.6. and 5.9., NCPPB 385 has started showing signs of alginate production, with BAM7, BAM8 and BAM9 binding to the sample. Two of the bacterial stains (NCPPB 385 and 1957) that exhibited alginate synthesis were grown in liquid culture in two different media, Kings broth and minimal media. The culture was left to incubate for 10 days, and aliquots were taken daily to measure the alginate production. With very limited alginate production observed on day 6 (Figure 5.5.), which is also seen in 5.9. The alginate production of NCPPB 385 when grown on KB, as detected by BAM7 and BAM10, increases significantly after day 6. (Figure 5.9.). The overall the alginate production of 385 as detected by BAM10, exceeds the alginate production from 1957. The alginate quantity can be compared within the sample set, as the data was normalised to the highest binding intensity spot, which for this data set is NCPPB 385 grown on KB, detected by BAM10. Both of the bacteria produce more alginate when grown on rich media (KB). It is likely that limited nutrients and sugar source in the minimal media has caused the bacteria to lower the metabolic rate and therefore slow the growth rate. A slower growth rate results in a smaller number of bacterial communities, making biofilm and alginate production slower.

LM7 has shown binding to NCPPB 1957 grown on KB. LM7 is known to bind to partially methyl-esterified epitope of pectic homogalacturonan (Willats et al., 2001), however it has been noted that it can bind to alginate (Torode et al., 2015). LM7 has shown higher binding intensity towards DAP (Figure 5.5 & 5.6), due to alginate from algae origin having a higher G-block content. l-Guluronic acid is a C-3 epimer of l-galacturonic acid, and homogalacturonan consists of α-1,4-linked D-galacturonic acid residues (Gacesa, 1991).

JIM5 and JIM7 are mAbs that recognise un-esterified (JIM5) and methyl-esterified (JIM7) epitopes of pectin (Knox et al., 1990), however binding has been recorded by JIM5 and JIM7 in Figure 5.9. As the supernatant contains bacteria, it is possible that JIM5 has bound to bacterial cell wall, as it was previously observed in Figure 2.7. Binding of JIM7 must be related to alginate synthesis and cross-reactivity between pectin and alginate. Binding recorded by LM19 to NCPPB 385 sample grown on KB, may be due to bacteria being present within the sample. LM19 and LM18 recognises the homogalacturonan domain of pectic polysaccharides, with LM19 showing similar binding properties to JIM5 (Verhertbruggen et al., 2009).

It is important to draw a comparison between homogalacturonan and alginate. Homogalacturonan contains contiguous stretches of (1-4)-a-D-galacturonic acid, with partial

methyl-esterification at the C-6 carboxyl (Mohnen, 1999). Alginate is a copolymer of galacturonic acid and mannuronic acid.

BAM 7 and BAM10 showed the highest binding intensities from all antibodies used in Figure 5.9. BAM7 was generated from immunising a rat with MM-blocks, a homopolymer of mannuronic acid, and BAM10 was generated by immunisation of a rat with GG-blocks, a homopolymer of guluronic acid. Despite BAM7 being closely related to BAM8 and BAM9, BAM7 has a different capacity when binding to pectic polysaccharides. BAM 8 and BAM9 recognise MG-blocks, which contain both monomers of mannuronic and guluronic acid (Torode et al., 2016).

LM16 was obtained by immunising a rat with an isolate of RGI derived from apple fruit (Verhoef et al., 2009). It is assumed that LM16 binds strongly to debranched arabinan (Verhertbruggen et al., 2009), however due to binding present in Figure 5.9, it is possible it also recognises epitopes of guluronic acid, as RGI is of pectic origin.

Alginate is a critical virulence factor, that contributes to severity and spread of infection in *Pseudomonas aeruginosa*. *P. aeruginosa* and *P. syringae* share the same alginate encoding genes (AlgR1 and algD) (Fakhr, Peñaloza-Vázquez, Chakrabarty and Bender, 1999). It has been confirmed that alginate plays a key role in *P. syringae* level of virulence and epiphytic fitness (Yu, Penaloza-Vazquez, Chakrabarty and Bender, 1999).

5.4 Conclusion

Bacterial biofilms play a critical role in the bacteria's ability to survive and successfully infect the host. Current methodology used for biofilm identification is Tissue Culture Plate (TCP), Tube method (TM), Congo Red Agar method (CRA), bioluminescent assay, piezoelectric sensors, and fluorescent microscopic examination (Hassan et al., 2011). Microarray offers a novel way of identifying and comparing bacterial biofilms, that goes beyond the binary outcome of presence or lack of presence of the biofilm. With further development of the methodology and additional molecular probes, it is possible to identify the microorganism with this methodology. Utilising a microarray robot and a selection of molecular probes offers additional insight into properties of alginate. These properties could be utilised for identification of pathogens, or pathogen groups. By creating alginate growth profiles of each bacterium in a selected media over a time course, bacteria are most likely to produce different quantities of alginate as it goes through the main three stages, adherence, proliferation, and dispersion. Differences in alginate production were be observed over the course of the week between NCPPB 385 and 1957.

5.5 Supplementary Figures

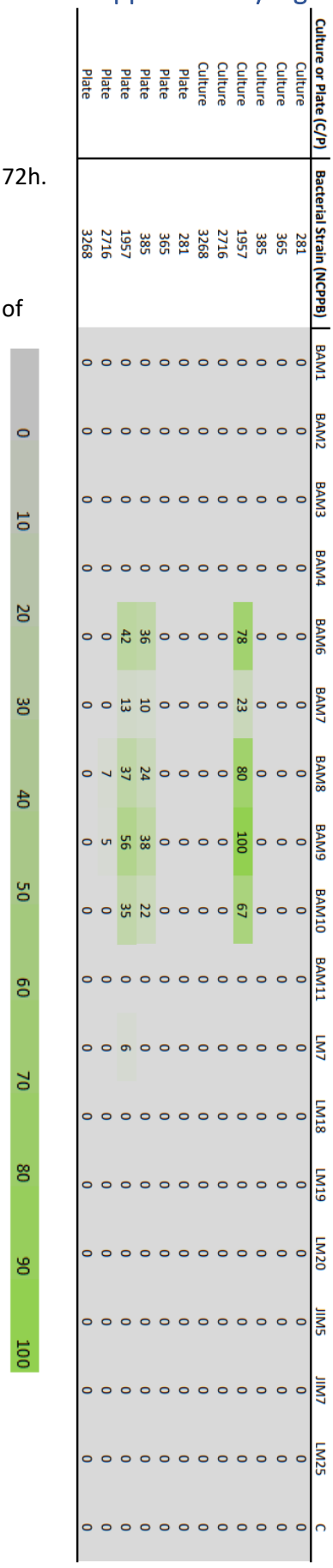

Figure 5.10. Heatmap showing production of alginate related polysaccharides by 6 different *P. syringae* pathovars when grown in liquid culture (culture), or on a solid media in a Petri dish (plate) after 72h. The production of alginate related polysaccharides is detected by a range of mAbs – BAM1, BAM2, BAM3, BAM4, BAM6, BAM7, BAM8, BAM9, BAM10, BAM11, LM7, LM18, LM19, LM20, JIM5, JIM7 and LM25. Negative control (C) is included in this heatmap, to show lack of cross-contamination of mAbs when handing microarrays. The control was probed with secondary antibody and stained normally.

Culture or Plate (C/P)	Bacterial Strain (NCPPB)	Day	BAM1	BAM2	BAM3	BAM4	BAM6	BAM7	BAM8	BAM9	BAM10	BAM11	LM7	LM18	LM19	LM20	JIM7	C
Starter culture	365	0	2	1	0	1	1	0	0	0	0	0	0	1	0	1	0	0
Culture	365	1	2	0	0	0	0	0	0	0	1	0	0	0	0	0	0	0
Culture	365	2	1	0	1	1	0	0	1	0	0	0	1	0	0	0	0	0
Culture	365	3	2	0	0	0	0	0	0	0	0	0	0	0	0	0	0	0
Culture	365	4	1	0	0	1	0	0	0	0	0	0	0	0	1	1	0	0
Culture	365	5	1	0	1	1	0	0	0	0	0	0	1	0	0	0	0	0
Culture	365	6	1	0	0	1	0	0	0	1	0	0	0	1	0	0	0	0
Plate	365	1	1	0	0	1	5	0	2	2	1	0	0	0	1	0	0	0
Plate	365	2	2	1	0	1	7	1	4	4	1	1	0	1	1	0	0	0
Plate	365	3	2	1	1	0	5	1	3	3	2	1	1	1	1	0	0	0
Plate	365	4	2	1	1	0	5	2	3	4	3	1	2	1	1	1	0	0
Plate	365	5	1	1	0	0	6	1	2	3	3	1	1	1	1	1	0	0
Plate	365	6	1	0	0	0	5	2	6	6	5	1	5	1	0	0	0	0
Defined Alginate PS (DAP)			2	0	1	1	16	22	31	48	20	1	45	1	0	0	0	0

Culture or Plate (C/P)	Bacterial Strain (NCPPB)	Day	BAM1	BAM2	BAM3	BAM4	BAM6	BAM7	BAM8	BAM9	BAM10	BAM11	LM7	LM18	LM19	LM20	JIM7	C
Starter culture	385	0	2	0	0	1	0	0	0	0	0	0	0	0	0	0	1	0
Culture	385	1	2	0	1	0	0	0	0	1	0	2	1	0	0	0	1	0
Culture	385	2	2	0	0	0	1	1	0	0	0	0	0	1	0	0	0	0
Culture	385	3	1	1	0	1	0	0	0	0	0	0	0	0	0	0	0	0
Culture	385	4	3	0	0	1	1	1	1	1	0	0	1	0	0	0	0	0
Culture	385	5	2	0	0	0	1	1	1	1	0	0	0	0	0	0	0	0
Culture	385	6	4	0	0	0	3	6	5	8	2	0	7	0	0	1	0	0
Plate	385	1	3	0	0	1	36	3	27	31	4	1	2	1	1	1	0	0
Plate	385	2	3	1	1	0	34	4	33	36	12	1	2	1	1	1	0	0
Plate	385	3	3	1	1	0	43	3	36	39	21	1	2	1	1	1	0	0
Plate	385	4	2	1	0	1	42	2	35	38	23	1	2	1	1	1	0	1
Plate	385	5	2	1	1	0	80	12	87	100	67	1	9	0	0	0	0	0
Plate	385	6	1	2	1	0	28	3	20	26	13	1	3	0	1	0	0	0
Defined Alginate PS (DAP)			2	0	1	1	16	22	31	48	20	1	45	1	0	0	0	0

Culture or Plate (C/P)	Bacterial Strain (NCPPB)	Day	BAM1	BAM2	BAM3	BAM4	BAM6	BAM7	BAM8	BAM9	BAM10	BAM11	LM7	LM18	LM19	LM20	JIM7	C
Starter culture	1957	0	1	0	0	1	0	0	1	0	0	0	0	0	1	0	0	0
Culture	1957	1	1	1	0	0	1	0	1	0	0	1	1	0	0	1	0	1
Culture	1957	2	1	0	1	1	1	0	1	1	1	0	0	0	0	0	0	0
Culture	1957	3	1	0	0	1	3	1	3	4	0	0	0	0	0	0	0	0
Culture	1957	4	2	0	0	1	24	2	24	37	0	0	2	0	0	0	0	0
Culture	1957	5	2	0	0	1	41	5	41	63	2	1	5	0	0	0	0	0
Culture	1957	6	1	0	0	1	48	8	49	71	2	0	8	0	0	0	0	0
Plate	1957	1	2	1	0	1	23	2	19	21	5	1	2	1	1	1	0	0
Plate	1957	2	1	1	0	1	31	4	25	30	18	1	3	2	1	1	0	0
Plate	1957	3	2	1	0	0	42	8	32	38	30	1	7	1	1	1	0	0
Plate	1957	4	2	1	1	1	63	11	51	60	67	1	13	1	1	1	0	1
Plate	1957	5	2	1	0	1	61	7	56	75	46	1	10	1	1	0	1	0
Plate	1957	6	1	1	0	1	38	11	45	54	36	1	14	1	0	0	0	0
Defined Alginate PS (DAP)			2	0	1	1	16	22	31	48	20	1	45	1	0	0	0	0

0	10	20	30	40	50	60	70	80	90	100

Figure 5.11. Heatmap showing production of alginate polysaccharides from three *P. syringae* pathovars (NCPPB 365, 385 and 1957) grown in liquid culture over the course of a week. The alginate production was detected by BAM1, BAM2, BAM3, BAM4, BAM6, BAM7, BAM8, BAM9, BAM10, BAM11, LM7, LM18, LM19, LM20 and JIM7. DAP was printed alongside this sample set as a positive control. Negative control (C) is included in this heatmap, to show lack of cross-contamination of mAbs when handing microarrays. The control was probed with secondary antibody and stained normally.

6. General Discussion

The objective of this thesis was to apply high-throughput methodology for screening of P*seudomonas syringae* pathovars. Another key aspect was utilising and developing methodology that would allow for additional applications of the microarray robot.

Despite several attempts at finding biomarkers, such as lipopolysaccharides within bacterial cell walls with microarray technology and TLC, no significant changes were observed between the pathovars (chapter 2.). The methodology used for profiling polysaccharides in bacterial cell walls using microarray robots did work, however the molecular probes available on the market for differentiating between pathovars were not available. It is entirely possible to isolate the lipopolysaccharides on the surface of each pathovar and create a library of monoclonal antibodies for each of them (Sattar, Jackson and Bradley, 2013) and then utilise the microarray technology to identify different pathovars. The work associated with isolation of these lipopolysaccharides and creating a library of monoclonal antibodies was not within the scope of this project.

Lipopolysaccharides not being a viable biomarker, due to lack of availability of relevant molecular probes. This results in the focus of the research shifting towards alternative biomarkers, such as enzymes. Biomarkers have a very broad definition, and with microarray robots being versatile, it was possible to develop a methodology for novel enzyme screening. Microarray technology has been successfully utilised for enzyme screening (Vidal-Melgosa et al., 2015, Duan, Cavanagh, Li and Walt, 2018), it was a viable course of action to develop a methodology to identify pathovar enzyme activity. Enzymes have been used as biomarkers in medicine, for diseases like myocardial infarction, jaundice, pancreatitis, cancer, and neurodegenerative disorders (Hemalatha et al., 2013). The methodology development began looking at epitope depletion of specific defined polysaccharide as detected by molecular probes, from which the enzymatic activity was inferred.

With bacteria being cultured in a laboratory setting becoming “domesticated”, enzymatic secretion is limited, and a desired enzymatic response must be carefully curated. It is impossible to imitate nature in a lab setting, making pathovar specific enzyme synthesis an impossible feat (Gibbons and Rinker, 2015). Method development focused on the high-

throughput aspect of enzyme screening. The bacterial strains were cultured in rich (Kings broth) and minimal media with an addition of defined polysaccharide as a carbon source. There was a difference observed in the enzymatic response, caused by different media used. The defined polysaccharide containing media source producing enzyme activity that was specific to the carbon source (Figures 3.5 – 3.11.). The methodology developed for epitope depletion can be utilised for a variety of substrates, as long as there are relevant probes are available.

This methodology would be of most significance to industry. Biofuel industry utilises lignocellulosic biomass for production of fuel, and uses enzymes such endoglucanases, cellobiohydrolases and β-glucosidases in order to breakdown the biomass (Zuccaro, Pirozzi and Yousuf, 2020). A high-throughput methodology would allow the industry to find novel enzyme activity for target molecules by printing the desired fraction from the product they require breaking down and treating it with microbial broths. The digested arrays would then be probed and analysed as outlined in chapter 3, to highlight microbial broths with activity of interest.

Due to the high cost of purchasing and installation of a microarray robot, it is possible to observe structural changes brought on by crude enzyme extracts with fluorescent microscopy. Methodology developed in chapter 4, focuses on utilising plant samples instead of defined polysaccharide standards to observe epitope depletion. Plant samples were treated with crude microbial enzymatic extracts and were then probed with molecular fluorescent probes, to observe changes within the plant structure when compared to control plants (untreated). A similar methodology has been used for commercial purified enzymes to characterise monoclonal antibodies (Mravec et al., 2017). Use of fluorescent microscopy provides qualitative data rather than quantitative, when used on plant roots in majority of chapter 4. This is due to physiological changes between samples. The fluorescence can be quantified using ImageJ to provide qualitative data when working with a sample set that does not have significant physiological variation between samples.

Biofilms are of significant interest to the medical and agricultural community, as biofilms are a key virulence factor that facilitate the spread of disease and aid the pathogen in evading the host's immune response. Microarray technology is capable of detecting alginate in liquid and

solid cultures as seen in chapter 5. It is possible to utilise microarray technology to check for biofilm presence in agricultural and medical settings, as it is faster than the majority of currently used culture-based methodology (Hassan et al., 2011). Due to the nature of biofilm being a community of bacteria suspended in matrix, it is not easy to quantify alginate production from bacteria on solid media, as sampling from individual colonies would be counter intuitive. With monoclonal probes being considered some of the most sensitive and specific molecular probes, a small alteration of the protocol should be able to accommodate the use of environmental swabs for biofilm identification and monitoring. A biofilm identification and monitoring methodology could be implemented in food manufacturing plants, to prevent the highly rampant food borne diseases.

The work carried out in this thesis has expanded the field of application of the microarray robot and provided more insight into enzymatic activity produced by *Pseudomonas syringae* pathovars. The methodologies developed have applications beyond the scope of the project and can be modified to suit the sample set of interest.

7. Final Conclusion

Microarray technology has a multitude of applications. Most of the microarray robots are being used for DNA and RNA work, due to lack of method development in other areas. The methodology used in chapter 2, for screening of pathovar specific epitopes using a selection of monoclonal antibodies works conceptually. However, a selection of custom or bacteria specific set of antibodies would need to be developed. The project funding was not able to support creation of custom monoclonal antibodies or purchasing a selection of more niche bacteria specific antibodies. There were only a handful of Pseudomonas species specific antibodies, however the risk of purchasing them was too high when the likelihood of them differentiating between over 50 different pathovars was extremely low. The project heavily relied upon a selection of monoclonal antibodies supplied by plantprobes.net (Paul Knox Laboratory, Leeds university).

Methodology developed for enzymatic activity screening in chapter 3 is a powerful tool for finding signs of enzymatic activity from crude microbial broths. The methodology needs minimal modification in order to a purified enzyme for its activity. Once an enzyme is purified, it's likely that its function is known, making the use of microarray machine not necessary. The application for this methodology would be to offer a primary perspective of enzymatic present in crude extract. Further action of the enzyme could be categorised with careful selection of defined standards and monoclonal antibodies, which would be costly. Use of high-performance-liquid-chromatography (HPLC) would be a more cost-efficient alternative that would offer insight into specific enzymatic activity.

Microscopy offered insight into structural significant of specific polysaccharides and offered additional insight into epitope specificities of monoclonal antibodies used. This novel methodology of using crude microbial enzyme extract on plant samples, showed which plant structures the plant pathogens are likely to damage and inhabit in nature. It is a relatively low-cost method of confirming enzymatic activity that could be applied to other materials with the same probing methods.

In conclusion, the microarray robot it a versatile and intricate bit of machinery. It allows to process a large sample set in a manageable time. During the duration of the PhD the research group was awarded a grant which allowed the group to purchase a new and updated microarray robot, (ArrayJet Marathon). The ArrayJet Marathon has a temperature regulation unit, which its predecessor (ArrayJet Sprint) did not have. During heatwaves in summer, the

ArrayJet Sprint was not able to function in a non-temperature-controlled laboratory, where it was placed. The temperature in the laboratory exceeded 25 ^{o}C most days during these heatwaves, making the robot unusable for 3 or 4 months of the year. During these months, a great deal of time was spent on maintenance work on these robots and focus of the work would shift towards methodologies that did not reply on the microarray robot. In the 3rd year of my PhD, the group secured the ArrayJet marathon that was easily able to withstand the hot temperature of the summer, and as a precautionary measure it was also based in a temperature-controlled laboratory.

While there is infrastructure within Newcastle University to facilitate using Microarray technology, it relies heavily on rich collection of molecular probes, relevant to field of study and MicroArray Pro software, which is quite dated. In the initial stages of the project, the software caused a lot of issues and required a lot of input from the IT department. The software was so old, that it was not possible to get in touch with the original developers of it. Alternative software was researched, however in literature most research groups that worked with microarrays would often have their own analysis software, developed in-house. Software not having support, advancement of data analysis is very limited, and the whole process heavily depends on it.

8. References

Adamczyk, B., Tharmalingam, T. & Rudd, P. (2012). Glycans as cancer biomarkers. *Biochimica et Biophysica Acta (BBA) - General Subjects*. 1820 (9). pp. 1347-1353.

Alderwick, L., Harrison, J., Lloyd, G. & Birch, H. (2015). The Mycobacterial Cell Wall—Peptidoglycan and Arabinogalactan. *Cold Spring Harbor Perspectives in Medicine*. 5 (8). p. a021113.

Alfano, J. & Collmer, A. (2004). Type III Secretion System Effector Proteins: Double Agents in Bacterial Disease and Plant Defense. *Annual Review of Phytopathology*. 42 (1). pp. 385-414.

Allison, S. & Vitousek, P. (2005). Responses of extracellular enzymes to simple and complex nutrient inputs. *Soil Biology and Biochemistry*. 37 (5). pp. 937-944.

Andersen, M., Boos, I., Marcus, S., Kračun, S., Rydahl, M., Willats, W., Knox, J. & Clausen, M. (2016). Characterization of the LM5 pectic galactan epitope with synthetic analogues of β-1,4-d-galactotetraose. *Carbohydrate Research*. 436. pp. 36-40.

Anderson, J., Pascuzzi, P., Xiao, F., Sessa, G. & Martin, G. (2006). Host-Mediated Phosphorylation of Type III Effector AvrPto Promotes Pseudomonas Virulence and Avirulence in Tomato. *The Plant Cell*. 18 (2). pp. 502-514.

Anon (2022). *Anthracnose*. [Online]. 2022. Integrated Pest Management. Available from: https://www.canr.msu.edu/ipm/diseases/anthracnose. [Accessed: 7 January 2022].

Anon (2022). *Bacterial canker*. [Online]. 2022. Love The Garden. Available from: https://www.lovethegarden.com/uk-en/article/bacterial-canker. [Accessed: 7 January 2022].

Anon (2022). *Holcus Leaf Spot of Corn*. [Online]. 2022. Crop protection network. Available from: https://cropprotectionnetwork.org/resources/articles/diseases/holcus-leaf-spot-of-corn. [Accessed: 7 January 2022].

Anon (2021). *How to get rid of Passionfruit Spots*. [Online]. 2021. Kings Plant Doctor. Available from: https://plantdoctor.co.nz/problem-finder/passionfruit-spots/. [Accessed: 7 January 2022].

Anon (2009). King's B medium. 2009 (7). pp. pdb.rec11326-pdb.rec11326.

Anon (2021). *National Collection of Plant Pathogenic Bacteria Catalogue*. [Online]. 2021. Ncppb.fera.defra.gov.uk. Available from: http://ncppb.fera.defra.gov.uk/ncppbresult.cfm. [Accessed: 6 December 2021].

Anon (2021). *NCPPB*. [Online]. 2021. Ncppb.fera.defra.gov.uk. Available from: http://ncppb.fera.defra.gov.uk/. [Accessed: 4 July 2021].

Anon (2022). *Powdery Mildew Treatment & Prevention (A How-To Guide) - Garden Design*. [Online]. 2022. GardenDesign.com. Available from: https://www.gardendesign.com/how-to/powdery-mildew.html. [Accessed: 7 January 2022].

Anon (1990). *Public health impact of pesticides used in agriculture*. Geneva: World Health Organization.

Anon (2022). *Rainy spring weather may lead to more leaf spot pathogens in the nursery*. [Online]. 2022. MSU Extension. Available from: https://www.canr.msu.edu/news/rainy_spring_weather_may_lead_to_more_leaf_spot_pathogens_in_the_nursery. [Accessed: 7 January 2022].

Anon (2022). *Rust*. [Online]. 2022. Love The Garden. Available from: https://www.lovethegarden.com/uk-en/garden-problem/rust. [Accessed: 7 January 2022].

Anon (2022). *Stem Rust of Wheat*. [Online]. 2022. Available from: https://cropprotectionnetwork.org/resources/articles/diseases/stem-rust-of-wheat. [Accessed: 7 January 2022].

Arvizu-Gómez, J., Hernández-Morales, A., Aguilar, J. & Álvarez-Morales, A. (2013). Transcriptional profile of *P. syringae pv. phaseolicola* NPS3121 at low temperature: Physiology of phytopathogenic bacteria. *BMC Microbiology*. 13 (1). p. 81.

Ates, O. (2015). Systems Biology of Microbial Exopolysaccharides Production. *Frontiers in Bioengineering and Biotechnology*. 3.

Atmodjo, M., Hao, Z. & Mohnen, D. (2013). Evolving Views of Pectin Biosynthesis. *Annual Review of Plant Biology*. 64 (1). pp. 747-779.

Balakshin, M., Capanema, E., Gracz, H., Chang, H. & Jameel, H. (2011). Quantification of lignin–carbohydrate linkages with high-resolution NMR spectroscopy. *Planta*. 233 (6). pp. 1097-1110.

Baldwin, L., Głazowska, S., Mravec, J., Fangel, J., Zhang, H., Felby, C., Willats, W. & Schjoerring, J. (2017). External nitrogen input affects pre- and post-harvest cell wall composition but not the enzymatic saccharification of wheat straw. *Biomass and Bioenergy*. 98. pp. 70-79.

Barnes, W. & Anderson, C. (2018). Release, Recycle, Rebuild: Cell-Wall Remodeling, Autodegradation, and Sugar Salvage for New Wall Biosynthesis during Plant Development. *Molecular Plant*. 11 (1). pp. 31-46.

Battistuzzi, F., Feijao, A. & Hedges, S. (2004). *BMC Evolutionary Biology*. 4 (1). p. 44.

BeMiller, J. (2019). Xanthan. *Carbohydrate Chemistry for Food Scientists*. pp. 261-269.

Bereswill, S., Bugert, P., Völksch, B., Ullrich, M., Bender, C. & Geider, K. (1994). Identification and relatedness of coronatine-producing *Pseudomonas syringae* pathovars by PCR analysis and sequence determination of the amplification products. *Applied and Environmental Microbiology*. 60 (8). pp. 2924-2930.

Block, A. & Alfano, J. (2011). Plant targets for *Pseudomonas syringae* type III effectors: virulence targets or guarded decoys?. *Current Opinion in Microbiology*. 14 (1). pp. 39-46.

Bordeaux, J., Welsh, A., Agarwal, S., Killiam, E., Baquero, M., Hanna, J., Anagnostou, V. & Rimm, D. (2010). Antibody validation. *BioTechniques*. 48 (3). pp. 197-209.

Boyd, A. & Chakrabarty, A. (1995). Pseudomonas aeruginosa biofilms: role of the alginate exopolysaccharide. *Journal of Industrial Microbiology*. 15 (3). pp. 162-168.

Brinsko, S., Blanchard, T., Varner, D., Schumacher, J., Love, C., Hinrichs, K. & Hartman, D. (2011). Examination of the Stallion for Breeding Soundness. *Manual of Equine Reproduction*. pp. 176-206.

Brust, H., Orzechowski, S. & Fettke, J. (2020). Starch and Glycogen Analyses: Methods and Techniques. *Biomolecules*. 10 (7). p. 1020.

Cammack, R. & Attwood, T. (2008). *Oxford dictionary of biochemistry and molecular biology*. Oxford: Oxford University Press.

Cao, B., Li, R., Xiong, S., Yao, F., Liu, X., Wang, M., Feng, L. & Wang, L. (2011). Use of a DNA Microarray for Detection and Identification of Bacterial Pathogens Associated with Fishery Products. *Applied and Environmental Microbiology*. 77 (23). pp. 8219-8225.

Cao, E., Chen, Y., Cui, Z. & Foster, P. (2003). Effect of freezing and thawing rates on denaturation of proteins in aqueous solutions. *Biotechnology and Bioengineering*. 82 (6). pp. 684-690.

Carezzano, M., Sotelo, J., Primo, E., Reinoso, E., Paletti Rovey, M., Demo, M., Giordano, W. & Oliva, M. (2017). Inhibitory effect ofThymus vulgarisandOriganum vulgareessential oils on virulence factors of phytopathogenic *Pseudomonas syringae* strains. *Plant Biology*. 19 (4). pp. 599-607.

Carpita, N. & McCann, M. (2015). Characterizing visible and invisible cell wall mutant phenotypes. *Journal of Experimental Botany*. 66 (14). pp. 4145-4163.

Castro, M. & Fontes, W. (2005). Plant Defense and Antimicrobial Peptides. *Protein & Peptide Letters*. 12 (1). pp. 11-16.

CAZy (2021). *CAZy - Carbohydrate-Active enZymes*. [Online]. 2021. Cazy.org. Available from: http://www.cazy.org/. [Accessed: 6 December 2021].

CAZy (2021). *CAZy - PL7*. [Online]. 2021. Cazy.org. Available from: http://www.cazy.org/PL7.html. [Accessed: 11 December 2021].

Cezairliyan, B. & Ausubel, F. (2017). Investment in secreted enzymes during nutrient-limited growth is utility dependent. *Proceedings of the National Academy of Sciences*. 114 (37). pp. E7796-E7802.

Chambers, J., Cleveland, W., Kleiner, B. & Tukey, P. (2018). *Graphical Methods for Data Analysis*.

Chew, S. & Yang, L. (2016). Biofilms. *Encyclopedia of Food and Health*. pp. 407-415.

Chialva, M., Fangel, J., Novero, M., Zouari, I., di Fossalunga, A., Willats, W., Bonfante, P. & Balestrini, R. (2019). Understanding Changes in Tomato Cell Walls in Roots and Fruits: The Contribution of Arbuscular Mycorrhizal Colonization. *International Journal of Molecular Sciences*. 20 (2). p. 415.

Chourasiya, S., Khillare, P. & Jyethi, D. (2014). Health risk assessment of organochlorine pesticide exposure through dietary intake of vegeTables grown in the periurban sites of Delhi, India. *Environmental Science and Pollution Research*. 22 (8). pp. 5793-5806.

Cid, M., Pedersen, H., Kaneko, S., Coutinho, P., Henrissat, B., Willats, W. & Boraston, A. (2010). Recognition of the Helical Structure of β-1,4-Galactan by a New Family of Carbohydrate-binding Modules. *Journal of Biological Chemistry*. 285 (46). pp. 35999-36009.

Clausen, M., Willats, W. & Knox, J. (2003). Synthetic methyl hexagalacturonate hapten inhibitors of anti-homogalacturonan monoclonal antibodies LM7, JIM5 and JIM7. *Carbohydrate Research*. 338 (17). pp. 1797-1800.

Cleveland, T. (2019). *Home, Yard & Garden Newsletter at the University of Illinois*. [Online]. 2019. Hyg.ipm.illinois.edu. Available from: http://hyg.ipm.illinois.edu/article.php?id=1100. [Accessed: 7 January 2022].

Colvin, K., Irie, Y., Tart, C., Urbano, R., Whitney, J., Ryder, C., Howell, P., Wozniak, D. & Parsek, M. (2011). The Pel and Psl polysaccharides provide *Pseudomonas aeruginosa* structural redundancy within the biofilm matrix. *Environmental Microbiology*. 14 (8). pp. 1913-1928.

Conway, J., Pierce, W., Le, J., Harper, G., Wright, J., Tucker, A., Zurawski, J., Lee, L., Blumer-Schuette, S. & Kelly, R. (2016). Multidomain, Surface Layer-associated Glycoside Hydrolases Contribute to Plant Polysaccharide Degradation by *Caldicellulosiruptor* Species. *Journal of Biological Chemistry*. 291 (13). pp. 6732-6747.

Cornuault, V., Buffetto, F., Rydahl, M., Marcus, S., Torode, T., Xue, J., Crépeau, M., Faria-Blanc, N., Willats, W., Dupree, P., Ralet, M. & Knox, J. (2015). Monoclonal antibodies indicate low-abundance links between heteroxylan and other glycans of plant cell walls. *Planta*. 242 (6). pp. 1321-1334.

Daher, F. & Braybrook, S. (2015). How to let go: pectin and plant cell adhesion. *Frontiers in Plant Science*. 6.

De Clerck, O., Bogaert, K. & Leliaert, F. (2012). Diversity and Evolution of Algae. *Advances in Botanical Research*. pp. 55-86.

Donlan, R. & Costerton, J. (2002). Biofilms: Survival Mechanisms of Clinically Relevant Microorganisms. *Clinical Microbiology Reviews*. 15 (2). pp. 167-193.

Donlan, R. (2001). Biofilm Formation: A Clinically Relevant Microbiological Process. *Clinical Infectious Diseases*. 33 (8). pp. 1387-1392.

Du Toit, S., Steyn, A. & Stumpf, R. (1986). Graphical Exploratory Data Analysis. *Springer Texts in Statistics*.

Du, H., Clarke, A.E. and Bacic, A. (1996) “Arabinogalactan-Proteins: A class of extracellular matrix proteoglycans involved in plant growth and development,” *Trends in Cell Biology*, 6(11), pp. 411–414. Available at: https://doi.org/10.1016/s0962-8924(96)20036-4.

Duan, B., Cavanagh, P., Li, X. & Walt, D. (2018). Ultrasensitive Single-Molecule Enzyme Detection and Analysis Using a Polymer Microarray. *Analytical Chemistry*. 90 (5). pp. 3091-3098.

Dudek, N., Sun, C., Burstein, D., Kantor, R., Aliaga Goltsman, D., Bik, E., Thomas, B., Banfield, J. & Relman, D. (2017). Novel Microbial Diversity and Functional Potential in the Marine Mammal Oral Microbiome. *Current Biology*. 27 (24). pp. 3752-3762.e6.

Ellis, M. (2016). *Bacterial Crown Gall of Fruit Crops*. [Online]. 2016. Ohioline.osu.edu. Available from: https://ohioline.osu.edu/factsheet/plpath-fru-19. [Accessed: 7 January 2022].

Engl, C., Waite, C., McKenna, J., Bennett, M., Hamann, T. & Buck, M. (2014). Chp8, a Diguanylate Cyclase from *Pseudomonas syringae pv. Tomato* DC3000, Suppresses the Pathogen-Associated Molecular Pattern Flagellin, Increases Extracellular Polysaccharides, and Promotes Plant Immune Evasion. *mBio*. 5 (3).

Esko, J., Doering, T. & Raetz, C. (2009). *Essentials of Glycobiology. 2nd edition*. 2nd Ed. Cold Spring Harbor Laboratory Press.

Fabich, H., Vogt, S., Sherick, M., Seymour, J., Brown, J., Franklin, M. & Codd, S. (2012). Microbial and algal alginate gelation characterized by magnetic resonance. *Journal of Biotechnology*. 161 (3). pp. 320-327.

Fakhr, M., Peñaloza-Vázquez, A., Chakrabarty, A. & Bender, C. (1999). Regulation of Alginate Biosynthesis in *Pseudomonas syringae pv. syringae*. *Journal of Bacteriology*. 181 (11). pp. 3478-3485.

Fey, J. & Maréchal-Drouard, L. (1999). Compilation and Analysis of Plant Mitochondrial Promoter Sequences: An Illustration of a Divergent Evolution between Monocot and Dicot Mitochondria. *Biochemical and Biophysical Research Communications*. 256 (2). pp. 409-414.

Fitzpatrick, M. (2014). *Measuring cell fluorescence using ImageJ — The Open Lab Book v1.0*. [Online]. 2014. Theolb.readthedocs.io. Available from: https://theolb.readthedocs.io/en/latest/imaging/measuring-cell-fluorescence-using-imagej.html. [Accessed: 22 December 2021].

Fredrickson, J., Zachara, J., Balkwill, D., Kennedy, D., Li, S., Kostandarithes, H., Daly, M., Romine, M. & Brockman, F. (2004). Geomicrobiology of High-Level Nuclear Waste-

Contaminated Vadose Sediments at the Hanford Site, Washington State. *Applied and Environmental Microbiology*. 70 (7). pp. 4230-4241.

Fries, M., Ihrig, J., Brocklehurst, K., Shevchik, V. & Pickersgill, R. (2007). Molecular basis of the activity of the phytopathogen pectin methylesterase. *The EMBO Journal*. 26 (17). pp. 3879-3887.

Gacesa, P. (1991) "Enzymic degradation of alginates," *International Journal of Biochemistry,* 24(4), pp. 545–552. Available at: https://doi.org/10.1016/0020-711x(92)90325-u.

Gal, A. (1968). Separation and identification of monosaccharides from biological materials by thin-layer chromatography. *Analytical Biochemistry*. 24 (3). pp. 452-461.

Galdiero, S., Falanga, A., Cantisani, M., Tarallo, R., Elena Della Pepa, M., D'Oriano, V. & Galdiero, M. (2012). Microbe-Host Interactions: Structure and Role of Gram-Negative Bacterial Porins. *Current Protein and Peptide Science*. 13 (8). pp. 843-854.

Ganapathi, Thumballi, Penna, Suprasanna, Rao, P.S.& Bapat & Vishwas (2004). Tobacco (Nicotiana tabacum L.) - A model system for tissue culture interventions and genetic engineering. *Indian Journal of Biotechnology*.. 3 (2). pp. 171-184.

Gerlt, J. (2016). Tools and strategies for discovering novel enzymes and metabolic pathways. *Perspectives in Science*. 9. pp. 24-32.

Ghigo, J. (2003). Are there biofilm-specific physiological pathways beyond a reasonable doubt?. *Research in Microbiology*. 154 (1). pp. 1-8.

Gibbons, J. & Rinker, D. (2015). The genomics of microbial domestication in the fermented food environment. *Current Opinion in Genetics & Development*. 35. pp. 1-8.

Ginsburg, I. (2002). Role of lipoteichoic acid in infection and inflammation. *The Lancet Infectious Diseases*. 2 (3). pp. 171-179.

Giorgi-Coll, S., Amaral, A., Hutchinson, P., Kotter, M. & Carpenter, K. (2017). Succinate supplementation improves metabolic performance of mixed glial cell cultures with mitochondrial dysfunction. *Scientific Reports*. 7 (1).

Gomila, M., Busquets, A., Mulet, M., García-Valdés, E. & Lalucat, J. (2017). Clarification of Taxonomic Status within the *Pseudomonas syringae* Species Group Based on a Phylogenomic Analysis. *Frontiers in Microbiology*. 8.

Goulson, D. (2014). Pesticides linked to bird declines. *Nature*. 511 (7509). pp. 295-296.

Gutiérrez-Barranquero, J., Cazorla, F. & de Vicente, A. (2019). *Pseudomonas syringae pv. syringae* Associated With Mango Trees, a Particular Pathogen Within the "Hodgepodge" of the *Pseudomonas syringae* Complex. *Frontiers in Plant Science*. 10.

Hahn, M. (2004). Broad diversity of viable bacteria in 'sterile' (0.2 µm) filtered water. *Research in Microbiology*. 155 (8). pp. 688-691.

Hammerschmidt, R. & Schultz, J. (1996). Multiple Defenses and Signals in Plant Defense against Pathogens and Herbivores. *Phytochemical Diversity and Redundancy in Ecological Interactions*. pp. 121-154.

Harris, P. (2009). Cell-wall Polysaccharides of Potatoes. *Advances in Potato Chemistry and Technology*. pp. 63-81.

Hassan, A., Usman, J., Kaleem, F., Omair, M., Khalid, A. & Iqbal, M. (2011). Evaluation of different detection methods of biofilm formation in the clinical isolates. *The Brazilian Journal of Infectious Diseases*. 15 (4). pp. 305-311.

Hayes, T., Case, P., Chui, S., Chung, D., Haeffele, C., Haston, K., Lee, M., Mai, V., Marjuoa, Y., Parker, J. & Tsui, M. (2006). Pesticide Mixtures, Endocrine Disruption, and Amphibian Declines: Are We Underestimating the Impact?. *Environmental Health Perspectives*. 114 (Suppl 1). pp. 40-50.

Hemalatha, T., UmaMaheswarI, T., Krithiga, G., Sankaranarayanan, P. & Puvanakrishnan, R. (2013). Enzymes in clinical medicine: an overview. *Indian journal of experimental biology*. 51 (10). pp. 777–788.

Henry, E., Yadeta, K. & Coaker, G. (2013). Recognition of bacterial plant pathogens: local, systemic and transgenerational immunity. *New Phytologist*. 199 (4). pp. 908-915.

Herth, W. & Schnepf, E. (1980). The fluorochrome, calcofluor white, binds oriented to structural polysaccharide fibrils. *Protoplasma*. 105 (1-2). pp. 129-133.

Hill, A. (2009). Microbiological stability of beer. *Beer*. pp. 163-183.

Høiby, N. (2017). A short history of microbial biofilms and biofilm infections. *APMIS*. 125 (4). pp. 272-275.

How to Spot, a. (2022). *How to Spot, Treat, and Prevent Chlorosis - Trees Unlimited*. [Online]. 2022. Trees Unlimited. Available from: https://treesunlimitednj.com/how-to-spot-treat-and-prevent-chlorosis/. [Accessed: 7 January 2022].

Hu, Wang, Yu, He, Qiao, Zhang & Wang (2019). Characterization and Antioxidant Activity of a Low-Molecular-Weight Xanthan Gum. *Biomolecules*. 9 (11). p. 730.

Hugouvieux-Cotte-Pattat, N. & Charaoui-Boukerzaza, S. (2009). Catabolism of Raffinose, Sucrose, and Melibiose in *Erwinia chrysanthemi* 3937. *Journal of Bacteriology*. 191 (22). pp. 6960-6967.

Huss, R. (2015). Biomarkers. *Translational Regenerative Medicine*. pp. 235-241.

Inaba, M. *et al.* (2015) "L-fucose-containing arabinogalactan-protein in radish leaves," *Carbohydrate Research*, 415, pp. 1–11. Available at: https://doi.org/10.1016/j.carres.2015.07.002.

Isla, M., OrdóÑez, R., Nieva Moreno, M., Sampietro, A. & Vattuone, M. (2002). Inhibition of Hydrolytic Enzyme Activities and Plant Pathogen Growth by Invertase Inhibitors. *Journal of Enzyme Inhibition and Medicinal Chemistry*. 17 (1). pp. 37-43.

Isleib, J. (2012). *Signs and symptoms of plant disease: Is it fungal, viral or bacterial?*. [Online]. 2012. Field Crops. Available from: https://www.canr.msu.edu/news/signs_and_symptoms_of_plant_disease_is_it_fungal_viral_or_bacterial. [Accessed: 7 January 2022].

Jacobs, J., Troxel, A., Ehrlich, Y., Spolnik, K., Bringas, J., Gregory, R. & Yassen, G. (2017). Antibacterial Effects of Antimicrobials Used in Regenerative Endodontics against Biofilm Bacteria Obtained from Mature and Immature Teeth with Necrotic Pulps. *Journal of Endodontics*. 43 (4). pp. 575-579.

Janda, A., Bowen, A., Greenspan, N. & Casadevall, A. (2016). Ig Constant Region Effects on Variable Region Structure and Function. *Frontiers in Microbiology*. 7.

Janeway, C., Travers, P., Walport, M. & Schlomchik, M. (2001). *Immunobiology, 5th edition: The Immune System in Health and Disease*. 5th Ed. New York: Garland Publishing.

Jung, J., Han, H., Jo, Y. & Koh, Y. (2003). Nested PCR Detection of *Pseudomonas syringae pv. actinidiae*, the Causal Bacterium. *Research in Plant Disease*. 9 (3). pp. 116-120.

Jutras, B., Lochhead, R., Kloos, Z., Biboy, J., Strle, K., Booth, C., Govers, S., Gray, J., Schumann, P., Vollmer, W., Bockenstedt, L., Steere, A. & Jacobs-Wagner, C. (2019). *Borrelia burgdorferi* peptidoglycan is a persistent antigen in patients with Lyme arthritis. *Proceedings of the National Academy of Sciences*. 116 (27). pp. 13498-13507.

Kang, X., Kirui, A., Dickwella Widanage, M., Mentink-Vigier, F., Cosgrove, D. & Wang, T. (2019). Lignin-polysaccharide interactions in plant secondary cell walls revealed by solid-state NMR. *Nature Communications*. 10 (1).

Kaplan, J. (2010). Biofilm Dispersal: Mechanisms, Clinical Implications, and Potential Therapeutic Uses. *Journal of Dental Research*. 89 (3). pp. 205-218.

Kar, M., Chourasiya, Y., Maheshwari, R. & Tekade, R. (2019). Current Developments in Excipient Science. *Basic Fundamentals of Drug Delivery*. pp. 29-83.

Kharbade, B. & Joshi, G. (1995). Thin-Layer Chromatographic and Hydrolysis Methods for the Identification of Plant Gums in Art Objects. *Studies in Conservation*. 40 (2). p. 93.

Kim, B., Park, J., Park, T., Bronstein, P., Schneider, D., Cartinhour, S. & Shuler, M. (2009). Effect of Iron Concentration on the Growth Rate of *Pseudomonas syringae* and the Expression of Virulence Factors in hrp -Inducing Minimal Medium. *Applied and Environmental Microbiology*. 75 (9). pp. 2720-2726.

Kim, B., Schneider, D., Cartinhour, S. & Shuler, M. (2010). Complex responses to culture conditions in *Pseudomonas syringae pv. Tomato* DC3000 continuous cultures: The role of iron in cell growth and virulence factor induction. *Biotechnology and Bioengineering*.

Kim, S. & Brandizzi, F. (2016). The plant secretory pathway for the trafficking of cell wall polysaccharides and glycoproteins. *Glycobiology*. 26 (9). pp. 940-949.

Kim, S., Chandrasekar, B., Rea, A., Danhof, L., Zemelis-Durfee, S., Thrower, N., Shepard, Z., Pauly, M., Brandizzi, F. & Keegstra, K. (2020). The synthesis of xyloglucan, an abundant plant cell wall polysaccharide, requires CSLC function. *Proceedings of the National Academy of Sciences*. 117 (33). pp. 20316-20324.

Klemm, D., Heublein, B., Fink, H. & Bohn, A. (2005). Cellulose: Fascinating Biopolymer and Sustainable Raw Material. *Angewandte Chemie International Edition*. 44 (22). pp. 3358-3393.

Knox, J., Linstead, P., King, J., Cooper, C. & Roberts, K. (1990). Pectin esterification is spatially regulated both within cell walls and between developing tissues of root apices. *Planta*. 181 (4).

Knox, P. (2021). *PlantProbes : Paul Knox Cell Wall Lab*. [Online]. 2021. Plantcellwalls.leeds.ac.uk. Available from: https://plantcellwalls.leeds.ac.uk/plantprobes/. [Accessed: 4 July 2021].

Kocincova, D. & Lam, J. (2011). Structural diversity of the core oligosaccharide domain of Pseudomonas aeruginosa lipopolysaccharide. *Biochemistry (Moscow)*. 76 (7). pp. 755-760.

Köhler, G. & Milstein, C. (1975). Continuous cultures of fused cells secreting antibody of predefined specificity. *Nature*. 256 (5517). pp. 495-497.

Kovacs-Simon, A., Titball, R. & Michell, S. (2011). Lipoproteins of Bacterial Pathogens. *Infection and Immunity*. 79 (2). pp. 548-561.

Krzywinski, M. & Altman, N. (2013). Error bars. *Nature Methods*. 10 (10). pp. 921-922.

Kumar, C. & Anand, S. (1998). Significance of microbial biofilms in food industry: a review. *International Journal of Food Microbiology*. 42 (1-2). pp. 9-27.

Kuthan, M., Devaux, F., Janderová, B., Slaninová, I., Jacq, C. & Palková, Z. (2003). Domestication of wild Saccharomyces cerevisiae is accompanied by changes in gene expression and colony morphology. *Molecular Microbiology*. 47 (3). pp. 745-754.

Lamport, D. (1966). The Protein Component of Primary Cell Walls. *Advances in Botanical Research*. pp. 151-218.

Laue, H., Schenk, A., Li, H., Lambertsen, L., Neu, T., Molin, S. & Ullrich, M. (2006). Contribution of alginate and levan production to biofilm formation by *Pseudomonas syringae*. *Microbiology*. 152 (10). pp. 2909-2918.

Le Goff, A., Renard, C., Bonnin, E. & Thibault, J. (2001). Extraction, purification and chemical characterisation of xylogalacturonans from pea hulls. *Carbohydrate Polymers*. 45 (4). pp. 325-334.

Lee, K., Marcus, S. & Knox, J. (2011). Cell Wall Biology: Perspectives from Cell Wall Imaging. *Molecular Plant*. 4 (2). pp. 212-219.

Lemuth, K. & Rupp, S. (2015). Microarrays as Research Tools and Diagnostic Devices. *RNA Technologies*. pp. 259-280.

Leroux, O., Sørensen, I., Marcus, S., Viane, R., Willats, W. & Knox, J. (2015). Antibody-based screening of cell wall matrix glycans in ferns reveals taxon, tissue and cell-type specific distribution patterns. *BMC Plant Biology*. 15 (1). p. 56.

Lievens, B. & Thomma, B. (2005). Recent Developments in Pathogen Detection Arrays: Implications for Fungal Plant Pathogens and Use in Practice. *Phytopathology*. 95 (12). pp. 1374-1380.

Limoli, D., Jones, C. & Wozniak, D. (2015). Bacterial Extracellular Polysaccharides in Biofilm Formation and Function. *Microbiology Spectrum*. 3 (3).

Lipman, N.S. *et al.* (2005) "Monoclonal versus polyclonal antibodies: Distinguishing characteristics, applications, and information resources," *ILAR Journal*, 46(3), pp. 258–268. Available at: https://doi.org/10.1093/ilar.46.3.258.

Lo, C. (2010). Effect of pesticides on soil microbial community. *Journal of Environmental Science and Health, Part B*. 45 (5). pp. 348-359.

Lombard, V., Bernard, T., Rancurel, C., Brumer, H., Coutinho, P. & Henrissat, B. (2010). A hierarchical classification of polysaccharide lyases for glycogenomics. *Biochemical Journal*. 432 (3). pp. 437-444.

Lombard, V., Golaconda Ramulu, H., Drula, E., Coutinho, P. & Henrissat, B. (2013). The carbohydrate-active enzymes database (CAZy) in 2013. *Nucleic Acids Research*. 42 (D1). pp. D490-D495.

Lovegrove, A., Edwards, C., De Noni, I., Patel, H., El, S., Grassby, T., Zielke, C., Ulmius, M., Nilsson, L., Butterworth, P., Ellis, P. & Shewry, P. (2015). Role of polysaccharides in food, digestion, and health. *Critical Reviews in Food Science and Nutrition*. 57 (2). pp. 237-253.

Ma, B., Simala-Grant, J. & Taylor, D. (2006). Fucosylation in prokaryotes and eukaryotes. *Glycobiology*. 16 (12). pp. 158R-184R.

Ma, J., Su, C., Hu, S., Chen, Y., Shu, Y., Yue, D., Zhang, B., Qi, Z., Li, S., Wang, X., Kuang, Y. & Cheng, P. (2020). The Effect of Residual Triton X-100 on Structural Stability and Infection Activity of Adenovirus Particles. *Molecular Therapy - Methods & Clinical Development*. 19. pp. 35-46.

Magro, P., Varvaro, L., Chilosi, G., Avanzo, C. & Balestra, G. (1994). Pectolytic enzymes produced by *Pseudomonas syringae pv. glycinea*. *FEMS Microbiology Letters*. 117 (1). pp. 1-5.

Malanovic, N. & Lohner, K. (2016). Antimicrobial Peptides Targeting Gram-Positive Bacteria. *Pharmaceuticals*. 9 (3). p. 59.

Manchester, K. (1995). Louis Pasteur (1822–1895) — chance and the prepared mind. *Trends in Biotechnology*. 13 (12). pp. 511-515.

Mann, E. & Wozniak, D. (2012). *Pseudomonas* biofilm matrix composition and niche biology. *FEMS Microbiology Reviews*. 36 (4). pp. 893-916.

Manning, M., Danson, E. & Calderone, C. (2018). Functional chararacterization of the enzymes TabB and TabD involved in tabtoxin biosynthesis by *Pseudomonas syringae*. *Biochemical and Biophysical Research Communications*. 496 (1). pp. 212-217.

Marcus, S., Verhertbruggen, Y., Hervé, C., Ordaz-Ortiz, J., Farkas, V., Pedersen, H., Willats, W. & Knox, J. (2008). Pectic homogalacturonan masks abundant sets of xyloglucan epitopes in plant cell walls. *BMC Plant Biology*. 8 (1).

Mathews, C., Holde, K. & Ahern, K. (2000). *Biochemistry*. San Francisco: Addison Wesley.

McGill, A. & Robinson, J. (1968). Organochlorine insecticide residues in complete prepared meals: A 12-month survey in S.E. England. *Food and Cosmetics Toxicology*. 6 (1). pp. 45-57.

Mellerowicz, E. & Gorshkova, T. (2011). Tensional stress generation in gelatinous fibres: a review and possible mechanism based on cell-wall structure and composition. *Journal of Experimental Botany*. 63 (2). pp. 551-565.

Mendis, M. & Simsek, S. (2014). Arabinoxylans and human health. *Food Hydrocolloids*. 42. pp. 239-243.

Mitchell, G., Chen, C. & Portnoy, D. (2016). Strategies Used by Bacteria to Grow in Macrophages. *Microbiology Spectrum*. 4 (3).

Mittelman, M. (2000). *Bacterial Biofilms and Biofouling: Translational Research in Marine Biotechnology*. Washington (DC): National Research Council (US) Board on Biology.

Mohnen, D. (1999). Biosynthesis of Pectins and Galactomannans. *Comprehensive Natural Products Chemistry*. pp. 497-527.

Moneo-Sánchez, M., Alonso-Chico, A., Knox, J., Dopico, B., Labrador, E. & Martín, I. (2018). β-(1,4)-Galactan remodelling in Arabidopsis cell walls affects the xyloglucan structure during elongation. *Planta*. 249 (2). pp. 351-362.

Monier, J. & Lindow, S. (2003). *Pseudomonas syringae* Responds to the Environment on Leaves by Cell Size Reduction. *Phytopathology®*. 93 (10). pp. 1209-1216.

Monteil, C., Yahara, K., Studholme, D., Mageiros, L., Méric, G., Swingle, B., Morris, C., Vinatzer, B. & Sheppard, S. (2016). Population-genomic insights into emergence, crop adaptation and dissemination of *Pseudomonas syringae* pathogens. *Microbial Genomics*. 2 (10).

Morris, C., Sands, D., Vinatzer, B., Glaux, C., Guilbaud, C., Buffière, A., Yan, S., Dominguez, H. & Thompson, B. (2008). The life history of the plant pathogen *Pseudomonas syringae* is linked to the water cycle. *The ISME Journal*. 2 (3). pp. 321-334.

Mravec, J., Kračun, S., Rydahl, M., Westereng, B., Pontiggia, D., De Lorenzo, G., Domozych, D. & Willats, W. (2017). An oligogalacturonide-derived molecular probe demonstrates the dynamics of calcium-mediated pectin complexation in cell walls of tip-growing structures. *The Plant Journal*. 91 (3). pp. 534-546.

Mukwaya, V., Wang, C. & Dou, H. (2018). Saccharide-based nanocarriers for targeted therapeutic and diagnostic applications. *Polymer International*. 68 (3). pp. 306-319.

Nelson, A., Dhimolea, E. & Reichert, J. (2010). Development trends for human monoclonal antibody therapeutics. *Nature Reviews Drug Discovery*. 9 (10). pp. 767-774.

Nelson, S. (2007). *Halo*. [Online]. 2007. Ctahr.hawaii.edu. Available from: https://www.ctahr.hawaii.edu/nelsons/glossary/Halo.htm. [Accessed: 7 January 2022].

Nicolaus, B., Kambourova, M. & Oner, E. (2010). Exopolysaccharides from extremophiles: from fundamentals to biotechnology. *Environmental Technology*. 31 (10). pp. 1145-1158.

Nighojkar, A., Patidar, M. & Nighojkar, S. (2019). Pectinases: Production and Applications for Fruit Juice Beverages. *Processing and Sustainability of Beverages*. pp. 235-273.

Novikova, O. & Solovyeva, T. (2009). Nonspecific porins of the outer membrane of Gram-negative bacteria: Structure and functions. *Biochemistry (Moscow) Supplement Series A: Membrane and Cell Biology*. 3 (1). pp. 3-15.

OERKE, E. (2005). Crop losses to pests. *The Journal of Agricultural Science*. 144 (1). pp. 31-43.

Ovod, V., Zdorovenko, E., Shashkov, A., Kocharova, N. & Knirel, Y. (2004). Structural diversity of O-polysaccharides and serological classification of *Pseudomonas syringae pv. garcae* and other strains of genomospecies 4. *Microbiology*. 73 (6). pp. 666-677.

Paczesny, J. & Mierzejewski, P. (2021). The use of probes and bacteriophages for the detection of bacteria. *Fluorescent Probes*. pp. 49-93.

Palková, Z. & Váchová, L. (2003). Ammonia signaling in yeast colony formation. *International Review of Cytology*. pp. 229-272.

Palková, Z. (2004). Multicellular microorganisms: laboratory versus nature. *EMBO reports*. 5 (5). pp. 470-476.

Passera, A., Compant, S., Casati, P., Maturo, M., Battelli, G., Quaglino, F., Antonielli, L., Salerno, D., Brasca, M., Toffolatti, S., Mantegazza, F., Delledonne, M. & Mitter, B. (2019). Not Just a Pathogen? Description of a Plant-Beneficial *Pseudomonas syringae* Strain. *Frontiers in Microbiology*. 10.

Patange, A., Boehm, D., Ziuzina, D., Cullen, P., Gilmore, B. & Bourke, P. (2019). High voltage atmospheric cold air plasma control of bacterial biofilms on fresh produce. *International Journal of Food Microbiology*. 293. pp. 137-145.

Pazos, M., Otten, C. & Vollmer, W. (2018). Bacterial Cell Wall Precursor Phosphatase Assays Using Thin-layer Chromatography (TLC) and High Pressure Liquid Chromatography (HPLC). *Bio-Protocol*. 8 (6).

Peltier, A., Bradley, C., Chilvers, M., Malvick, D., Mueller, D., Wise, K. & Esker, P. (2012). Biology, Yield loss and Control of *Sclerotinia* Stem Rot of Soybean. *Journal of Integrated Pest Management*. 3 (2). pp. 1-7.

Peña, M., Kong, Y., York, W. & O'Neill, M. (2012). A Galacturonic Acid–Containing Xyloglucan Is Involved in *Arabidopsis* Root Hair Tip Growth. *The Plant Cell*. 24 (11). pp. 4511-4524.

Pensinger, D., Schaenzer, A. & Sauer, J. (2018). Do Shoot the Messenger: PASTA Kinases as Virulence Determinants and Antibiotic Targets. *Trends in Microbiology*. 26 (1). pp. 56-69.

Pettolino, F., Walsh, C., Fincher, G. & Bacic, A. (2012). Determining the polysaccharide composition of plant cell walls. *Nature Protocols*. 7 (9). pp. 1590-1607.

Preston, L., Bender, C. & Schiller, N. (2001). Analysis and Expression of algL, which Encodes Alginate Lyase in *Pseudomonas Syringae Pv. Syringae*. *DNA Sequence*. 12 (5-6). pp. 455-461.

Rajagopal, M. & Walker, S. (2015). Envelope Structures of Gram-Positive Bacteria. *Current Topics in Microbiology and Immunology*. pp. 1-44.

Rajam, M., Weinstein, L. & Galston, A. (1985). Prevention of a plant disease by specific inhibition of fungal polyamine biosynthesis. *Proceedings of the National Academy of Sciences*. 82 (20). pp. 6874-6878.

Raveendran, S., Parameswaran, B., Ummalyma, S., Abraham, A., Mathew, A., Madhavan, A., Rebello, S. & Pandey, A. (2018). Applications of Microbial Enzymes in Food Industry. *Food Technology and Biotechnology*. 56 (1).

Reem, N., Pogorelko, G., Lionetti, V., Chambers, L., Held, M., Bellincampi, D. & Zabotina, O. (2016). Decreased Polysaccharide Feruloylation Compromises Plant Cell Wall Integrity and Increases Susceptibility to Necrotrophic Fungal Pathogens. *Frontiers in Plant Science*. 7.

Rietschel, E., Kirikae, T., Schade, F., Mamat, U., Schmidt, G., Loppnow, H., Ulmer, A., Zähringer, U., Seydel, U., Di Padova, F., Schreier, M. & Brade, H. (1994). Bacterial endotoxin: molecular relationships of structure to activity and function. *The FASEB Journal*. 8 (2). pp. 217-225.

Riley, M., Williamson, M. & Maloy, O. (2002). Plant Disease Diagnosis. *Plant Health Instructor*.

Ritika, B. & Utpal, D. (2014). An overview of fungal and bacterial biopesticides to control plant pathogens/diseases. *African Journal of Microbiology Research*. 8 (17). pp. 1749-1762.

Roach, P. & Zeeman, S. (2016). Glycogen and Starch. *Encyclopedia of Cell Biology*. pp. 263-270.

Rollenske, T., Szijarto, V., Lukasiewicz, J., Guachalla, L., Stojkovic, K., Hartl, K., Stulik, L., Kocher, S., Lasitschka, F., Al-Saeedi, M., Schröder-Braunstein, J., von Frankenberg, M., Gaebelein, G., Hoffmann, P., Klein, S., Heeg, K., Nagy, E., Nagy, G. & Wardemann, H. (2018). Cross-specificity of protective human antibodies against Klebsiella pneumoniae LPS O-antigen. *Nature Immunology*. 19 (6). pp. 617-624.

Ropartz, D. & Ralet, M. (2020). Pectin Structure. *Pectin: Technological and Physiological Properties*. pp. 17-36.

Routledge, S. (2012). Beyond de-foaming: the effects of antifoams on bioprocess productivity. *Computational and Structural Biotechnology Journal*. 3 (4). p. e201210001.

Ruiz-Villalba, A., van Pelt-Verkuil, E., Gunst, Q., Ruijter, J. & van den Hoff, M. (2017). Amplification of nonspecific products in quantitative polymerase chain reactions (qPCR). *Biomolecular Detection and Quantification*. 14. pp. 7-18.

Rydahl, M., Kračun, S., Fangel, J., Michel, G., Guillouzo, A., Génicot, S., Mravec, J., Harholt, J., Wilkens, C., Motawia, M., Svensson, B., Tranquet, O., Ralet, M., Jørgensen, B., Domozych, D. & Willats, W. (2017). Development of novel monoclonal antibodies against starch and ulvan - implications for antibody production against polysaccharides with limited immunogenicity. *Scientific Reports*. 7 (1).

S. Chidan Kumar, C., Chandraju, S., Mythily, R., Ahmad, T. & M. Made Gowda, N. (2012). Extraction of Sugars from Black Gram Peels by Reversed-Phase Liquid Chromatography

Systems and Identification by TLC and Mass Analysis. *Advances in Analytical Chemistry of Scientific & Academic Publishing*. 2 (4). pp. 32-36.

Sadovskaya, I. & Guérardel, Y. (2019). Simple Protocol to Purify Cell Wall Polysaccharide from Gram-Positive Bacteria and Assess Its Structural Integrity. *Methods in Molecular Biology*. pp. 37-45.

Salmeán, A., Guillouzo, A., Duffieux, D., Jam, M., Matard-Mann, M., Larocque, R., Pedersen, H., Michel, G., Czjzek, M., Willats, W. & Hervé, C. (2018). Double blind microarray-based polysaccharide profiling enables parallel identification of uncharacterized polysaccharides and carbohydrate-binding proteins with unknown specificities. *Scientific Reports*. 8 (1).

Sattar, A., Jackson, S. & Bradley, G. (2013). The potential of lipopolysaccharide as a real-time biomarker of bacterial contamination in marine bathing water. *Journal of Water and Health*. 12 (1). pp. 105-112.

Schulz, G. (2002). The structure of bacterial outer membrane proteins. *Biochimica et Biophysica Acta (BBA) - Biomembranes*. 1565 (2). pp. 308-317.

Sequeira, L. (1984). Plant-Bacterial Interactions. *Cellular Interactions*. pp. 187-211.

Sergeeva, L. & Vreugdenhil, D. (2002). In situ staining of activities of enzymes involved in carbohydrate metabolism in plant tissues. *Journal of Experimental Botany*. 53 (367). pp. 361-370.

Shao, X., Xie, Y., Zhang, Y. & Deng, X. (2019). Biofilm Formation Assay in Pseudomonas syringae. *Bio-Protocol*. 9 (10).

Sherma, J. (2006). Thin-Layer Chromatography. *Encyclopedia of Analytical Chemistry*.

Siddiqui, A., Musharraf, S., Choudhary, M. & Rahman, A. (2017). Application of analytical methods in authentication and adulteration of honey. *Food Chemistry*. 217. pp. 687-698.

Siddiqui, M. (2010). Monoclonal antibodies as diagnostics; an appraisal. *Indian Journal of Pharmaceutical Sciences*. 72 (1). p. 12.

Silhavy, T., Kahne, D. & Walker, S. (2010). The Bacterial Cell Envelope. *Cold Spring Harbor Perspectives in Biology*. 2 (5).

Singh, J., Kundu, D., Das, M. & Banerjee, R. (2019). Enzymatic Processing of Juice From Fruits/VegeTables: An Emerging Trend and Cutting Edge Research in Food Biotechnology. *Enzymes in Food Biotechnology*. pp. 419-432.

Singh, R., Kumar, M., Mittal, A. & Mehta, P. (2016). Microbial enzymes: industrial progress in 21st century. *3 Biotech*. 6 (2).

Sørensen, I. & Willats, W. (2010). Screening and Characterization of Plant Cell Walls Using Carbohydrate Microarrays. *Methods in Molecular Biology*. pp. 115-121.

Srey, S., Jahid, I. & Ha, S. (2013). Biofilm formation in food industries: A food safety concern. *Food Control*. 31 (2). pp. 572-585.

Stinson, E., Osman, S., Heisler, E., Siciliano, J. & Bills, D. (1981). Mycotoxin production in whole tomatoes, apples, oranges, and lemons. *Journal of Agricultural and Food Chemistry*. 29 (4). pp. 790-792.

Strahl, H. & Errington, J. (2017). Bacterial Membranes: Structure, Domains, and Function. *Annual Review of Microbiology*. 71 (1). pp. 519-538.

Strange, R. & Scott, P. (2005). Plant Disease: A Threat to Global Food Security. *Annual Review of Phytopathology*. 43 (1). pp. 83-116.

Tang, W., Fernandez, J., Sohn, J. & Amemiya, C. (2015). Chitin Is Endogenously Produced in Vertebrates. *Current Biology*. 25 (7). pp. 897-900.

Teegarden, D. (2004). *Polymer chemistry*. Arlington: NSTA Press.

Teitzel, G. & Parsek, M. (2003). Heavy Metal Resistance of Biofilm and Planktonic Pseudomonas aeruginosa. *Applied and Environmental Microbiology*. 69 (4). pp. 2313-2320.

Teo, S., Liew, K., Shamsir, M., Chong, C., Bruce, N., Chan, K. & Goh, K. (2019). Characterizing a Halo-Tolerant GH10 Xylanase from Roseithermus sacchariphilus Strain RA and Its CBM-Truncated Variant. *International Journal of Molecular Sciences*. 20 (9). p. 2284.

Thomas, N., Schwessinger, B., Liu, F., Chen, H., Wei, T., Nguyen, Y., Shaker, I. & Ronald, P. (2016). XA21-specific induction of stress-related genes followingXanthomonasinfection of detached rice leaves. *PeerJ*. 4. p. e2446.

Torode, T., Marcus, S., Jam, M., Tonon, T., Blackburn, R., Hervé, C. & Knox, J. (2015). Monoclonal Antibodies Directed to Fucoidan Preparations from Brown Algae. *PLOS ONE*. 10 (2). p. e0118366.

Torode, T., Siméon, A., Marcus, S., Jam, M., Le Moigne, M., Duffieux, D., Knox, J. & Hervé, C. (2016). Dynamics of cell wall assembly during early embryogenesis in the brown algaFucus. *Journal of Experimental Botany*. 67 (21). pp. 6089-6100.

Toth, I. & Birch, P. (2005). Rotting softly and stealthily. *Current Opinion in Plant Biology*. 8 (4). pp. 424-429.

Toth, I., Bell, K., Holeva, M. & Birch, P. (2002). Soft rot *erwiniae:* from genes to genomes. *Molecular Plant Pathology*. 4 (1). pp. 17-30.

Ünal Turhan, E., Erginkaya, Z., Korukluoğlu, M. & Konuray, G. (2019). Beneficial Biofilm Applications in Food and Agricultural Industry. *Health and Safety Aspects of Food Processing Technologies*. pp. 445-469.

Urtuvia, V., Maturana, N., Acevedo, F., Peña, C. & Díaz-Barrera, A. (2017). Bacterial alginate production: an overview of its biosynthesis and potential industrial production. *World Journal of Microbiology and Biotechnology*. 33 (11).

Uttamchandani, M. & Moochhala, S. (2010). Microarray-based enzyme profiling: Recent advances and applications (Review). *Biointerphases*. 5 (3). pp. FA24-FA31.

Van Der Heijden, M., Bakker, R., Verwaal, J., Scheublin, T., Rutten, M., Van Logtestijn, R. & Staehelin, C. (2006). Symbiotic bacteria as a determinant of plant community structure and plant productivity in dune grassland. *FEMS Microbiology Ecology*. 56 (2). pp. 178-187.

van Meer, G., Voelker, D. & Feigenson, G. (2008). Membrane lipids: where they are and how they behave. *Nature Reviews Molecular Cell Biology*. 9 (2). pp. 112-124.

Verhertbruggen, Y., Marcus, S., Haeger, A., Ordaz-Ortiz, J. & Knox, J. (2009). An extended set of monoclonal antibodies to pectic homogalacturonan. *Carbohydrate Research*. 344 (14). pp. 1858-1862.

Verhertbruggen, Y., Marcus, S., Haeger, A., Verhoef, R., Schols, H., McCleary, B., McKee, L., Gilbert, H. & Paul Knox, J. (2009). Developmental complexity of arabinan polysaccharides and their processing in plant cell walls. *The Plant Journal*. 59 (3). pp. 413-425.

Verhoef, R., Lu, Y., Knox, J., Voragen, A. & Schols, H. (2009). Fingerprinting complex pectins by chromatographic separation combined with ELISA detection. *Carbohydrate Research*. 344 (14). pp. 1808-1817.

Veronese, P., Ruiz, M., Coca, M., Hernandez-Lopez, A., Lee, H., Ibeas, J., Damsz, B., Pardo, J., Hasegawa, P., Bressan, R. & Narasimhan, M. (2003). In Defense against Pathogens. Both Plant Sentinels and Foot Soldiers Need to Know the Enemy. *Plant Physiology*. 131 (4). pp. 1580-1590.

Vester, J., Glaring, M. & Stougaard, P. (2014). Discovery of novel enzymes with industrial potential from a cold and alkaline environment by a combination of functional metagenomics and culturing. *Microbial Cell Factories*. 13 (1).

Vidal-Melgosa, S., Pedersen, H., Schückel, J., Arnal, G., Dumon, C., Amby, D., Monrad, R., Westereng, B. & Willats, W. (2015). A New Versatile Microarray-based Method for High Throughput Screening of Carbohydrate-active Enzymes. *Journal of Biological Chemistry*. 290 (14). pp. 9020-9036.

Vidarsson, G., Dekkers, G. & Rispens, T. (2014). IgG Subclasses and Allotypes: From Structure to Effector Functions. *Frontiers in Immunology*. 5.

Voiniciuc, C., Pauly, M. & Usadel, B. (2018). Monitoring Polysaccharide Dynamics in the Plant Cell Wall. *Plant Physiology*. 176 (4). pp. 2590-2600.

Voisin, S., Kus, J., Houliston, S., St-Michael, F., Watson, D., Cvitkovitch, D., Kelly, J., Brisson, J. & Burrows, L. (2007). Glycosylation of *Pseudomonas aeruginosa* Strain Pa5196 Type IV Pilins with Mycobacterium-Like α-1,5-Linked d-Ara-f Oligosaccharides. *Journal of Bacteriology*. 189 (1). pp. 151-159.

Vollmer, W., Blanot, D. & De Pedro, M. (2008). Peptidoglycan structure and architecture. *FEMS Microbiology Reviews*. 32 (2). pp. 149-167.

von Schantz, L., Håkansson, M., Logan, D., Walse, B., Österlin, J., Nordberg-Karlsson, E. & Ohlin, M. (2012). Structural basis for carbohydrate-binding specificity—A comparative assessment of two engineered carbohydrate-binding modules. *Glycobiology*. 22 (7). pp. 948-961.

Wade, W. (2002). Unculturable bacteria--the uncharacterized organisms that cause oral infections. *JRSM*. 95 (2). pp. 81-83.

Wang, V., Chua, S., Cao, B., Seviour, T., Nesatyy, V., Marsili, E., Kjelleberg, S., Givskov, M., Tolker-Nielsen, T., Song, H., Loo, J. & Yang, L. (2013). Engineering PQS Biosynthesis Pathway for Enhancement of Bioelectricity Production in *Pseudomonas aeruginosa* Microbial Fuel Cells. *PLoS ONE*. 8 (5). p. e63129.

Wang, X. & Quinn, P. (2010). Endotoxins: Lipopolysaccharides of Gram-Negative Bacteria. *Subcellular Biochemistry*. pp. 3-25.

Willats, W., McCartney, L., Steele-King, C., Marcus, S., Mort, A., Huisman, M., van Alebeek, G., Schols, H., Voragen, A., Le Goff, A., Bonnin, E., Thibault, J. & Knox, J. (2003). A xylogalacturonan epitope is specifically associated with plant cell detachment. *Planta*. 218 (4). pp. 673-681.

Willats, W., Orfila, C., Limberg, G., Buchholt, H., van Alebeek, G., Voragen, A., Marcus, S., Christensen, T., Mikkelsen, J., Murray, B. & Knox, J. (2001). Modulation of the Degree and Pattern of Methyl-esterification of Pectic Homogalacturonan in Plant Cell Walls. *Journal of Biological Chemistry*. 276 (22). pp. 19404-19413.

Williams, E. & Williams, H. (2015). *A History of Science; Volume 4*. Creative Media Partners, LLC.

Williams, R. & Fraústo da Silva, J. (2006). Outline of Biological Chemical Principles: Components, Pathways and Controls. *The Chemistry of Evolution*. pp. 125-192.

Wilson, J. & Hunt, T. (2002). *Molecular biology of the cell, 4th edition*. New York: Garland Science.

Wilson, M. & Bernstein, H. (2016). Surface-Exposed Lipoproteins: An Emerging Secretion Phenomenon in Gram-Negative Bacteria. *Trends in Microbiology*. 24 (3). pp. 198-208.

Wolf, D., Dao, T., Scott, H. & Lavy, T. (1989). Influence of Sterilization Methods on Selected Soil Microbiological, Physical, and Chemical Properties. *Journal of Environmental Quality*. 18 (1). pp. 39-44.

Wolf, S., Mouille, G. & Pelloux, J. (2009). Homogalacturonan Methyl-Esterification and Plant Development. *Molecular Plant*. 2 (5). pp. 851-860.

Wood, I., Pearson, B., Garcia-Gutierrez, E., Havlickova, L., He, Z., Harper, A., Bancroft, I. & Waldron, K. (2017). Carbohydrate microarrays and their use for the identification of molecular markers for plant cell wall composition. *Proceedings of the National Academy of Sciences*. p. 201619033.

Xie, Y., Shao, X. & Deng, X. (2019). Regulation of type III secretion system in *Pseudomonas syringae*. *Environmental Microbiology*. 21 (12). pp. 4465-4477.

Xin, X., Kvitko, B. & He, S. (2018). *Pseudomonas syringae*: what it takes to be a pathogen. *Nature Reviews Microbiology*. 16 (5). pp. 316-328.

Yang, Y. & Anderson, C. (2020). Biosynthesis, Localisation, and Function of Pectins in Plants. *Pectin: Technological and Physiological Properties*. pp. 1-15.

Ye, J., Joseph, S., Ji, M., Nielsen, S., Mitchell, D., Donne, S., Horvat, J., Wang, J., Munroe, P. & Thomas, T. (2017). Chemolithotrophic processes in the bacterial communities on the surface of mineral-enriched biochars. *The ISME Journal*. 11 (5). pp. 1087-1101.

Yi, W., Liu, X., Li, Y., Li, J., Xia, C., Zhou, G., Zhang, W., Zhao, W., Chen, X. & Wang, P. (2009). Remodeling bacterial polysaccharides by metabolic pathway engineering. *Proceedings of the National Academy of Sciences*. 106 (11). pp. 4207-4212.